

Republic of Iraq
Ministry of Higher Education and Scientific Research
Al-Nahrain University
College of Science
Department of Chemistry



Spectrophotometric Determination for Single and Multi Components of Drugs

A Thesis

*Submitted to the College of Science /Al-Nahrain University as a partial
fulfillment of the requirements for the Degree of Master of Science in
Chemistry*

By

Marwah Sabah yones

B.Sc. Chemistry /college of science / Baghdad University

Supervised by

Dr. Khaleda H. Al-Saidi

(Assist. Prof.)

Oct. 2014

Dhul Hijjah 1435

بِسْمِ اللَّهِ الرَّحْمَنِ الرَّحِيمِ

يَرْفَعِ اللَّهُ الَّذِينَ آمَنُوا مِنْكُمْ
وَالَّذِينَ أُوتُوا الْعِلْمَ دَرَجَاتٍ وَاللَّهُ
بِمَا تَعْمَلُونَ خَبِيرٌ

صدق الله العظيم
المجادلة (11)

Supervisor (s) Certification

We, certify that this thesis entitled *Spectrophotometric determination for single and multi components of drugs* was prepared by *Marwah Sabah yones* under our supervision at the College of Science/ Al-Nahrain University as partial fulfillment of the requirements for the Degree of master of science in chemistry.

Signature:

Name: Dr. Khaleda H. Al-Saidi

Scientific Degree: Assist. Prof.

Date: / / 2014

Signature

Name:

Scientific Degree:

Date: / / 2014

In view of the available recommendation, I forward this thesis for debate by the Examining Committee.

Signature:

Name: Dr. Nasreen R . Jber

Scientific Degree: Assist. Prof.

Title: Head of the Department of Chemistry, College of Science

Al-Nahrain University

Date: / / 2014

Committee Certification

We, the Examining Committee, certify that we have read this thesis entitled”
Spectrophotometric determination for single and multi components of drugs” and
examined the student (Marwah Sabah yones) in its contents and that in our opinion, it
is accepted for the Degree of Master of Science in Chemistry.

Signature:

Name: **Sarmad B. Dikran**

Scientific Degree: **prof. Dr.**

Date:

(Chairman)

Signature:

Name: **Dheaa S. Zageer**

Scientific Degree: **Dr.**

Date:

(Member)

Signature:

Name: **Yehya K. Albayati**

Scientific Degree: **Assist. prof. Dr.**

Date:

(Member)

Signature:

Name:

Scientific Degree:

Date:

(Member)

Signature:

Name: **Khaleda H. Al-saidi**

Scientific Degree: **Assist. prof. Dr.**

Date:

(Member)

I, hereby certify upon the decision of the examining committee.

Signature:

Name: **Hadi M. A. Abood**

Scientific Degree: **Prof. Dr.**

Title: Dean of the College of Science, Al- Nahrain University

Date:

الإهداء

الى الشمعة التي احترقت لتنير دربي....

والدي العزيز

الى من بنت فاعلى الله مقامها...
الى من زرعت فحصدت طيب ثمارها...
الى من سهرت وافنت سني عمرها...

أمي الغالية

الى من غرس في نفسي الامل...
الى القلب الكبير...

زوجي الغالي

الى شمسي وضياء نهاري...

ولدي

الى من تقر بهم عيني...
الى من برويتهم يزول همي...
الى من بحبهم أستمد عزمي...

أخوتي وأخواتي

إليهم جميعا اهدي ثمرة جهدي عرفانا بفضلهم

مروة

Acknowledgments

I wish to express my deepest gratitude and appreciation to my supervisor Dr. Khaleda H. Al-saidi for her patience, supervision and encouragement during the course of my study.

I am sincerely thankful to Dr. Nasreen R. Jber the Head of Chemistry Department at AL-Nahrain University for all the facilities that he offered during my research.

Finally, I would like to thank my Husband, parents, brothers and my sisters as well as all my friends for their support and encourage me.

Marwa sabah

2014

<i>Summary</i>	<i>Page No.</i>
<i>Chapter One: Introduction</i>	
1-1-Spectroscopy and Beer's Law	1
1-2-Beer's law Deviations	3
1-3-UV-Visible spectrophotometry	4
1-4-UV-VIS Instrumentation	4
1-4-1- Sources	4
1-4-2- Wavelength Selection	5
1-4-3- Sample Compartment	6
1-4-3-1- Single-Beam Spectrophotometer	6
1-4-3-2- Double-Beam Designs	6
1-4-4-Detectors	7
1-5-General Applications of UV/Visible	8
1-5-1-Applications of UV/Visible for Drugs Analyses	8
1-6-Derivative Spectrophotometric Analysis	10
1-6-1-Basic Characteristics of Derivative Spectrophotometry	10
1-6-1-1-Derivative Spectrophotometry (DS), Derivation	10
1-6-1-2-Increase of Spectra Resolution	11
1-6-1-3-Elimination of the Influence of Baseline Shift and Matrix Interferences	12
1-6-1-4-Enhancement of the Detectability of Minor Spectral Features	12
1-6-1-5-Precise Determination of the Positions of Absorption Maxima	13
1-6-1-6-Signal to Noise Ratio (SNR)	14
1-6-2-Quantitative Analysis	14
1-7-Application of Derivative Spectrophotometry (DS)	15
1-8-Sulphamethoxazole and Trimethoprim	17
1-8-1-Sulphamethoxazole	17
1-8-2-Trimethoprim	17
1-8-3-Sulphamethoxazole and Trimethoprim mixture	18
1-8-4-Analysis of Sulphamethoxazole and Trimethoprim	18
1-9-Paracetamol and Caffeine	19
1-9-1-Paracetamol	19
1-9-2-Caffeine	19
1-9-3-Paracetamol and Caffeine mixture	20
1-9-4-Analysis of Paracetamol and Caffeine	20
1-10-Paracetamol and Hyoscine	22
1-10-1-Hyoscine Butyl bromide	22

1-10-2-Paracetamol and Hyoscine mixture	22
1-10-3-Analysis of Paracetamol and Hyoscine	22
1-11-Aim of the work	23
1-12-Future Work	23
Chapter TWO: Experimental part	Page No.
2-1-Instruments and Equipment's	25
2-2-Chemicals	25
2-3-Preparation of Standard Solutions	26
2-4-Preparation of pharmaceuticals samples	28
2-5-UV- Measurement	29
2-6-Interfering Effect using UV Measurements	29
2-7-Sample Analyses	30
Chapter Three: Results and Discussion	
3-1-Sulfamethoxazole	31
3-1-1-Normal Spectroscopy	31
3-1-2-Derivative Spectrophotometry (DS)	31
3-1-2-1-Selection of Optimum Instrumental Conditions	32
3-1-2-2-First Derivative	32
3-1-2-3-Second Derivative	33
3-1-2-4-Third Derivative	34
3-1-2-5-Fourth Derivative	35
3-2-Trimethoprim	38
3-2-1-Normal Spectroscopy	38
3-2-2-Derivative Spectrophotometry	38
3-2-2-1-First Derivative	39
3-2-2-2-Second Derivative	40
3-2-2-3-Third Derivative	41
3-2-2-4-Fourth Derivative	43
3-3-Binary Mixture	46
3-3-1-Sulphmethoxazole with Trimethoprim Mixture	46
3-3-1-1-First Derivative	47
3-3-1-2-Second Derivative	49

3-3-1-3-Third Derivative	49
3-3-1-4-Fourth Derivative	52
3-4-Interferences study	59
3-5-Analysis of Pharmaceutical Samples	61
3-5-1-Sulphamethaxzole with Trimethoprim Mixture	61
3-6-Paracetamol	63
3-6-1-Normal Spectroscopy	63
3-6-2-Derivative Spectrophotometry	63
3-6-2-1-Selection of Optimum Instrumental Conditions	63
3-6-2-2-First Derivative	63
3-6-2-3-Second Derivative	64
3-6-2-4-Third Derivative	64
3-6-2-5-Fourth Derivative	64
3-7-Caffeine	68
3-7-1-Normal Spectroscopy	68
3-7-2-Derivative Spectrophotometry	68
3-7-2-1-First Derivative	68
3-7-2-2-Second Derivative	68
3-7-2-3-Third Derivative	69
3-7-2-4-Fourth Derivative	69
3-8-Binary Mixture	73
3-8-1-Paracetamol with Caffeine Mixture	73
3-8-1-1-First Derivative	73
3-8-1-2-Second Derivative	75
3-8-1-3-Third Derivative	77
3-8-1-4-Fourth Derivative	79
3-9-Interferences study	84
3-10-Analysis of Pharmaceutical Samples	85
3-10-1-Paracetamol with Caffeine Mixture	85
3-11-Hyoscine-n-butyl bromide	87
3-11-1-Normal Spectroscopy	87
3-11-2-Derivative Spectrophotometry	87

3-11-2-1-Selection of Optimum Instrumental Conditions	87
3-11-2-2-First Derivative	87
3-11-2-3-Second Derivative	88
3-11-2-4-Third Derivative	88
3-11-2-5-Fourth Derivative	88
3-12-Binary Mixture	91
3-12-1-Paracetamol with Hyoscine Mixture	91
3-12-1-1-First Derivative	91
3-12-1-2-Second Derivative	95
3-12-1-3-Third Derivative	97
3-12-1-4-Fourth Derivative	99
3-13-Interferences study	103
3-14-Analysis of Pharmaceutical Samples	104
3-14-1-Paracetamol with Hyoscine Mixture	104

Summary

This research includes determination of drugs SMX, TMP, CAF, HYO and PAR using derivative spectrophotometry (first, second, third and fourth derivative) were developed for binary mixture by applying zero-crossing technique for pure synthetic mixture and their pharmaceutical formulation as follows:

1. SMX with TMP mixture: SMX was determined by applying $1^{\text{D}}\&4^{\text{D}}$ teach s at 288.0 and 257.8 nm (zero crossing point of TMP) with linear concentration ranges (2-30) and (2-25) mg/L , $r = 0.9996$ and $r = 0.9992$ LOD = 0.750 and LOD = 0.360 mg/L and TMP was determined by applying 4^{D} teach at 251.5 nm (zero crossing point of SMX) with concentration range (2-30) mg/L , $r = 0.9995$ and LOD = 0.382mg/L . The RSD were 0.255, 0.280 and 1.136 for SMX and TMP respectively and applied for (TRIMOL-400SMX, 80TMP mg) and (METHOPRIM-400SMX,80TMP mg).

2. PAR with CAF mixture: PAR was determined by applying 3^{D} teach at 275.8 nm (zero crossing point of CAF).With linear concentration range (2-35) mg/L , $r = 0.9987$ and LOD=0.445mg/L . And CAF was determined by applying 4^{D} teach at 294.7 nm (zero crossing point of PAR). With linear concentration range (2-35) mg/L , $r = 0.9995$ and LOD = 0.162 mg/L . The RSD was 0.222 for PAR and 0.130 for CAF and applied for (PANADOL EXTRA-500PAR, 65CAF mg).

3. PAR with HYO mixture: PAR was determined by applying $1^{\text{D}}\&2^{\text{D}}$ teach s at 297.4 and 303.5 nm (zero crossing point of HYO) with linear concentration ranges (2-30) and (2-30) mg/L , $r = 0.9998$ and $r = 0.9987$ LOD = 0.081 and LOD = 0.250 mg/L and HYO was determined by applying 1^{D} teach at 215.9 nm (zero crossing point of PAR) with

concentration range (2-25) mg/L , $r = 0.9997$ and $LOD = 0.091\text{mg/L}$. The RSD were 0.107, 0.400 and 0.342 for PAR and HYO respectively and applied for (SPAZMOTEK PLUS-500PAR,10HYO mg).

This thesis has mainly been structured in three different chapters, each one containing the following information:

Chapter one provides a short historical review with the analytical performance characteristics of UV-visible are described. The applications of UV and DS in pharmaceutical and SMX, TMP, CAF, HYO and PAR analyses and their mixture .the general and specific objectives of thesis are reported.

Chapter two corresponds to the experimental part. Reagents, instruments, procedures and detail protocols for the preparation of standard solution and pharmaceutical sample which used in this study are reported.

Chapter three contains the experimental results and discussion that lead to the possibility of successful applications which used DS to determine the concentration of each material in drugs.

List of tables

<i>Number of Tables</i>	<i>The title of Tables</i>	<i>Page No.</i>
1-1	Some applications of UV/Visible for drug analysis	9
1-2	Some applications of Derivative spectrophotometry for determination of some mixtures.	15
1-3	Some teach s for the analyses of Sulphamethoxazole and Trimethoprim	18
1-4	Some teach s for the analyses of Paracetamol and Caffeine.	21
1-5	Some teach s for the analyses of Paracetamol and Hyoscine.	23
3-1	The parameters obtained from the calibration curves for normal and DS teach s of SMX.	37
3-2	The relative error and recovery for the determination standard sample of 20 mg/L SMX by using normal and DS teach s.	37
3-3	The parameters obtained from the calibration curves for Normal and DS teach of TMP.	45
3-4	The relative error and recovery for the determination synthetic sample of 20 mg/L TMP by using normal and DS teach	46
3-5	The relative error and recovery for the determination SMX in the presence of TMP at 288 nm using ¹ D teach.	48
3-6	The relative error and recovery for the determination SMX in the presence of TMP at 251.4 nm using ³ D teach .	50
3-7	The relative error and recovery for the determination TMP in the presence of SMX at 258.6 nm using ³ D teach .	51
3-8	The relative error and recovery for the determination SMX in the presence of TMP at 246.2 nm using ⁴ D teach .	54
3-9	The relative error and recovery for the determination SMX in the presence of TMP at 257.8 nm using ⁴ D teach .	54
3-10	The relative error and recovery for the determination TMP in the presence of SMX at 251.5 nm using ⁴ D teach .	56
3-11	The relative error and recovery for the determination TMP in the presence of SMX at 237.6 nm using ⁴ D teach .	57
3-12	The parameters obtained from the calibration curves for DS teach. of SMX and TMP.	59
3-13	Statistical data for the calibration curves that used to determine SMX and TMP in their mixture.	59
3-14	The relative error and recovery for the determination of Trimol sample (20mg/L SMX + 4mg/L TMP) by using DS teach .	61
3-15	The relative error and recovery for the determination of Methoprim sample (20mg/L SMX + 4mg/L TMP) by using DS teach.	62
3-16	Statistical data for the determination of (SMX + TMP) in their mixture in pure and pharmaceutical form by ⁴ D teach.	63
3-17	The parameters obtained from the calibration curves for normal and DS teach s of PAR.	67
3-18	The relative error ,recovery and standard deviation for the determination	68

	synthetic sample of 20 mg/L PAR by using normal and DS teach .	
3-19	The parameters obtained from the calibration curves for normal and DS teach of CAF.	72
3-20	The relative error, recovery and standard deviation for the determination synthetic sample of 20 mg/L CAF by using normal and DS teach .	73
3-21	The relative error and recovery for the determination PAR in the presence of CAF at 273.6 nm using ¹ D teach .	75
3-22	The relative error and recovery for the determination CAF in the presence of PAR at 223.7 nm using ² D teach .	76
3-23	The relative error and recovery for the determination CAF in the presence of PAR at 278.8 nm using ² D teach .	77
3-24	The relative error and recovery for the determination PAR in the presence of CAF at 275.8 nm using ³ D teach .	78
3-25	The relative error and recovery for the determination CAF in the presence of PAR at 268.6 nm using ³ D teach .	79
3-26	The relative error and recovery for the determination PAR in the presence of CAF at 264.8 nm using ⁴ D teach .	81
3-27	The relative error and recovery for the determination CAF in the presence of PAR at 230.4 nm using ⁴ D teach .	82
3-28	The relative error and recovery for the determination CAF in the presence of PAR at 294.7 nm using ⁴ D teach .	82
3-29	The parameters obtained from the calibration curves for DS teach. of .PAR and CAF	84
3-30	Statistical data for the calibration curves that used to determine PAR and CAF in their mixture.	84
3-31	The relative error and recovery for the determination of Panadol extra sample (20 mg/L PAR + 3mg/L CAF) by using DS teach s.	86
3-32	Statistical data for the determination of (PAR + CAF) in their mixture in pure and pharmaceutical form by ³ D for PAR & ⁴ D for CAF.	87
3-33	The parameters obtained from the calibration curves for DS teach s of HYO.	91
3-34	The relative error and recovery for the determination synthetic sample of 20 mg/L HYO by using DS teach .	91
3-35	The relative error and recovery for the determination PAR in the presence of HYO at 257.5 nm using ¹ D teach.	93
3-36	The relative error and recovery for the determination PAR in the presence of HYO at 297.4 nm using ¹ D teach.	94
3-37	The relative error and recovery for the determination HYO in the presence of PAR at 215.9 nm using ¹ D teach.	95
3-38	The relative error and recovery for the determination PAR in the presence of HYO at 245.4 nm using ² D teach.	96
3-39	The relative error and recovery for the determination PAR in the presence of HYO at 268.2 nm using ² D teach.	97
3-40	The relative error and recovery for the determination PAR in the presence of HYO at 303.5 nm using ² D teach.	97
3-41	The relative error and recovery for the determination PAR in the presence of HYO at 237.1 nm using ³ D teach .	99
3-42	The relative error and recovery for the determination PAR in the presence of HYO at 214.0 nm using ³ D teach	99

3-43	The relative error and recovery for the determination PAR in the presence of HYO at 219.7 nm using ⁴ D teach .	101
3-44	The relative error and recovery for the determination PAR in the presence of HYO at 266.3 nm using ⁴ D teach .	101
3-45	The parameters obtained from the calibration curves for DS teach. of PAR and HYO.	103
3-46	Statistical data for the calibration curves that used to determine PAR and HYO in their mixture.	104
3-47	The relative error and recovery for the determination of Spasmodic plus sample (25mg/L PAR + 0.5mg/L HYO) by using DS teach s.	106
3-48	Statistical data for the determination of (PAR + HYO) in their mixture in pure and pharmaceutical form by ² D for PAR and ¹ D for HYO.	107

List of figures

Figure No.	The Figure name	Page No.
1-1	Absorption of radiation by a sample	2
1-2	Deviation from Beer's law often manifests them by a nonlinear portion of the Beer's law plot at the higher concentration.	3
1-3	An illustration of the double-beam design utilizing two cuvette holders in the sample compartment.	7
3-1	Calibration curve of normal spectra for SMX 6-25 mg/L at P = 256.7 nm.	31
3-2	Calibration curve of ¹ D spectra for SMX 2-30 mg/L at V= 269.2 nm.	32
3-3	Calibration curve of ² D spectra for SMX 2-30 mg/L at P = 276.0 nm.	33
3-4	Calibration curve of ² D spectra for SMX 4-25 mg/L at V = 258.5nm.	33
3-5	Calibration curve of ³ D spectra for SMX 6–25 mg/L at P = 267.4 nm.	34
3-6	Calibration curve of ³ D spectra for SMX 2-30 mg/L at V =251.1 nm.	34
3-7	Calibration curve of ⁴ D spectra for SMX 6-25 mg/L at P = 259.4 nm.	35
3-8	Calibration curve of ⁴ D spectra for SMX 4-25 mg/L at V = 274 nm.	35
3-9	Spectra of 2-30 mg/L SMX a- Normal spectrum b- First derivative(S=3,λ=2) c- Second derivative(S=5,λ=4) d- Third derivative (S=40,λ=8) e- Fourth derivative(S=160,λ=16)	36
3-10	Calibration curve of normal spectra for TMP 2-30 mg/L at P = 288 nm.	38
3-11	Calibration curve of ¹ D spectra for TMP 2-30 mg/L at P = 272.2nm.	39
3-12	Calibration curve of ¹ D spectra for TMP 2-30 mg/L at V = 245.6 nm.	39
3-13	Calibration curve of ¹ D spectra for TMP 2-30 mg/L at V = 301.5 nm.	40
3-14	Calibration curve of ² D spectra for TMP 2-30 mg/L at P = 250.7 nm.	40
3-15	Calibration curve of ² D spectra for TMP 2-30 mg/L at V = 241.7 nm.	41
3-16	Calibration curve of ³ D spectra for TMP 2-30 mg/L at P = 246.1 nm.	42
3-17	Calibration curve of ³ D spectra for TMP 2-30 mg/L at V = 256.2 nm.	42
3-18	Calibration curve of ³ D spectra for TMP 2-35 mg/L at V = 286.0 nm.	42
3-19	Calibration curve of ⁴ D spectra for TMP 2-30 mg/L at P = 241.0 nm.	43
3-20	Calibration curve of ⁴ D spectra for TMP 2-30 mg/L at V = 251.3 nm.	43
3-21	Spectra of 2-30 mg/L TMP a- Normal spectrum b- First derivative(S=3,λ=2) c- Second derivative(S=5,λ=4) d- Third derivative (S=40,λ=8) e- Fourth derivative(S=160,λ=16)	44
3-22	¹ D spectra for (4-25) mg/L SMX and (4) mg/L TMP (zero crossing) at 288 nm.	47
3-23	Calibration curve of ¹ D spectra for SMX 2-30 mg/L at V = 288nm.	47
3-24	³ D spectra for (8-25) mg/L SMX and (4)mg/L TMP (zero crossing) at 251.4nm.	49
3-25	Calibration curve of ³ D spectra for SMX 2-30 mg/L at V = 251.4nm.	50
3-26	³ D spectra for (8-25) mg/L TMP and (20) mg/L SMX (zero crossing) at 258.6nm.	51
3-27	Calibration curve of ³ D spectra for TMP 2-30 mg/L at V = 258.6nm.	51
3-28	⁴ D spectra for (8-25) mg/L SMX and (4) mg/L TMP (zero crossing) at 246.2 and 257.8nm.	53
3-29	Calibration curve of ⁴ D spectra for SMX 2-30 mg/L at V = 246.2nm.	53
3-30	Calibration curve of ⁴ D spectra for SMX 2-30 mg/L at P= 257.8nm.	54
3-31	⁴ D spectra for (8-25) mg/L TMP and (20) mg/L SMX (zero crossing) at 251.5 and 237.6nm.	55
3-32	Calibration curve of ⁴ D spectra for TMP 2-30 mg/L at V= 251.5nm	56
3-33	Calibration curve of ⁴ D spectra for TMP4-30 mg/L at P= 237.6nm.	56

3-34	Spectra of 8-25 mg/L SMX, 8-25 mg/L TMP a- Normal spectrum of 20 mg/L for each SMX and TMP. b- First derivative(S=3, λ =2) c- Second derivative(S=5, λ =4) d- Third derivative (S=40, λ =8) e- Fourth derivative(S=160, λ =16)	58
3-35	Normal spectra for analyzed preparation(a)Mix with drug (b)Mix with (Av,Ge,Mg,St,Su)	60
3-36	Spectra of 2-30 mg/L PAR ,a- Normal spectrum b- First derivative(S=10, λ =2) c- Second derivative(S=60, λ =4) d- Third derivative (S=100, λ =8) e- Fourth derivative(S=300, λ =16)	65
3-37	Spectra of 2-30 mg/L CAF ,a- Normal spectrum b- First derivative(S=10, λ =2) c- Second derivative(S=60, λ =4) d- Third derivative (S=100, λ =8) e- Fourth derivative(S=300, λ =16)	70
3-38	¹ D spectra for (8-25) mg/L PAR and (8) mg/L CAF (zero crossing) at 273.6nm.	73
3-39	² D spectra for(8-25) mg/L CAF and(8)mg/L PAR (zero crossing) at 223.7 and 278.8nm	75
3-40	³ D spectra for (8-25) mg/L PAR and (8) mg/L CAF (zero crossing) at 275.8 nm.	77
3-41	³ D spectra for (8-25) mg/L CAF and (8) mg/L PAR (zero crossing) at 268.6nm.	78
3-42	⁴ D spectra for (8-25) mg/L PAR and (8) mg/L CAF (zero crossing) at 264.8nm.	80
3-43	⁴ D spectra for (8-25) mg/L CAF and (8) mg/L PAR (zero crossing) at 230.4 and 294.7nm.	81
3-44	Spectra of 8-25 mg/L PAR 8-25 mg/LCAF a- Normal spectrum of 20 mg/L for each PAR and CAF. b- First derivative(S=10, λ =2) c- Second derivative(S=60, λ =4) d- Third derivative (S=100, λ =8) e- Fourth derivative(S=300, λ =16)	83
3-45	Spectra of 0.5-35 mg/L HYO ,a- Normal spectrum b- First derivative(S=6, λ =2) c- Second derivative(S=25, λ =4) d- Third derivative (S=75, λ =8) e- Fourth derivative(S=150, λ =16)	85
3-46	Spectra of 0.5-35 mg/L HYO ,a- Normal spectrum b- First derivative(S=6, λ =2) c- Second derivative(S=25, λ =4) d- Third derivative (S=75, λ =8) e- Fourth derivative(S=150, λ =16)	89
3-47	¹ D spectra for (8-25) mg/L PAR and (8) mg/L HYO (zero crossing) at 257.5 and 297.4nm.	92
3-48	¹ D spectra for (8-25) mg/L HYO and (8) mg/L PAR (zero crossing) at 215.9nm.	94
3-49	² D spectra for (8-25) mg/L PAR and (8) mg/L HYO (zero crossing) at 245.5, 268.2 and 303.5nm.	95
3-50	³ D spectra for (8-25) mg/L PAR and (8) mg/L HYO (zero crossing) at 237.1 and 214.0nm.	98
3-51	⁴ D spectra for (8-25) mg/L PAR and (8) mg/L HYO (zero crossing) at 219.7 and 266.3nm.	100
3-52	Spectra of 8-25 mg/L PAR 8-25 mg/LHYO a- Normal spectrum of 25 mg/L for each PAR and HYO. b- First derivative(S=6 λ =2) c- Second derivative(S=25, λ =4) d- Third derivative (S=75, λ =8) e- Fourth derivative(S=150, λ =16)	102
3-53	Normal spectra for analyzed preparation.(a)Mix with drug (b)Mix with Tit.	104
3-54	Calibration carve for standard addition teach (SAM) for HYO by using 1D teach at V=215.9nm.	105

List of abbreviation

$\Delta\lambda$	Delta lambda
A	absorbance
a	absorbivity
Av.	Avicel
b	Path length(cm)
BDD	Boron-doped diamond
c	concentration
CAF	Caffeine
COX	cyclooxygenase
DPV	Differential pulse voltammetry
DS	Derivative spectrophotometry
ϵ	Molar absorptivity
ER	Relative error
F.W.	Formula weight
Ge.	Gelatin
HT	Hydrogen terminated
HYO	Hyoscine n-butyl bromide
IR	Infrared
LOD	Limit of detection
LOQ	Limit of quantification
m	slope
MCP	Meta cresol purple
Mg	Magnesium stearate
Mix	mixture
ⁿ D	Derivative order
OT	oxygen terminated
P	Peak
PAR	Paracetamol
r	Correlation coefficient
RC	Recovery
RSD	Relative standard deviation
S	Scaling factor
SAM	Standard addition method
SC	Sildenafil citrate
SD _B	Standard deviation for blank
SMX	Sulphamethoxazole
SNR	Signal noise ratio
St.	Starch
Su.	Sucrose

T	transmittance
Tit.	Titanium dioxide
TMP	Trimethoprim
UV-VIS	Ultraviolet-visible
V	Valley
W	Band width
δ	Standard deviation

Chapter One

Introduction

Introduction

1.1. Spectroscopy and Beer's Law:

When light passes through an absorbing sample, the power of the light emerging from the sample is decreased. Assume the power of a beam of monochromatic (i.e., single wavelength) radiation is p_0 . This beam is passed through a sample that can absorb radiation of this wavelength, as shown in Fig. (1.1). The emerging light beam has an power equal to p , where $p_0 \geq p$. If no radiation is absorbed by the sample, then $p = p_0$. If any amount of radiation is absorbed, then $p < p_0$. The transmittance T is defined as the ratio of p to p_0 :⁽¹⁾

$$T = \frac{p}{p_0} \quad \dots 1-1$$

The transmittance is the fraction of the original light that passes through the sample. Therefore, the range of allowed values for T is from 0 to 1. The ratio p/p_0 remains relatively constant even if p_0 changes; hence, T is independent of the actual intensity p_0 . To study the quantitative absorption of radiation by samples it is useful to define another quantity, the absorbance A where:

$$A = \log\left(\frac{p_0}{p}\right) = \log\left(\frac{1}{T}\right) = -\log T \quad \dots 1-2$$

When no light is absorbed, then $p = p_0$ and $A = 0$. Two related quantities are also used in spectroscopy, the percent transmittance, %T, which equals $T \times 100$, and the percent absorption, %A, which is equal to $100 - \%T$.⁽²⁾

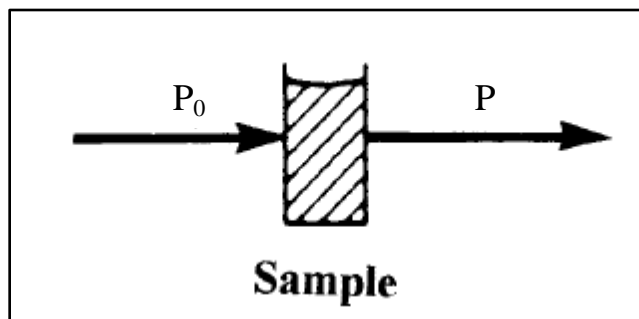


Figure (1-1): Absorption of radiation by a sample

If we perform a similar experiment keeping the path length constant by using only one cell but change the concentration of the absorbing species, we find the same relationship between p , A , and concentration as we found for path length. A linear relationship exists between the absorbance A and the concentration c of the absorbing species in the sample, a very important quantity! Because A is linear with respect to path length b and concentration c we can write the following equation:⁽¹⁾

$$A = abc \quad \dots 1-3$$

The term “a” is proportionality constant called the absorptivity. The absorptivity is a measure of the ability of the absorbing species in the sample to absorb light at the particular wavelength used. Absorptivity is a constant for a given chemical species at a specific wavelength. If the concentration is expressed in molarity (mol/L or M), then the absorptivity is called the molar absorptivity, and is given the symbol ϵ . The usual unit for path length is centimeters, cm, so if the concentration is in molarity, M, the unit for molar absorptivity is $M^{-1} \text{ cm}^{-1}$. Beer discovered the proportional relationship between concentration and absorbance at constant path length in 1852. Equation (1-3), which summarizes the relationship between absorbance, concentration of the species measured, sample path length, and the absorptivity of the species is known as the Beer–Lambert–Bouguer Law or, more commonly, as Beer’s Law.⁽²⁾

1.2. Beer's law Deviations:

Deviations from Beer's law are an evidence when the Beer's law plot is not linear. This is probably most often observed at the higher concentrations of the analyte, as indicated in Fig. (1-2). Such deviations can be either chemical or instrumental. Instrumental deviations occur because it is not possible for an instrument to be accurate at extremely high or extremely low transmittance values—values that are approaching either 0 or 100% T . The normal working range is between 15 and 80%, corresponding to absorbance values between 0.10 and 0.82. It is recommended that standards be prepared to measure in this range and that unknown samples be diluted if necessary.⁽³⁾

Deviations due to chemical interferences occur when a high or low concentration of the analyte causes chemical equilibrium shifts in the solution that directly or indirectly affect its absorbance. It may be necessary in these instances to work in a narrower concentration range than expected. This means that unknown samples may also need to be further diluted, as in the instrumental deviation case.⁽⁴⁾

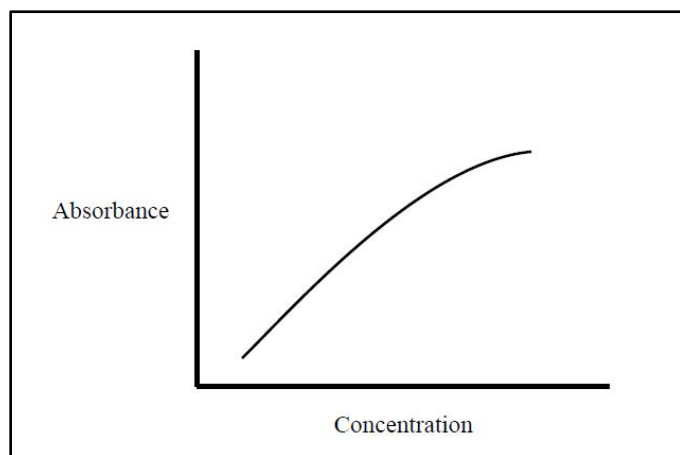


Figure (1-2): Deviation from Beer's law often manifests themselves by a nonlinear portion of the Beer's law plot at the higher concentration.

1.3. UV-Visible spectrophotometry:

The absorption and emission of radiation in the near ultraviolet (UV) and visible region of the spectrum (wavelength range 200–900 nm) are the result of valence electron transitions. In atomic spectra, this can give rise to absorption or emission lines which are characteristic of the element, and thus form the basis of a range of elemental analysis techniques. In molecules, however, the outer energy levels are much more numerous, because the bonds have vibrational, rotational, and stretching energy states associated with them, the energy levels of which are also quantized and can be shown as multiple lines on energy level diagrams. The absorption spectra of molecular species therefore consist of broad bands rather than sharp lines, as is the case with atomic spectra. Nevertheless, the frequency or wavelength of these bands gives important and quantifiable information about the bonds present in the sample.⁽⁵⁾

1.4. UV-VIS Instrumentation:

1.4.1. Sources:

In reality, special light sources are used in order to provide an optimum-quality light beam for the region of the spectrum utilized. An ideal light source is one that emits an intense continuous spectrum of light across an entire region of the spectrum, such as the visible region, while also exhibiting a long life. A light source used frequently for visible light absorption studies is the tungsten filament source.⁽⁶⁾ If an instrument is meant strictly for visible light studies, then this lamp is the only one present in the instrument. Such an instrument is often referred to as a **colorimeter**. A light source used frequently for ultraviolet absorption studies is the deuterium lamp. If an instrument is meant strictly for ultraviolet work, then the deuterium lamp is the only light source present and the instrument is called a **UV**

spectrophotometer. Often, both a tungsten filament lamp and a deuterium lamp are present and are individually selectable. Also, instead of having two independently selectable sources, a light source that can be used for both ultraviolet and visible studies, the xenon arc lamp, may be present. In these latter two cases, the instrument is called a **UV-VIS spectrophotometer.**⁽⁷⁾

1.4.2. Wavelength Selection:

In order to plot the absorption spectrum of a compound or complex ion, we must be able to carefully control the wavelengths from the broad spectrum of wavelengths emitted by the source so that we can measure the absorbance at each wavelength. Additionally, in order to perform quantitative analysis by Beer's law, we need to be able to carefully select the wavelength of maximum absorption, also from this broad spectrum of wavelengths, in order to plot the proper absorbance at each concentration. These facts dictate that we must be able to filter out the unwanted wavelengths and allow only the wavelength of interest to pass.

There are two common types of wavelength selection devices-filters or monochromators. The filters used in spectroscopy are usually based on interference. They are used to monitor light at fixed wavelengths. Monochromators are the best wavelength-selection device known until now. In a classic monochromator, the incoming light is passed through the entrance slit, goes to the grating where it is diffracted, and after that goes to the exit slit, which selects part of the resulting spectrum. The narrower the slits, the better is the spectral resolution and the lower the output intensity.⁽⁶⁾

In the newly developed monochromators, based on diode array, no exit slit is employed. Instead, the spectrum is directed to a linear array of photodetectors. The size of the single detector determines the spectral resolution. These monochromators are significantly cheaper, possess no moving parts and are very

reliable. Additional advantages are simultaneous access to the whole spectrum and integrated optoelectronic conversion. However, their resolution is lower in comparison to their standalone counterparts; furthermore, as they rely on diode arrays, they are mostly used at high light intensities.⁽⁸⁾

1.4.3. Sample Compartment:

Following the wavelength selection by the monochromator, the beam passes on to the sample compartment where the sample solution, held in the cuvette, is positioned in its path. The sample compartment is an enclosure with a lid that can be opened and closed in order to insert and remove the cuvette. When the lid is closed, the compartment should be relatively free of **stray light**.⁽⁶⁾

1.4.3.1. Single-Beam Spectrophotometer:

In a single-beam spectrophotometer, the monochromatic light beam created by the monochromator passes directly through the sample solution held in the cuvette and then proceeds to the detector. This is the most inexpensive design and is especially useful for routine absorbance measurements for which the wavelength of maximum absorbance (the wavelength to be used) is known in advance without having to scan a particular wavelength range to determine it.⁽⁹⁾

1.4.3.2. Double-Beam Designs:

Probably the most popular, and the most advantageous, double-beam design is one in which the light emerging from the monochromator is chopped into two beams that take parallel but separate paths through the sample compartment. In the sample compartment are two cuvette holders, one to hold the blank and one to simultaneously hold the sample being measured. One of the two beams passes through the blank and is called the reference beam. The other passes through the sample and is called the sample beam. The beams are recombined with a second chopper prior to reaching the detector. See Fig. (1-3) The detector is programmed

to the chopping frequency and can differentiate between the two beams. This design allows the instrument's electronics, or computer software, to self-adjust for the blank reading at each wavelength a split second before taking the sample reading. Thus both disadvantages of the single-beam systems (the tedium and the time factor) are done away with while also rapidly scanning the wavelength range of interest (by motor-driven dispersing element rotation) to obtain the molecular absorption spectrum.⁽¹⁰⁾

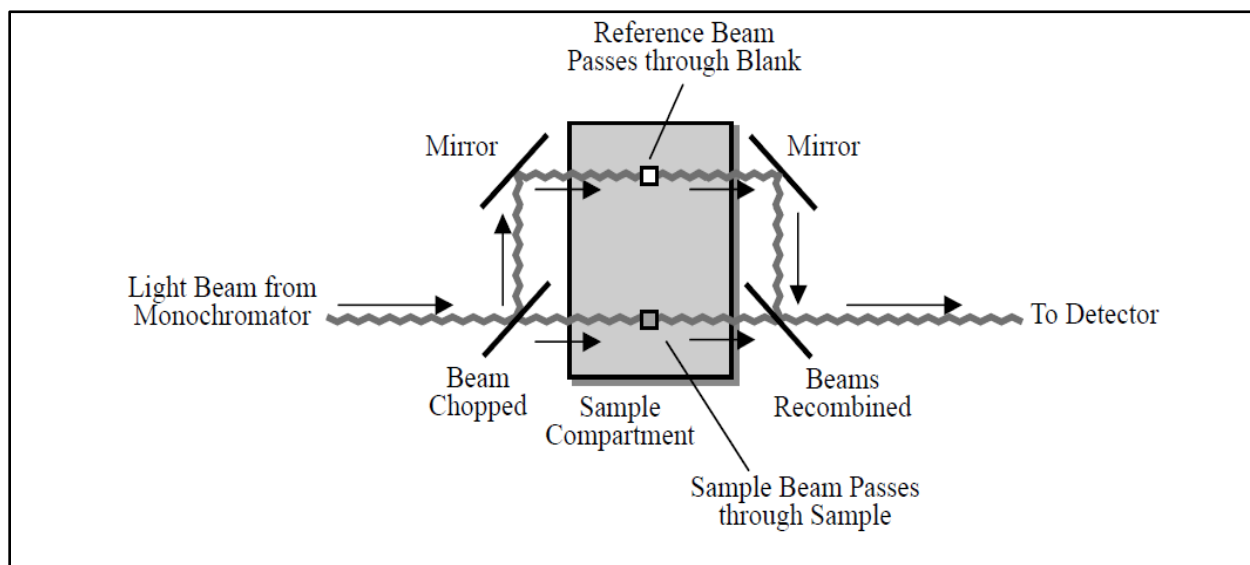


Figure (1-3): An illustration of the double-beam design utilizing two cuvette holders in the sample compartment.

1.4.4. Detectors:

Photomultiplier tubes or photodiodes (light sensors) are used as detectors in UV-VIS spectrophotometers, while thermo couples (heat sensors) are used as detectors for infrared (IR) spectrometry. This is the reason UV-VIS instruments are called spectrophotometers while IR instrument are called spectrometers.^(11,12)

1.5. General Applications of UV/Visible:

Wide applications of UV/Visible spectroscopy include numbers of inorganic metals, organic compounds, and biochemical species absorbed ultraviolet or visible radiation and are thus amenable to direct quantitative determination. Many non-absorbing species can also be determined after chemical conversion to absorbing derivatives. It has been estimated that over 90% of analyses performed in clinical laboratories are based upon UV/Visible spectroscopy.⁽¹³⁾ The typical applications of UV absorption spectroscopy include the determination of poly nuclear aromatic compounds such as steroids, pesticides residue in the sub microgram level, dyestuff material Vitamins, drugs, various applications of visible spectrophotometric methods have been developed for analysis of different colored metal complexes and colored compounds.⁽¹⁴⁾

1.5.1.Applications of UV/Visible for Drags Analyses:

The Spectrophotometric procedures are widely used for pharmaceutical analysis with advantages of determining sample directly, rapidly and simplicity. Table (1-1) shows some applications of UV/Visible in pharmaceuticals.

Table 1-1:-Some applications of UV/Visible for drug analysis.

Pharmaceuticals	Method	Wavelength λ_{\max}	Linear rang	Molar absorptivity (L/mol.cm)	Correlation coefficient	Ref.
Levofloxacin	The method is based on using a solvent composed of water : methanol : acetonitrile (9:0.5:0.5).	292 nm	1.0–12.0 ($\mu\text{g/ml}$)	2.427×10^3	0.9998	15
Ampicillin Trihydrate	Method A based on formation of pink complex by the reaction with ferric chloride and 2, 2 bipyridyl. Method B based on formation of orang complex by the reaction with ferric chloride and 1, 10 phenanthroline.	A= 500 nm B= 523 nm	A= 1-10 B= 1-12 (mcg/ml)	A= 1.624×10^3 B= 3.090×10^3	A= 0.9990 B= 0.9997	16
Amoxicillin	The drug produce a bluish-green colored soluble charge-transfer complex with metol in the presence of potassium persulphate in alkaline medium	620 nm	5-60 ($\mu\text{g/ml}$)	2.726×10^3	0.9994	17
Sildenafil	The method is based on the formation of ion-association complex of sildenafil citrate (SC) with metacresol purple (MCP) in acidic buffer solution.	410 nm	3-70 (mg/L)	7.86×10^3	0.9993	18
Adrenaline	The method is based on the reaction of adrenaline with vanadium (V) in acidic solution.	488 nm	0.5–140 ($\mu\text{g/ml}$)	2.015×10^3	0.9992	19
Paracetamol	The method is based on the reaction with iron(III) sulfate. The produced iron(II) reacts with potassium hexacyanoferrate (III) forming Prussian blue colored product	710 nm	0.1 – 7.0 ($\mu\text{g/ml}$)	3.477×10^4	0.9969	20
Ascorbic acid	The method is based on the formation of colored azo dye by diazotization of 2, 4-dichloroaniline followed by azo-coupling reaction between the resulting product and ascorbic acid.	535 nm	2 – 70 ($\mu\text{g/ml}$)	2.315×10^3	0.9998	21
Metformin	The method is based on the oxidation of metformin by a known excess of sodium hypochlorite in alkaline medium.	385 nm	0.5 – 4.0 ($\mu\text{g/ml}$)	2.0×10^4	0.9999	22
Sumatriptan Succinate	Two methods were developed using different solvents, 0.1 M HCl (method A) and acetonitrile (method B).	A= 226 nm B= 228 nm	0.2–6.0 ($\mu\text{g/ml}$)	A= 7.59×10^4 B= 7.81×10^4	0.9999	23

1.6. Derivative Spectrophotometric Analysis:

The derivative method using UV/Visible and IR Spectrophotometry was introduced in 1953⁽²⁴⁾. The rapid progress in the technology of microcomputers has made it possible to directly present the first, second and higher order derivative spectra. The great interest towards derivative spectrophotometry (DS) is due to the increased resolution of spectral bands, reducing the effect of spectral background interferences⁽²⁵⁾. For these reasons, the qualitative and quantitative DS procedures applied in the analysis of complex systems is completely avoided. General analytical applications of UV/Visible DS have been reviewed for the period till 2005^(26,27). Other review of the application of DS for determination of the equilibrium constants is reported⁽²⁸⁾.

1.6.1. Basic Characteristics of Derivative Spectrophotometry

1.6.1.1. Derivative Spectrophotometry (DS), Derivation:

The Principle of operation of this technique is based on the measurement of the changes in intensity or absorbance, manually or automatically by certain instrument. The approach is based on the idea that the wavelength scan rate, $(d\lambda/dt)$ is constant, then the derivative of the intensity with respect to the wavelength, $(dI/d\lambda)$ is proportional to the derivative of the intensity with respect to the time, (dI/dt) , which is measured by means of its electronic differentiation⁽²⁵⁾:

$$(dI/d\lambda) = (dI/dt)/(d\lambda/dt) \quad \dots 1-4$$

1.6.1.2. Increase of Spectra Resolution:

The DS that enhanced the resolution of overlapping spectral bands is the consequence of differentiation which discriminates against broad bands in favor of a sharp peak to an extent which increases parallel to derivative order. This property depends on the band width for two simple band shapes, and in practical spectroscopy; the amplitude in the n-th derivative order (nD) is inversely related to the n-th power of the band width (W) of the original spectrum:

$$({}^nD) = 1/(W)^n \quad \dots 1-5$$

Thus, two bands (X and Y) are of the same intensity, but of different width, the derivative amplitude of the sharper band (X) is greater than that of the broader one (Y) by factor that increases with increasing derivative order:

$${}^nD(X)/{}^nD(Y) = (W_Y/W_X)^n \quad \dots 1-6$$

The relative increase of the amplitude of sharper band compared to that of the broader one in higher derivatives represents the most important factor responsible for the increase of sensitivity and selectivity in DS. Fig. (1-4) show the effect of derivative order (zeroth, second and fourth) on the relative amplitude of the two bands. ⁽²⁵⁾

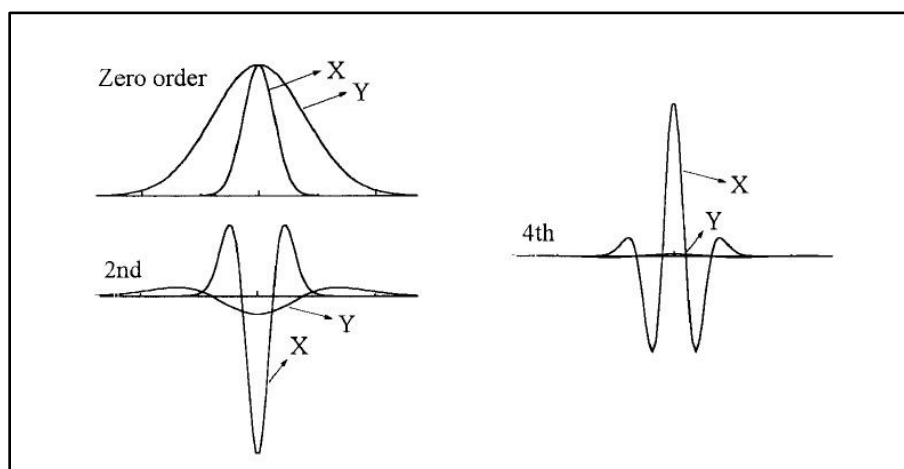


Figure (1-4): The effects of derivative order (zeroth, second and fourth) on the relative amplitude of two bands (X and Y) are of the same intensity, but with band width ratio 1:3.

1.6.1.3. Elimination of the Influence of Baseline Shift and Matrix Interferences:

The great blank absorbance and matrix interferences are caused by absorption of scattering by turbid solution and suspensions. All these can be overcome by derivatisation. The order of derivatisation depends on the order of the polynomial function used to describe interferences ⁽²⁵⁾. In general, if n represents the highest degree of the polynomial equation used to define interference, then interference is reduced to a constant using the nth order derivative and is completely eliminated in the nth derivative:

$$P = a_0 + a_1\lambda + a_2\lambda^2 + \dots a_n\lambda^n \quad \dots 1-7$$

$$d^n p / d \lambda^n = n_j a_n \quad \dots 1-8$$

$$(d^{(n+1)} p) / (d \lambda^{(n+1)}) = 0 \quad \dots 1-9$$

In many cases matrix interference can be approximated by linear function ($p = a\lambda + b$). The first derivative yields a function where the interference is reduced to a constant ($dp/d\lambda = a$) and the second order derivative transformation the interference is completely eliminated ($d^2p/d^2\lambda = 0$).⁽²⁹⁾

1.6.1.4. Enhancement of the Detectability of Minor Spectral Features:

Derivatisation of broad spectra increases both possibility of detection and measurement of minor spectral features and discrimination against interference. Derivative transformation of broad spectra does not increase the number of intrinsic data, but visually enhances the subtle changes in them. A great number of theoretical and practical investigations have been developed in this regard ⁽³⁰⁻³²⁾.

1.6.1.5. Precise Determination of the Positions of Absorption Maxima:

When a single peak spectrum has a broad band as its main feature, the position of absorption maximum can be only approximately determined. The first derivative of this band ($dA/d\lambda$) passes through zero at the peak maximum, minimum and shoulder points Fig.1-4 and can be used to accurately locate the peak position. In contrast, the second and even higher derivatives ($d^2A/d\lambda^2$, $d^4A/d\lambda^4$...etc.) contain a peak of changeable sign (negative in second order, positive in the fourth order...etc.) which has the same position as a peak maximum in the normal spectrum. The width of this peak progressively decreases with increasing order of the even derivative, which causes a sharpening of the peak enabling its exact identification. In the higher derivatives order ($n \geq 6$) the satellites of adjacent bands may interfere, thus limiting the observed resolution, also the peaks of certain components might be shifted, compared to their original position⁽³³⁾.

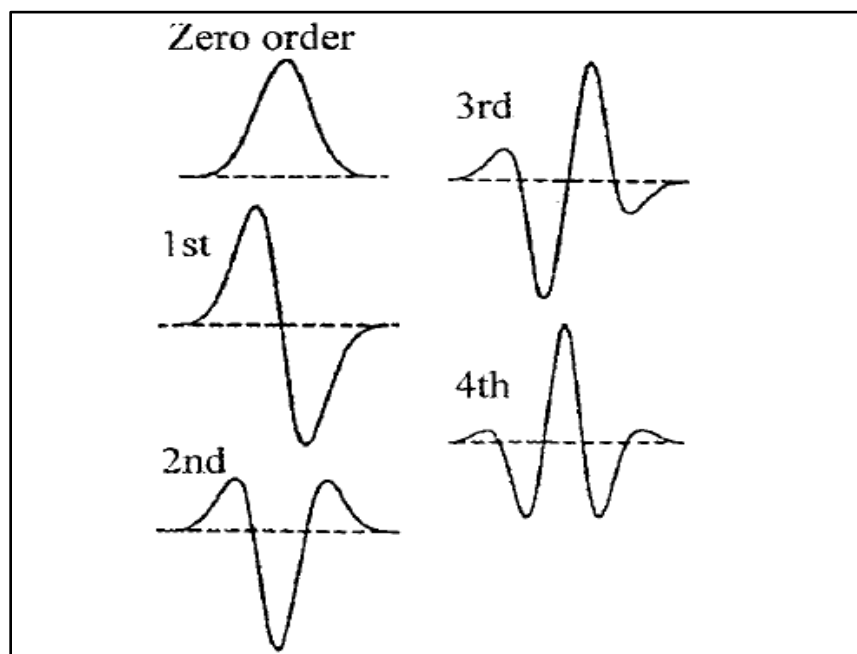


Figure (1-5): The characteristic profiles of derivative orders of a Gaussian band.

1.6.1.6. Signal to Noise Ratio (SNR):

The main disadvantage of the derivative technique is the SNR becomes worse as the order of the derivative increases. A detailed study on the effect of derivatisation on the SNR, and has been described by O'Haver. The practical derivative technique includes some degree of smoothing to control the increasing in the noise. The selection of the optimum smoothing ratio depends on the purpose for the application of derivative technique, when it is used to remove or reduce a broad-band back ground; significantly larger smoothing ratio may be employed ⁽³⁴⁾.

1.6.2. Quantitative Analysis:

The application of DS for quantitative analysis is based on the same requirement as normal spectrophotometry, i.e., the validity of Beer's law and the additivity of absorbance for the derivative spectra of the n-th order at wavelength λ , these laws can be represented by the following equation: ⁽³³⁾

$${}^nD = d^n A / d\lambda^n = (d^n / d\lambda^n) \epsilon c b \quad \dots \text{1-10}$$

$${}^nD(T) = {}^nD(X) + {}^nD(Y) + \dots \quad \dots \text{1-11}$$

Where A is the absorbance, ϵ is the molar absorptivity, c is the concentration, b, is the band length and ${}^nD(T)$ the total derivative amplitude, which is equal to the algebraic sum of each absorbing component X, Y, etc. The most important methods used for the construction of a calibration curve are: peak-peak, peak-baseline, peak-tangent and zero-crossing technique, which allow quantization of one chromophore X overlapped by the absorption band of another Y ⁽³²⁾.

1.7. Application of Derivative Spectrophotometry (DS):

Derivative Spectrophotometry (DS) is widely applied in inorganic and organic analysis, toxicology, and clinical analysis, analysis of pharmaceutical products, amino acids and proteins, in analysis of food and in environmental chemistry. In general, the application of DS is not limited to any particular case or field, but it can be used whenever quantitative or qualitative investigations of broad spectra are difficult. Table (1-2) shows some applications of derivative Spectrophotometry.

Table 1-2:-Some applications of Derivative spectrophotometry for determination of some mixtures.

Compounds	Method	Wavelength λ_{\max}	Linear rang ($\mu\text{g/mL}$)	Correlation coefficient	Ref .
Amiloride hydrochloride	¹ D	P= 340.0 nm	2-40	0.9997	35
	¹ D	V= 382.0 nm		0.9998	
hydrochlorothiazide	¹ D	V= 285.0 nm	2-40	0.9996	
	² D	V= 239.0 nm		0.9995	
Cephalexin monohydrate	¹ D	P= 264.0 nm	8-80	0.9999	36
	² D	V= 263.8 nm			
Amoxicillin	¹ D	V= 238.2 nm	10-50	0.9999	
	² D	V= 250.5 nm	5-50		
Salbutamol sulfate	¹ D	P= 257.0 nm	5-45	0.9998	37
Ketotifen fumarate	¹ D	P= 278.0 nm	5-35	0.9998	
Paracetamol	¹ D	V= 249.3 nm	20-40	0.9970	38
	¹ D ratio	P= 274.8 nm		0.9986	
Ibuprofen	¹ D	V= 242.0 nm	12-32	0.9996	
	¹ D ratio	V= 230.4 nm		0.9977	

Compounds	Method	Wavelength λ_{\max}	Linear rang ($\mu\text{g/mL}$)	Correlation coefficient	Ref .
Ofloxacin	¹ D ¹ D ratio	V= 303.6 nm V= 290.0 nm	0.5-30 0.5-25	0.9990	39
Flavoxate hydrochloride	¹ D ¹ D ratio	P= 329.3 nm V= 254.0 nm	0.5-70 0.5-30	0.9990	
Amoxicillin	¹ D ² D	V= 283.5 nm P= 229.0 nm	2-100 2-90	0.9993 0.9995	40
Potassium clavulanate	¹ D ² D	V= 229.0 nm V= 239.5 nm	10-80 10-90	0.9995 0.9999	
Promethazine hydrochloride	¹ D ² D	V= 216.5 nm P= 258.8 nm	2-30	0.9997 0.9996	41
Paracetamol	¹ D ¹ D	V= 274.07 nm P= 299.20 nm	2-30	0.9994 0.9996	
Cobalt (II)	¹ D	P= 492.8 nm V= 519.8 nm	0.10-2.50	0.9947 0.9976	42
Iron (III)	¹ D	V= 500.3 nm	0.50-6.00	0.9978	
Cobalt (II)	¹ D	V= 549.0 nm	0.293- 4.124	0.9994	43
Nickel (II)	¹ D	P= 546.0 nm	0.291- 4.676	0.9994	
Copper	³ D	P= 472.0 nm	1-30	0.9999	44
Nickel	³ D	P= 501.0 nm	1-30	0.9998	
Amiloride Hydrochloride	¹ D ² D ratio	P= 285.0 nm V= 311.0 nm	1-15	0.9999	45
Hydrochlorothiazide	³ D ² D ratio	V= 265.0 nm P= 290.0 nm	2-25	0.9999	
Timolol Maleate	¹ D ¹ D ratio	V= 315.4 nm V= 314.8 nm	3-20 1-20	0.9999	

1.8. Sulphamethoxazole and Trimethoprim:⁽⁴⁶⁾

1.8.1. Sulphamethoxazole:

Sulphamethoxazole (SMX), 4-Amino-N-(5-methylisoxazol-3-yl) benzene sulphon-amide, which has the empirical formula ($C_{10}H_{11}N_3O_3S$), as shown in Fig. (1-6), is white, or almost white crystalline powder with molecular weight 253.3 g/mole, practically insoluble in water, freely soluble in acetone, sparingly soluble in alcohol, slightly soluble in ether. It dissolves in dilute solutions of sodium hydroxide.

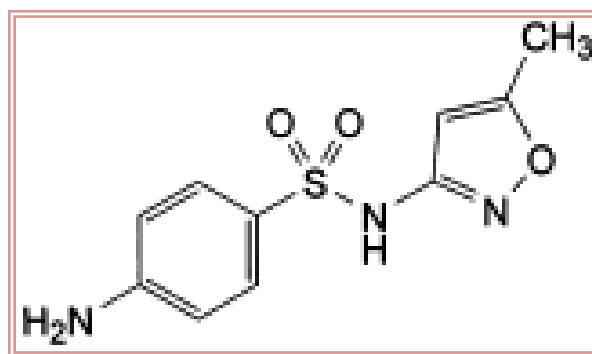


Figure 1-6: Structure formula of sulphamethoxazole.

1.8.2. Trimethoprim:

Trimethoprim (TMP), 5-(3,4,5-Trimethoxy benzyl)pyrimidine-2,4-diamine, which has the empirical formula ($C_{14}H_{18}N_4O_3$), as shown in Fig. (1-7), is white, or yellowish-white powder with molecular weight 290.32 g/mole, very slightly soluble in water and slightly soluble in alcohol. It dissolves in dilute solutions of sodium hydroxide.

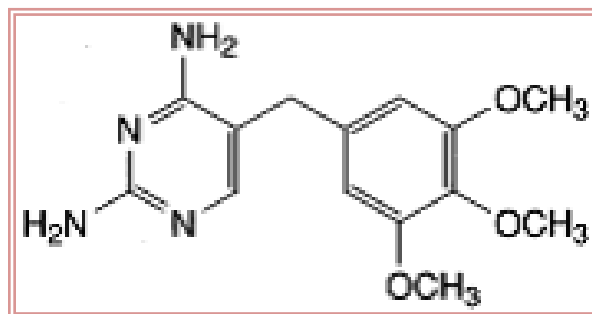


Figure 1-7: Structure formula of trimethoprim.

1.8.3. Sulphamethoxazole and Trimethoprim mixture:

The combination of (SMX) and (TMP) are used for the treatment of infections caused by susceptible bacterial organisms, follows the practical application of the principle that if two drugs act on sequential steps in the pathway of an obligate enzymatic reaction in bacteria, the result of their combination will be supra-additive.⁽⁴⁷⁾ The optimal ratio of the two agents for their synergistic activity has been found to be 5:1.⁽⁴⁸⁾

1.8.4. Analysis of Sulphamethoxazole and Trimethoprim:

Various methods have been reported for the simultaneous determination of the combination of SMX and TMP in pharmaceutical formulations and biological fluids, Table (1-3) shows some of these methods.

Table 1-3: Some methods for the analyses of Sulphamethoxazole and Trimethoprim.

Method	Reagents used	Linear rang (µg/mL)	Ref.
Spectrophotometry	The method depends on ¹ D zero-crossing for TMP at 237.6nm and for SMX at 259nm.	4-20 for TMP 4-25 for SMX	49
	Based on multivariate calibrations PLS and PCR with optimum number of factors was selected by using the cross-validation method.	0.4-6 for TMP 2-15 for SMX	50
	Based on a direct determination of SMX after diazotization and coupling with 2-naphthol by visible spectrophotometry and an indirect determination of TMP in the UV region by difference was developed.	20-65 for TMP 40-130 for SMX	51
High Performance Liquid Chromatography (HPLC)	Primidone was used as internal standard. Chromatography was performed on a C18 column (250 mm × 4.6 mm, 5 µm) under isocratic elution with 50 mM aqueous sodium dihydrogen phosphate–acetonitrile–triethylamine (100:25:0.5, v/v), pH 5.9. Detection was made at 240 nm	0.125-2 for TMP 0.39-50 for SMX	52
	Using antipyrine as the internal standard. Separation of the compounds was achieved on a reverse-phase C8 column packed with 5 microm dimethyl octadecylsilyl bonded amorphous silica (4.6 mm x 250 mm) column using a mobile phase consisted of potassium hydrogen phosphate, acetonitrile, methanol and water adjusted to pH 6.2.	LOQ =10 ng/mL for TMP and 50 ng/mL for SMX	53

Method	Reagents used	Linear rang ($\mu\text{g/mL}$)	Ref.
Electrophoresis	A rapid method for simultaneous determination of these compounds using CE with capacitively coupled contactless conductivity detection.	3.6-58 for TMP 3.1-50 for SMX	54
Electrochemically	Based on hydrogen- (HT) and oxygen-terminated (OT) boron-doped diamond (BDD) electrodes, the HT-BDD electrode presented two well-defined oxidation peaks at 920 and 1100 mV vs. Ag/AgCl for sulfamethoxazole and trimethoprim, respectively	LOD = 3.92 $\mu\text{g/mL}$ for TMP and 3.65 $\mu\text{g/mL}$ for SMX	55

1.9. Paracetamol and Caffeine:⁽⁴⁶⁾

1.9.1. Paracetamol:

Paracetamol (PAR), N-(4-Hydroxyphenyl) acetamide, which has the empirical formula ($\text{C}_8\text{H}_9\text{NO}_2$), as shown in Fig. (1-8), is white, or almost white crystalline powder with molecular weight 151.2 g/mole, Sparingly soluble in water, freely soluble in alcohol, very slightly soluble in methylene chloride.

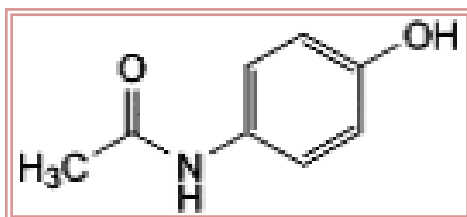


Figure 1-8: Structure formula of paracetamol.

1.9.2. Caffeine:

Caffeine (CAF), 1,3,7-Trimethyl-3,7-dihydro-1H-purine-2,6-dione, which has the empirical formula ($\text{C}_8\text{H}_{10}\text{N}_4\text{O}_3$), as shown in Fig. (1-9), is white, or almost white, crystalline powder or silky with molecular weight 194.2 g/mole, Sparingly soluble in water, freely soluble in boiling water, slightly soluble in ethanol (96 %). It dissolves in concentrated solutions of alkali benzoates or salicylates.

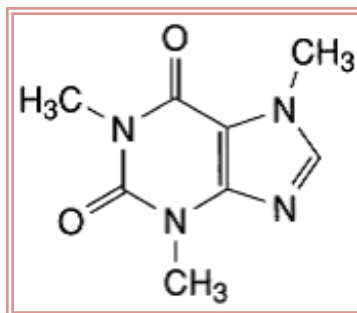


Figure 1-9: Structure formula of caffeine.

1.9.3. Paracetamol and Caffeine mixture:

The use of the mixture of paracetamol and caffeine as an analgesic and antipyretic is well established in pharmaceutical formulation.⁽⁵⁶⁾ The antipyretic, analgesic and anti-inflammatory effect of paracetamol is due to inhibiting prostaglandin synthesis cyclooxygenase-1(COX-1) and cyclooxygenase-2 (COX-2).^(57, 58) Caffeine is used as a stimulant, due to acts on the central nervous system.⁽⁵⁹⁾ It used in migraine attack, child birth and avoid postpartum hemorrhage.⁽⁵⁶⁾

1.9.4. Analysis of Paracetamol and Caffeine:

Various methods have been reported for the simultaneous determination of the combination of PAR and CAF in pharmaceutical formulations and biological fluids, Table (1-4) shows some of these methods.

Table 1-4: Some methods for the analyses of Paracetamol and Caffeine.

Method	Reagents used	Linear rang (µg/mL)	Ref.
Spectrophotometry	Method A involved simultaneous equation method. The two wavelengths 243 nm (λ_{\max} of Paracetamol) and 273 nm (λ_{\max} of Caffeine). Method B involved formation of Q-absorbance equation at isobestic point (259.5 nm).	2-16 for PAR 2-32 for CAF	60
	This method is based on difference in the rate of oxidation of the compounds with Cu(II)-neocuproine system and formation of Cu(II)-neocuproine complex, which is monitored at 453 nm and at pH 5.0 in the presence of dodecyl sulfate.	1.5-7.0 for PAR 0.1-3.0 for CAF	61
High Performance Liquid Chromatography (HPLC)	The separation was achieved on a C ₁₈ column at a flow rate of 1.5 ml/min with UV detection at 220 nm. The mobile phase was composed of 1mM phosphate buffer pH3.0–acetonitrile (85:15 v/v) containing 0.2 % triethylamine (v/v).	31.25-250 for PAR 4.06-32.50 for CAF	62
	This method was carried out on C ₁₈ column with mobile phase methanol and water in the ratio of 40:60 (by volume) at the flow rate 1.0 mL/minute. The detection was carried out at λ_{\max} =243 nm	10-100 for PAR 10-100 for CAF	63
	Using an inertsil ODS C ₁₈ column with 0.05M dibasic phosphate buffer: acetonitrile (93: 07; v/v) as the mobile phase. The flow rate of the mobile phase was adjusted to 1.5 ml/min and the column oven temperature was kept at 30 °C.	400-600 for PAR 24-36 for CAF	64
	Using a µ-Bondapak C8 column by isocratic elution with a flow rate of 1.0 ml/min. The mobile phase composition was 0.01 M KH ₂ PO ₄ -methanol-acetonitrile-isopropyl alcohol (420: 20: 30: 30) (v/v/v/v) and spectrophotometric detection was carried out at 215 nm.	0.409-400 for PAR 0.151-200 for CAF	65
Electro-chemically	Using differential pulse voltammetry (DPV) with the cathodically pre-treated boron-doped diamond (BDD) electrode, a separation of about 550 mV between the peak oxidation potentials of paracetamol and caffeine present in binary mixtures.	7.56×10^{-2} -12.54 for PAR 9.71×10^{-2} -16.11 for CAF	66

1.10. Paracetamol and Hyoscine⁽⁴⁶⁾

1.10.1. Hyoscine Butylbromide:

Hyoscine Butylbromide (HYO), (1R,2R,4S,5S,7s,9r)-9-Butyl-7-[[[(2S)-3-hydroxy-2-phenylpropanoyl]oxy]-9-methyl-3-oxa-9-azoniatricyclo [3.3.1.0^{2,4}] nonane bromide, which has the empirical formula (C₂₁H₃₀BrNO₄), as shown in Fig. (1-10), is white, or almost white crystalline powder with molecular weight 440.4 g/mole, Freely soluble in water and in methylene chloride, sparingly soluble in anhydrous ethanol.

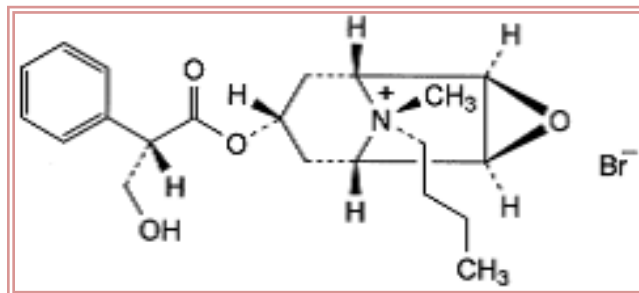


Figure 1-10: Structure formula of hyoscine.

1.10.2. Paracetamol and Hyoscine mixture:

The combination of (PAR) and (HYO) are used for the relief of smooth muscle spasm (cramps) of the gastrointestinal and genitourinary system, it is effective in the treatment of recurrent crampy abdominal pain.⁽⁶⁷⁾

1.10.3. Analysis of Paracetamol and Hyoscine:

Various methods have been reported for the simultaneous determination of the combination of PAR and HYO in pharmaceutical formulations and biological fluids, Table (1-5) shows some of these methods.

Table 1-5: Some methods for the analyses of Paracetamol and Hyoscine.

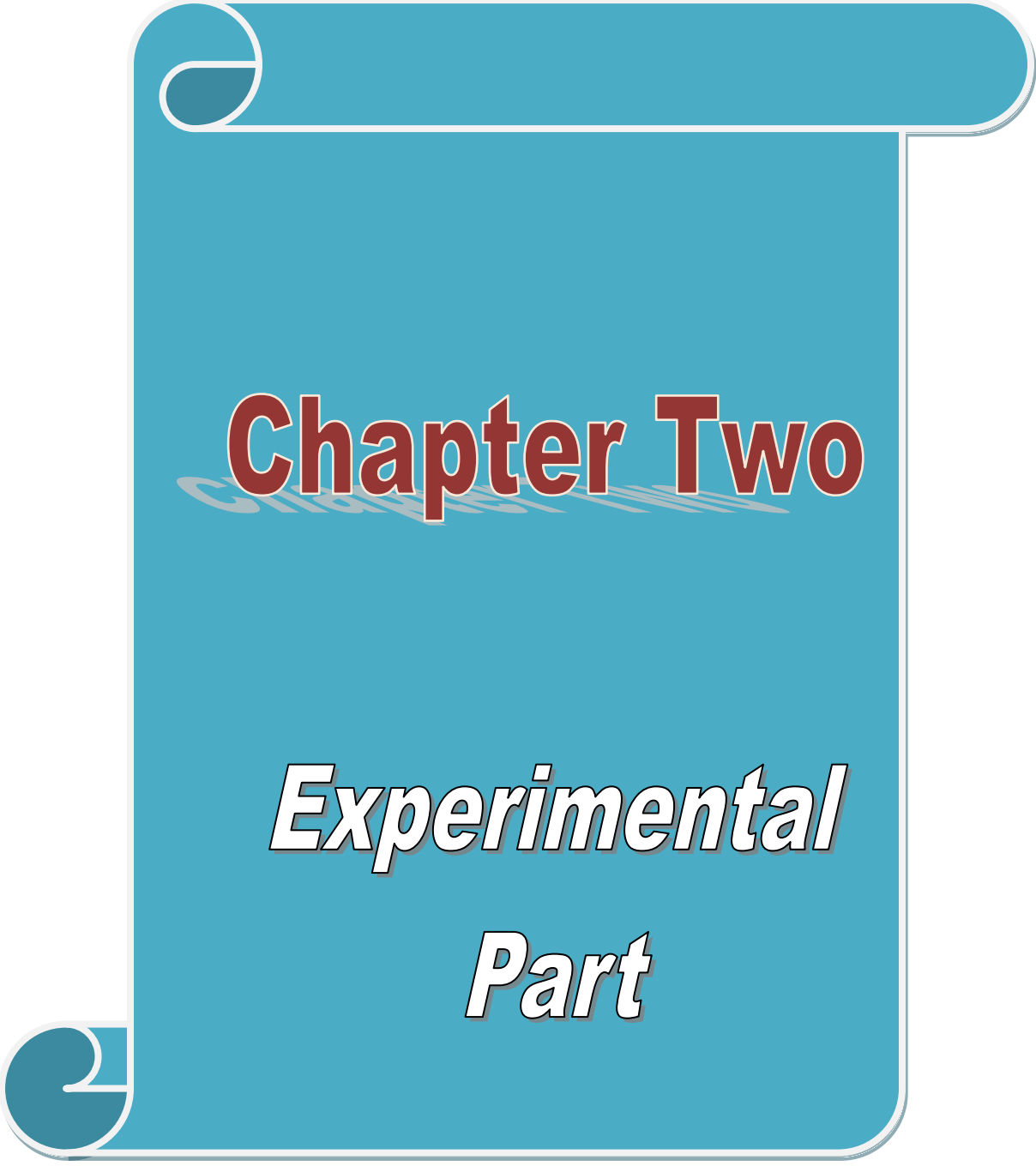
Method	Reagents used	Linear rang (µg/mL)	Ref.
Spectrophotometry	By precipitating hyoscine N-butyl bromide with ammonium reineckate at pH 6,0 selectively and reading the absorbance of the solution of the precipitate in acetone at 525.0 nm for hyoscine N-butyl bromide by measuring the dA/dλ values at 254.5 nm in the first derivative spectra of the remaining solution for paracetamol.	RSD= 0.10 % RC= 99.8 % for PAR RSD= 0.90 % RC= 98.3 % for CAF	68
High Performance Liquid Chromatography (HPLC)	In this method, HBB and PAR were separated on RP-18 W/ UV ₂₅₄ TLC plates using developing mobile phase consisting of methanol: citrate buffer (pH=1.5):tri-fluoroacetic acid (70:30:0.1, by volume) at room temperature.	2-14 for PAR 2-12 for HYO	69
	The separation was performed on a BDS C-18 column. The mobile phase consisted of a mixture of acetonitrile: ammonium acetate 0.2M, (30:70, v/v) pumped at a flow rate 1.2 mL/min. The UV detector was operated at 254 nm.	LOD = 0.67 µg/mL for PAR and 1.05 µg/mL for HYO	70
	Using C ₁₈ (25 cm×4.6 mm i.d. 5 µm particle size) column as a stationary phase and water: methanol (50:50, v/v pH adjusted to 3.9 with CF ₃ COOH acid) as a mobile phase, maintaining the flow rate at 1.0 mL min ⁻¹ with UV detection at 210 nm.	5-200 for PAR 2-50 for HYO	71

1.11. Aim of the work:

The aim of this project is to determine of each drug by used UV spectrophotometry to developed based on derivative spectra methods for the determination of sulfamethaxazole , trimethoprim, paracetamol ,hyoscine-n-butyl bromid and caffeine drugs and binary mixtures of sulfamethaxazole with trimethoprim, paracetamol with hyoscine-n-butyl bromid and paracetamol with caffeine then the pharmaceutical sample were studied in this work.

1.12. Future Work:

1. Analyzing and determination of other types of drugs and antibiotic.
2. Analyzing and determination of other types of binary mixtures for drugs and antibiotic.
3. Analyzing and determination of other types of tertiary mixtures for drugs and antibiotic.
4. Study the interferences of metals with drugs.
5. Apply in derivative ratio spectra method for resolution of binary and ternary mixtures.
6. Apply in double divisor-ratio spectra derivative method for resolution of binary and ternary mixtures.
7. Apply in H-point standard methods (HPSAM) which is one of the mathematical treatment data procedures utilized for analysis of multi-component system.



Chapter Two

Experimental

Part

Experimental part

2.1. Instruments and Equipment:

1. Double-beam UV-Visible spectrophotometer model (UV-1650 PC) SHIMADZO (Japan), interfaced with computer via a SHIMADZU UV probe data system program (Version 1.10), using 1.00 cm quartz cells.
2. Sartorius Handy 4digits Analytical Balance (GMBH, H110, Germany).
3. Micropipettes (200-1000 μ l) Swiss made.

2.2. Chemicals:

1. Sodium hydroxide obtained from (BDH).
2. Standard antibiotic drugs: sulphamethoxazole (SMX) ($C_{10}H_{11}N_3O_3S$; F.W. 253.3) , trimethoprim(TMP) ($C_{14}H_{18}N_4O_3$; F.W. 290.3), paracetamol (PAR) ($C_8H_9NO_2$; F.W. 251.2), caffeine(CAF) ($C_8H_{10}N_4O_2$; F.W. 194.2) and hyocscine-n-butyl bromide (HYO) ($C_{21}H_{30}BrNO_4$; F.W. 440.4) were purchased from the State Company of Drug Industries and Medical Appliances (IRAQ-SDI- Samara). All drugs were used as working standards without further purification.
3. Pharmaceuticals drugs:
 - 3.1. Co-trimoxazole tablet
 - 3.1.1. (TRIMOL-400SMX, 80TMP mg) made by Julphar pharmaceutical limited company (U.A.E).
 - 3.1.2. (METHOPRIM-400SMX,80TMP mg) made by the State Company of Drug Industries and Medical Appliances IRAQ-SDI- Samara.

- 3.2. Panadol extra tablet (PANADOL EXTRA-500PAR, 65CAF mg) made by Glaxosmithkline Dungarvan pharmaceutical limited company (Ireland).
- 3.3. Spazmotek plus tablet (SPAZMOTEK PLUS-500PAR,10HYO mg) made by Bilim pharmaceutical limited Company (Turkey).
4. Interferences material (Starch, Gelatin, Magnesium setrate, Avecil, Sucrose, and Titanium dioxide) obtained from (BDH).

2.3. Preparation of Solutions:

1. (0.1M) Sodium hydroxide was prepared by dissolving (4.00g) of sodium hydroxide in (1L) distilled water.
2. Stock solutions of (250 mg/L) standard for (SMX) and (TMP) were prepared by dissolving (0.0250 g) in sodium hydroxide solution (0.1M) and diluted to 100 ml volumetric flask with the same solution. Series of pure single drug standards (2, 4, 6, 8, 10, 15, 20, 25 and 30 mg/L) for (SMX) and (TMP) were prepared by diluting stock solutions with (0.1 M) sodium hydroxide solution.
3. Stock solutions of (250 mg/L) standard for (PAR) , (CAF) and (HYO) were prepared by dissolving (0.025g) in distilled water and diluted to 100 ml volumetric flask with the same solution, Series of pure single drug standards (2, 4, 6, 8, 10, 15, 20, 25 and 30 mg/L)for (PAR), (CAF) and (HYO) were prepared by diluting Stock solutions with distilled water.
4. Two series of binary mixtures for standard drugs (SMX) and (TMP) solutions were prepared.

First series of mixture solutions were prepared by using a constant concentration of (20 mg/L) for (SMX) with different concentrations (2, 4, 6, 8, 10, 15, 20, and 25 mg/L) of (TMP), while the second series of mixture contains

a fixed concentration (4 mg/L) of (TMP) with different concentration of (2, 4, 6, 8, 10, 15, 20, and 25mg/L) of (SMX).

5. Solutions for binary mixtures of standard drugs (PAR) and (CAF) solutions were prepared by two series.

First series of mixture solutions were prepared by using a constant concentration of (20 mg/L) for(PAR) with different concentrations (2, 4, 6, 8, 10, 15, 20, and 25 mg/L) of (CAF),while the second series of mixture contains a constant concentration (3 mg/L) of (CAF) with different concentration of (2, 4, 6, 8, 10, 15, 20, and 25mg/L) of (PAR).

6. Solutions for binary mixtures of standard drugs (PAR) and (HYO) solutions were prepared by two series.

First series of mixture solutions were prepared by using a constant concentration of (25 mg/L) for(PAR) with different concentrations (0.5, 1, 2, 4, 6, 8, 10, 15, 20, and 25 mg/L) of (HYO),while the second series of mixture contains a constant concentration (0.5 mg/L) of (HYO) with different concentration of (2, 4, 6, 8, 10, 15, 20, and 25mg/L) of (PAR).

7. Stock solutions (250 mg/L) for study the interferences were prepared by dissolving (0.0125 g) of each interfere substances (starch, gelatin, magnesium setrate, avecil and sucrose) in 50 mL of 0.1 M NaOH solution. Serial standard solutions of interfered substances were prepared by dilution of stock solutions (250 mg/L) with 0.1 M NaOH solution. Serial standard solutions of(Titanium dioxide) interfered substances were prepared by dilution of stock solutions (250 mg/L) with distilled water.

2.4. Preparation of pharmaceuticals samples:

1. 10 tablets of each pharmaceutical preparation Co-Trimoxazole (MITHOPRIM-400SMX, 80TMP and TRIMOL) were accurately weighted and found to be (0.0519 g) and (0.0647 g) respectively, then grind to a fine powder, Then (0.0685 g) of these powders were dissolved in 100 mL of (0.1 M) sodium hydroxide then filtrated, the clear solution were taken and filed up to 100 mL. The resultant solutions may be contained 400 mg/L (SMX) and 80 mg/L (TMP). Other working solutions were prepared by dilution with (0.1M) NaOH.
2. 10 tablets of the pharmaceutical preparation Paracetamol-Caffeine (PANADOL EXTRA-500PAR,65CAF) was accurately weighted and found to be (6.8589 g), then grind to a fine powder, Then (0.0685 g) of this powder was dissolved in 100 mL distilled water then filtrated, the clear solution were taken and filed up to 100 mL. The resultant solution may be contained 500 mg/L (PAR) and 65 mg/L (CAF). Other working solutions were prepared by dilution with distilled water.
3. 10 tablets of the pharmaceutical preparation Hyoscine-n-butylbromide-Paracetamol (SPAZMOTЕК PLUS-500PAR,10HYO) was accurately weighted and found to be (6.8345 g),then grind to a fine powder, Then (0.0683 g) of this powder was dissolved in 100 mL distilled water then filtrated, the clear solution were taken and filed up to 100 mL. The resultant solution may be contained 500 mg/L (PAR) and 10 mg/L (HYO), Other working solutions were prepared by dilution with distilled water.
4. Standard addition method for the pharmaceutical Hyoscine-n-butylbromide-Paracetamol (SPAZMOTЕК PLUS-500PAR,10HYO) solutions were

prepared by taken fixed volume (5ml) from (0.5) mg/L HYO from pharmaceutical sample to 7 volumetric flask with different concentration (0,1, 5, 8, 10, 12 and 15 mg/L)of standard Hyoscine-n-butylbromide in 10ml volumetric flask.

2.5. UV- Measurement:

The absorption spectra of the sulfamethaxazole and trimethoprim, were measured from 400 to 200 nm against (0.1 M) sodium hydroxide while paracetamol, caffeine and hyoscine-n-butyl bromid were measured from 400 to 200 nm against distilled water as blank. The wavelength at absorption maxima (λ_{max}) were identified. Calibration curves were constructed for these drugs at their respective (λ_{max}).The derivative spectra 1D , 2D , 3D and 4D have been derived from their normal spectra for each drug by the computer via a SHIMADZU UV probe data system program and the parameters S and $\Delta\lambda$ were optimized. The suitable wavelengths peak (P) and valley (V) at (λ_{max}) were identified for standard drug.

Calibration curves of each derivative were constructed and the best was of them used to determine the concentrations of each drug. Derivative spectra 1D , 2D , 3D and 4D have been derived from normal spectrum (zero order) for binary drug mixture of SMX with TMP, PAR with CAF, and PAR with HYO. Calibration curves of suitable derivative and at suitable wavelength were constructed for these standard drugs, which were used to determine the concentration of each drug present in the mixtures.

2.6. Interference Effect using UV Measurements:

The effect of some interfering species on the determination of the sulfamethoxazole with trimethoprim, paracetamol with hyoscin-n-butyl bromid and paracetamol with caffeine were studied using normal UV spectrophotometry

and derivative spectrophotometry. The solution of each of interferers species was prepared (starch, gelatin, magnesium setrate, avecil, sucrose and Titanium dioxide),ten time greater than the concentration for each drug.

2.7. *Sample Analyses:*

Different concentrations for binary synthetic samples of sulfamethoxazole with trimethoprim, paracetamol with caffeine and paracetamol with hyoscin-n-butyl bromid and a pharmaceutical drug (TRIMOL-400), (METHOPRIM-400),(PANADOL EXTRA-500) and (SPAZMOTEK PLUS-500) were directly measured, using derivative with suitable wavelength depending on the calibration curves of single each drug.

Chapter Three

Results and Discussion

Part One:

3.1. Sulfamethoxazole:

3.1.1. Normal Spectroscopy:

Normal UV spectrum of Sulfamethoxazole has an absorption maxima of wavelengths at 256.7 nm with a molar absorptivity (ϵ) $1.74903 \times 10^4 \text{ L.mol}^{-1}.\text{cm}^{-1}$, as shown in figure (3-9-a). The calibration curve is linear in the concentration range 6-25 mg/L as shown in the figures (3-1). The LOD was 0.179mg/L and the LOQ was 0.598mg/L. The linear regression equations and correlation coefficients for the calibration curves are listed in table (3-1).

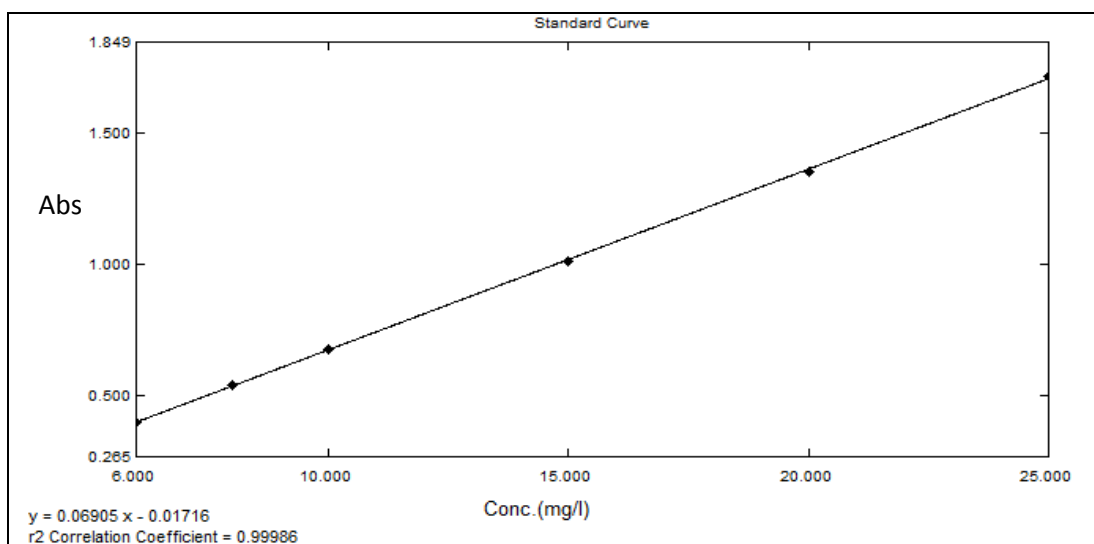


Figure (3-1) Calibration curve of normal spectra for SMX 6-25 mg/L at $\lambda = 256.7 \text{ nm}$.

3.1.2. Derivative Spectrophotometry (DS):

The UV derivative 1D , 2D , 3D and 4D spectra have derived from normal spectra of SMX. All peaks and valleys less than 240.0 nm cannot be used, because they gave noisy signals.

3.1.2.1. Selection of Optimum Instrumental Conditions:

The scaling factor affects only on the derivative amplitude, Weak derivative amplitude needs to high scaling factor to give a good peak high, The suitable scaling factor that chosen to give good peak were 3, 5, 40 and 160 for 1D , 2D , 3D and 4D respectively for the SMX and TMP. However, if the value of $\Delta\lambda$ is too large, the spectral intensity signal of the first derivative deteriorates, ⁽⁴⁶⁾. The suitable $\Delta\lambda$ that optimized to give good selectivity were 2, 4, 8 and 16 for 1D , 2D , 3D and 4D respectively for the SMX, TMP.

3.1.2.2. First Derivative:

First derivative spectra for SMX have derived from normal spectra using (scale factor = 3) and ($\Delta\lambda = 2$), as shown in figure (3-9-b). 1D spectra shows P at 246.4 nm, and V at 269.2 nm. The P = 246.4 nm cannot be used because they have weak 1D value. The calibration curves was constructed for wavelengths 269.2nm, as shown in figures (3-2). The linear equations, correlation coefficients and the concentration ranges for the calibration curves are listed in table (3-1).

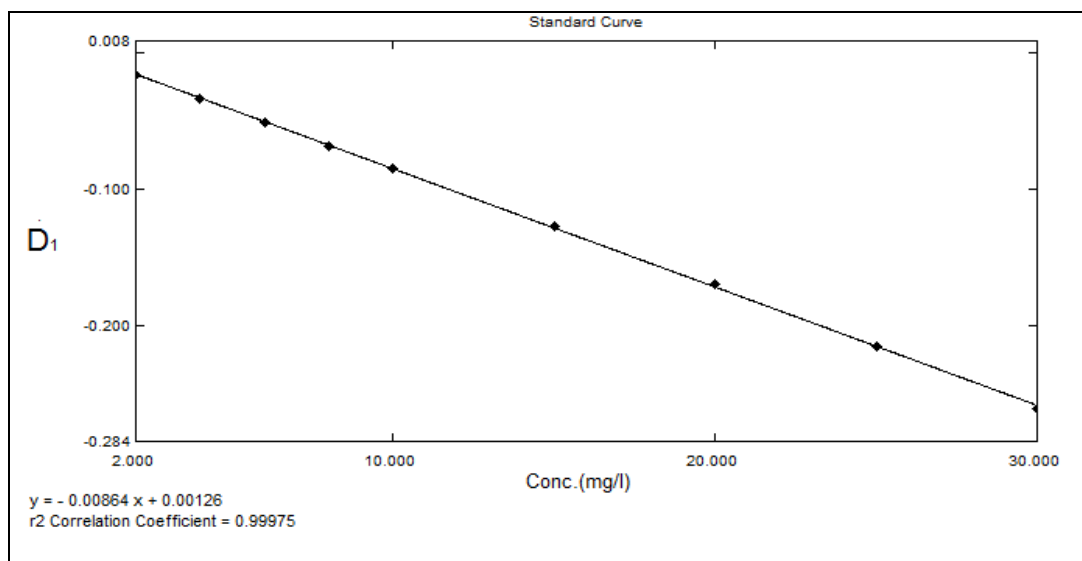


Figure (3-2) Calibration curve of 1D spectra for SMX 2-30 mg/L at $V = 269.2$ nm.

3.1.2.3. Second Derivative:

²D spectra for SMX have derived from normal spectra using ($S = 5$), with ($\Delta\lambda = 4$), as shown in figure (3-9-c). ²D spectra show peak(P) at 276.0 nm, and V at 258.5 nm. Calibration curves were constructed at wavelengths 276.0 and 258.5 nm, as shown in figures (3-3) and (3-4) respectively. The linear equations, correlation coefficients and the concentration ranges for the calibration curves are listed in table (3-1).

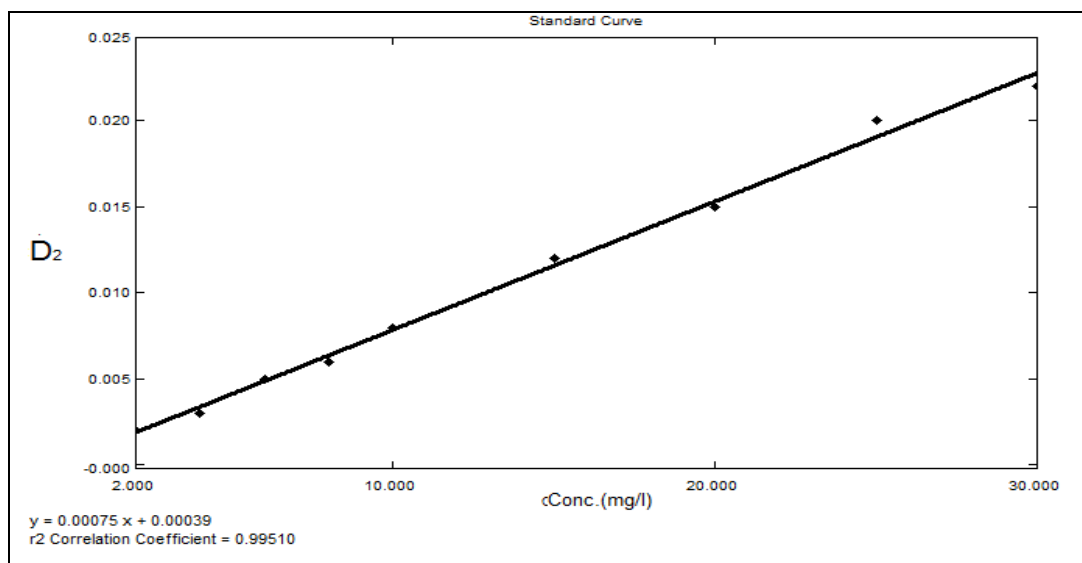


Figure (3-3) Calibration curve of ²D spectra for SMX 2-30 mg/L at P = 276.0 nm.

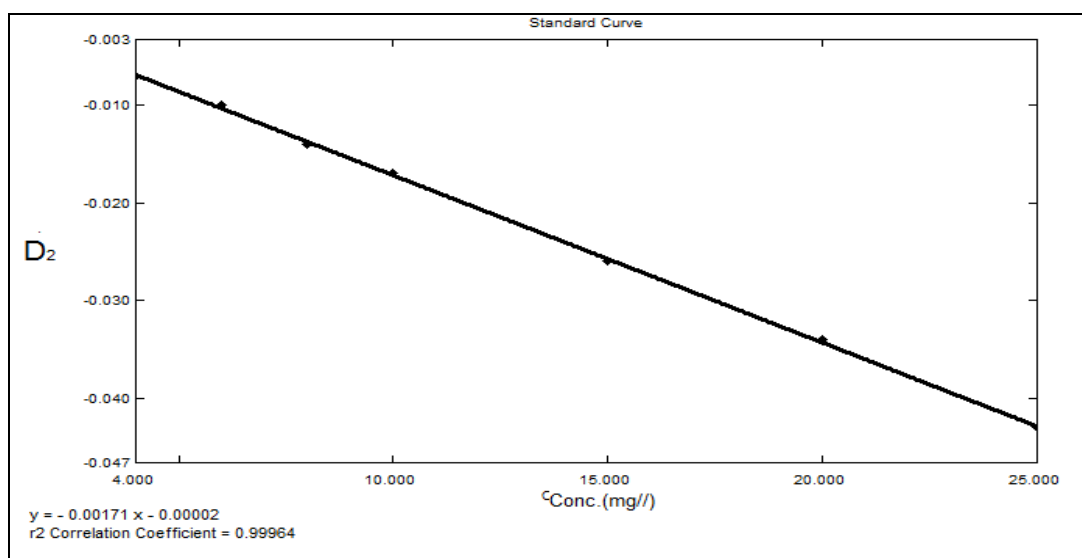


Figure (3-4) Calibration curve of ²D spectra for SMX 4-25 mg/L at V = 258.5nm.

3.1.2.4. Third Derivative:

³D spectra for SMX have derived from normal spectra using ($S = 40$), with ($\Delta\lambda = 8$). Figure (3-9-d) shows that ³D spectra have P at 267.4 nm, and V at 251.1 nm. Calibration curves were constructed at 267.4 and 251.1 nm, as shown in figures (3-5) and (3-6) respectively. The linear equations, correlation coefficients and the concentration ranges for the calibration curves are listed in table (3-1).

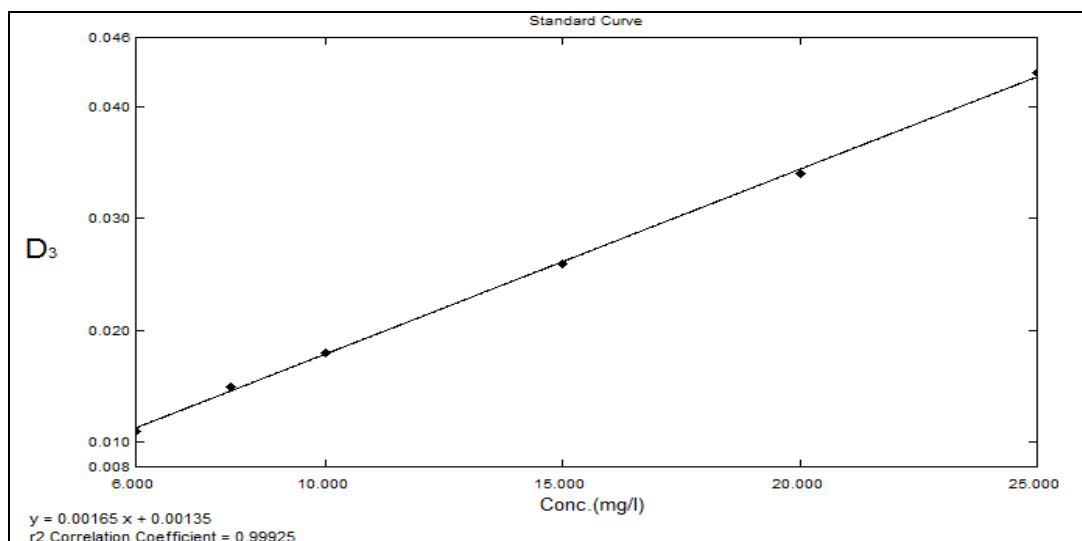


Figure (3-5) Calibration curve of ³D spectra for SMX 6–25 mg/L at P = 267.4 nm.

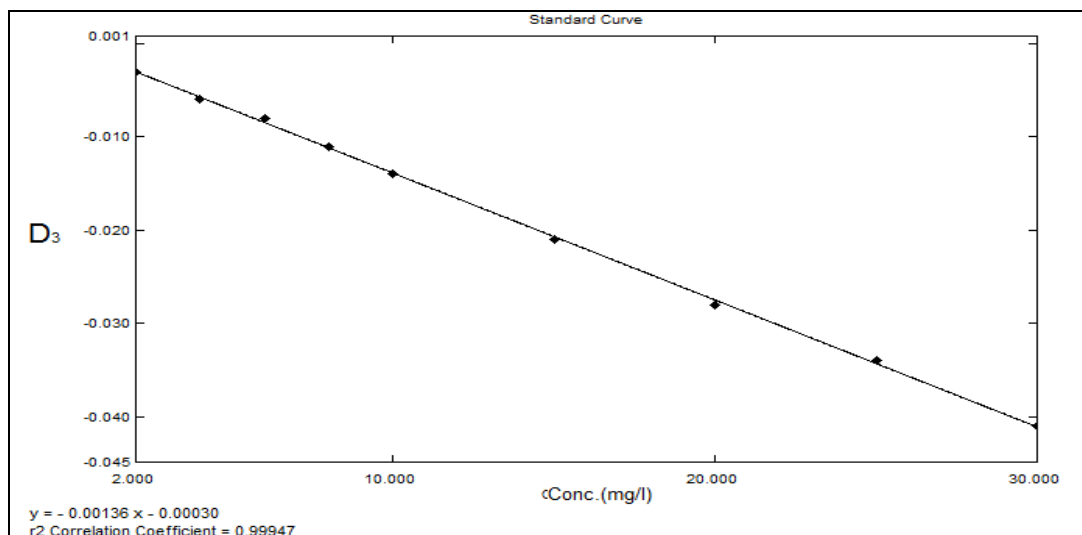


Figure (3-6) Calibration curve of ³D spectra for SMX 2–30 mg/L at V = 251.1 nm.

3.1.2.5. Fourth Derivative:

4D spectra for SMX have derived from normal spectra using ($S = 160$), with ($\Delta \lambda = 16$). Figure (3-9-e) shows 4D spectra with P at 259.4 nm, and two V at 246.0 and 274.0 nm. The V = 246.0 nm not be used because they have weak 4D value. Calibration curves were constructed for the wavelengths 259.4 and 274.0 nm, as shown in figures (3-7) and (3-8) respectively. The linear equations, correlation coefficients and the concentration ranges for the calibration curves are listed in table (3-1).

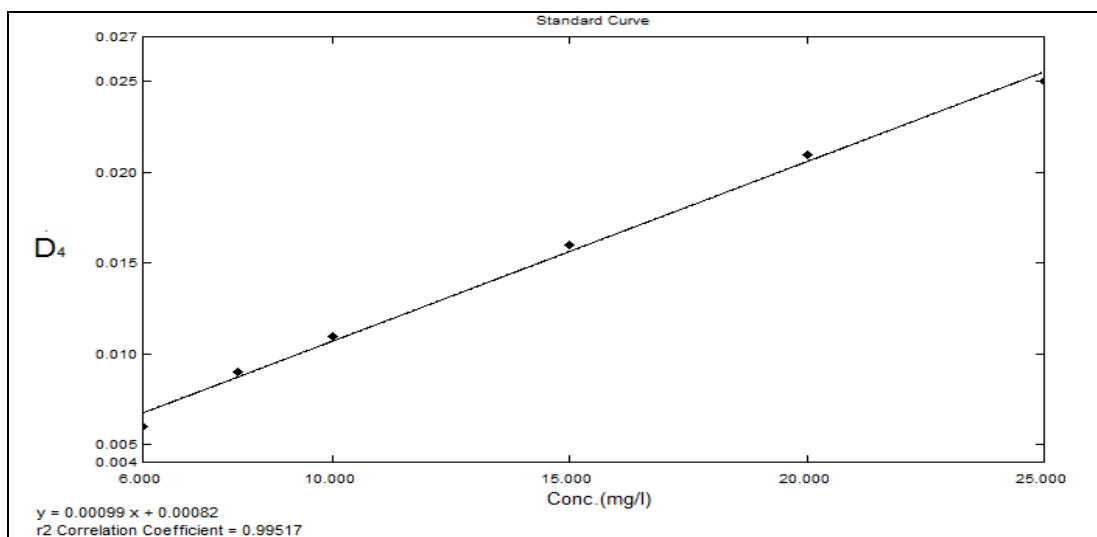


Figure (3-7) Calibration curve of 4D spectra for SMX 6-25 mg/L at P = 259.4 nm.

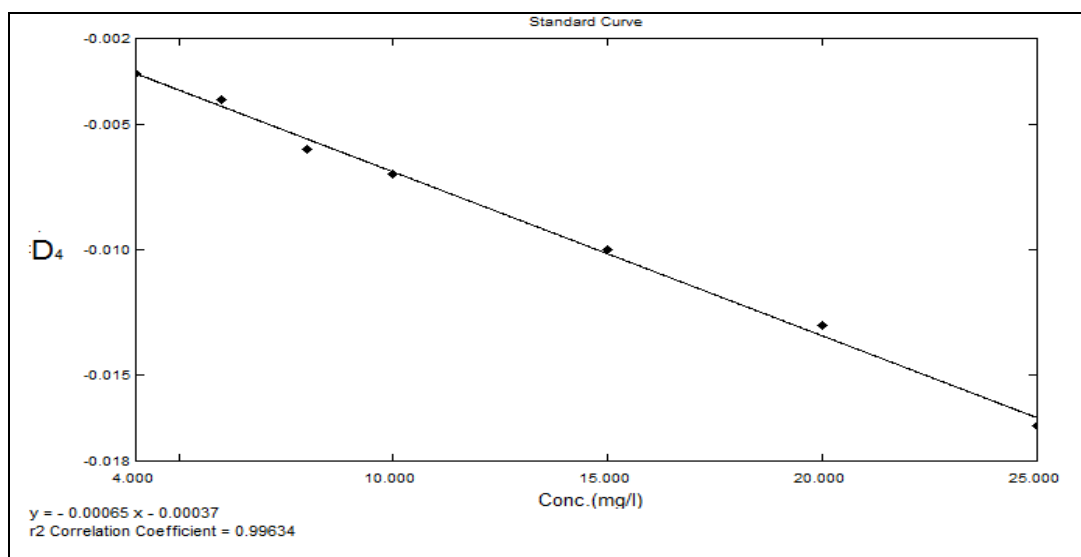


Figure (3-8) Calibration curve of 4D spectra for SMX 4-25 mg/L at V = 274 nm.

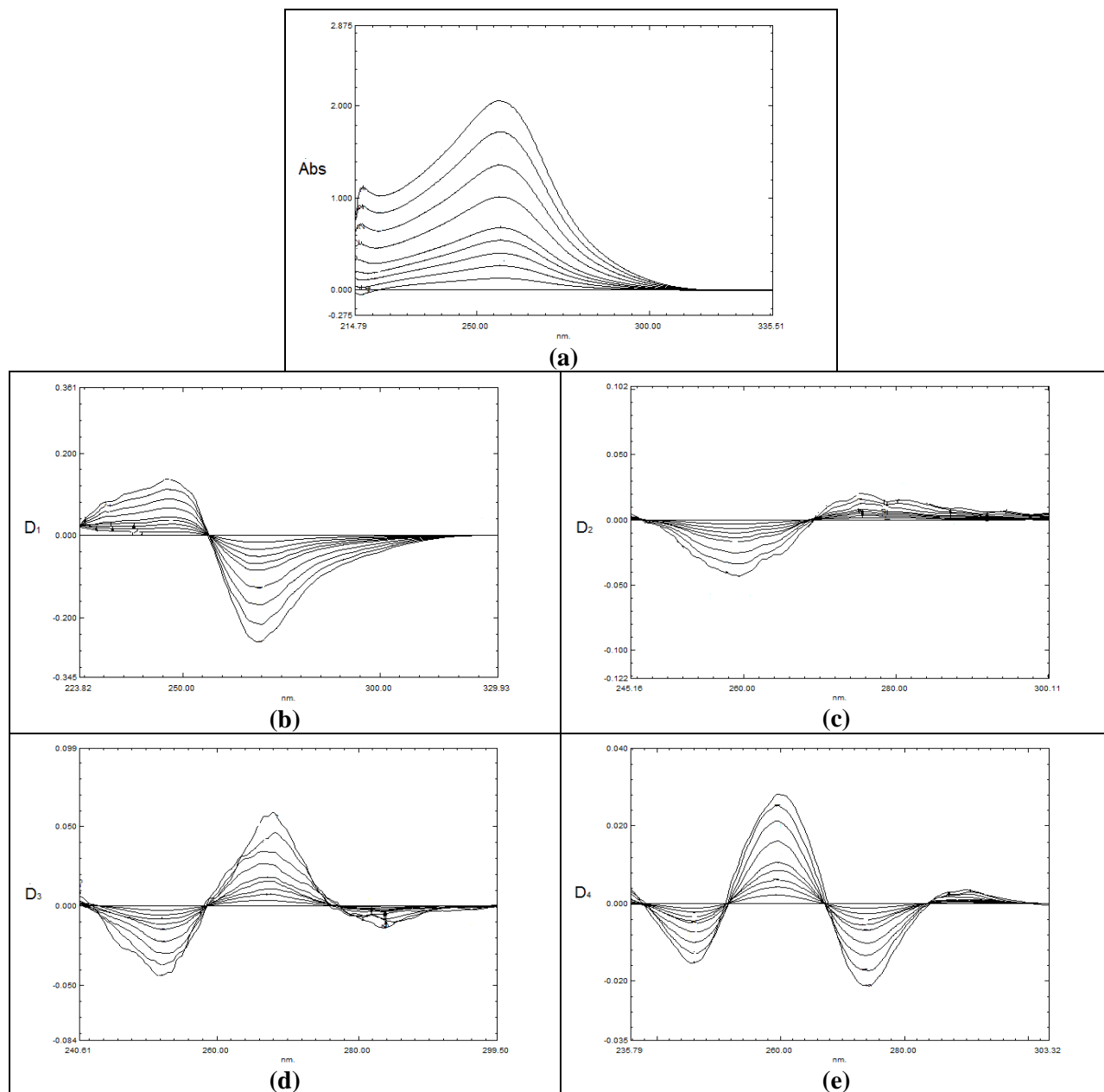


Fig. (3-9) Spectra of 2-30 mg/L SMX, a- Normal spectra b- First derivative spectra(S=3, λ =2) c- Second derivative spectra (S=5, λ =4) d- Third derivative spectra (S=40, λ =8) e- Fourth derivative spectra (S=160, λ =16).

Table (3-1): The parameters obtained from the calibration curves for normal and DS teach. of SMX.

Teach.	Conc. range mg/L	λ (nm)	Equation	r	*LOD mg/L	*LOQ mg/L
Normal	2-30	P=256.7	Y= 0.06905x-0.01716	0.9999	0.179	0.598
¹ D	2-30	V=269.2	Y=-0.00864x+0.00126	-0.9998	0.200	0.666
² D	2-30	P=276.0	Y= 0.00075x+0.00039	0.9975	0.530	1.765
	4-25	V=258.5	Y=-0.00171x-0.00002	-0.9998	0.268	0.894
³ D	6-25	P=267.4	Y= 0.00165x+0.00135	0.9996	0.193	0.644
	2-30	V=251.1	Y=-0.00136x+0.00030	-0.9997	0.485	1.616
⁴ D	6-25	P=259.4	Y= 0.00099x+0.00082	0.9975	0.214	0.714
	4-25	V=274.0	Y=-0.00065x-0.00037	-0.9981	0.484	1.614

* LOD = $3SD_B/m$, LOQ = $10SD_B/m$; where SD_B = standard deviation of blank; m = slope. ⁽⁴⁶⁾

Sulfamethoxazole can be determined using the above teach.. The results for determination standard samples of SMX (20 mg/L) and the relative errors are listed in table (3-2).

Table (3-2): The relative error and recovery for the determination standard sample of 20 mg/LSMX by using normal and DS teach.

Teach.	λ (nm)	SMX found mg/L	Er. %	RC %	δ_{n-1}
Normal	P=256.7	19.886	-0.57	99.43	0.115
¹ D	V=269.2	19.696	-1.52	98.48	0.076
² D	P=276.0	19.593	-2.04	97.97	0.038
	V=258.5	19.821	-0.89	99.11	0.048
³ D	P=267.4	19.746	-1.27	98.73	0.035
	V=251.1	20.356	1.78	101.78	0.071
⁴ D	P=259.4	20.403	2.01	102.02	0.034
	V=274.0	19.008	-4.96	95.04	0.043

The results of table (3-2) show the high value of the relative error refers to weak absorbance such as for 4D at 274.0 nm.

3.2. Trimethoprim:

3.2.1. Normal Spectroscopy:

Normal UV spectrums of TMP has one absorption maximum wavelengths at 288.0 nm with a molar absorptivity (ϵ) $0.69381 \times 10^4 \text{ L.mol}^{-1}.\text{cm}^{-1}$, as shown in figure (3-21-a). The calibration curves are linear in the concentration range 2-30 mg/L for 288.0 nm, as shown in the figures (3-10). The LOD were $0.162 \mu\text{g mL}^{-1}$ and the LOQ was 0.541 mg/L . The linear regression equations and correlation coefficients for the calibration curves are listed in table (3-3).

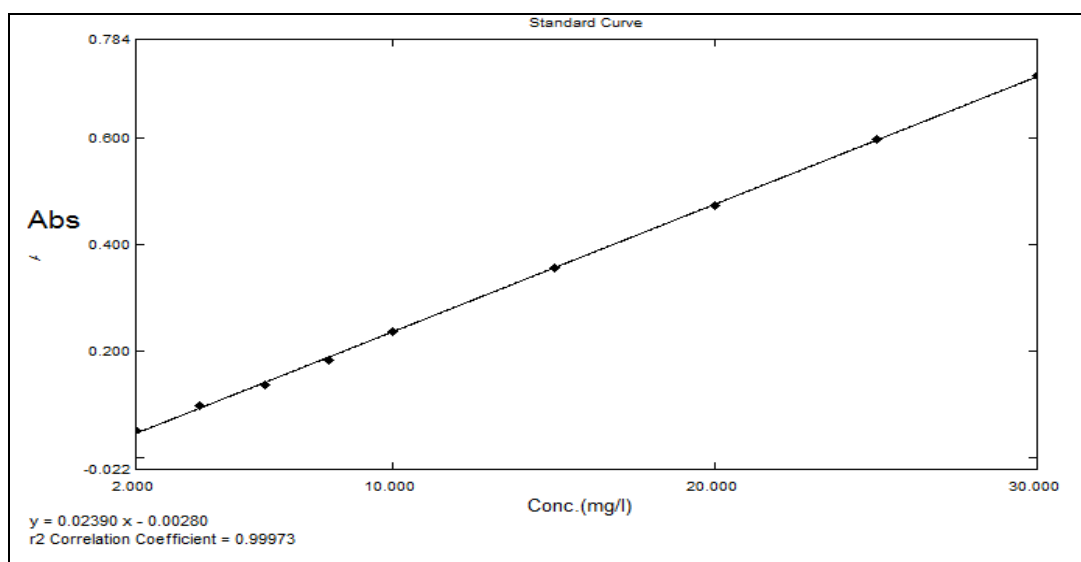


Figure (3-10) Calibration curve of normal spectra for TMP 2-30 mg/L at $\lambda = 288 \text{ nm}$.

3.2.2. Derivative Spectrophotometry:

The UV derivative spectra 1D , 2D , 3D and 4D have derived from normal spectrum of TMP as shown in fig.(3-21).

3.2.2.1. First Derivative:

¹D spectra for TMP have derived from normal spectra using ($S = 3$), with ($\Delta\lambda = 2$). Figure (3-21-b) shows that ¹D spectra have P at 272.2 nm and two V at 245.6 and 301.5 nm. Calibration curves were constructed for the wavelengths 272.2, 245.6 and 301.5 nm, as shown in figures (3-11) to (3-13) respectively. The linear dynamic ranges, the linear equations and correlation coefficients of the calibration curves are listed in table (3-3).

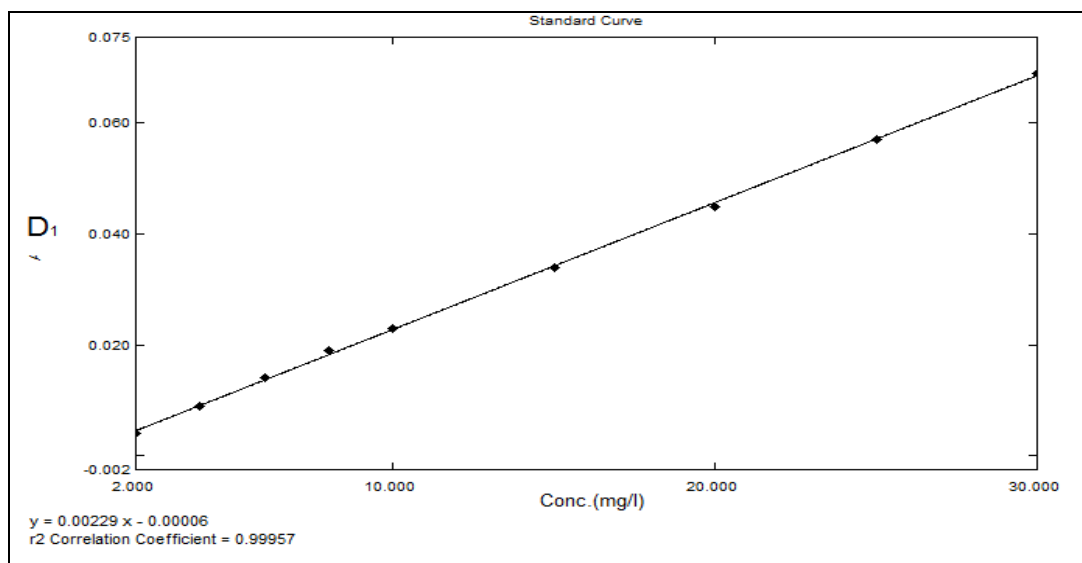


Figure (3-11) Calibration curve of ¹D spectra for TMP 2-30 mg/L at P = 272.2 nm.

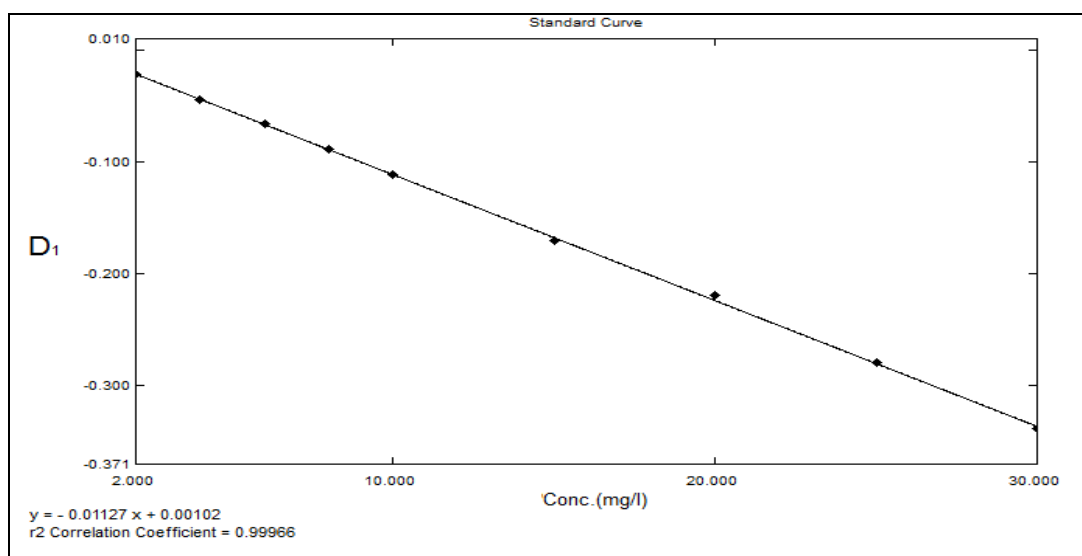


Figure (3-12) Calibration curve of ¹D spectra for TMP 2-30 mg/L at V = 245.6 nm.

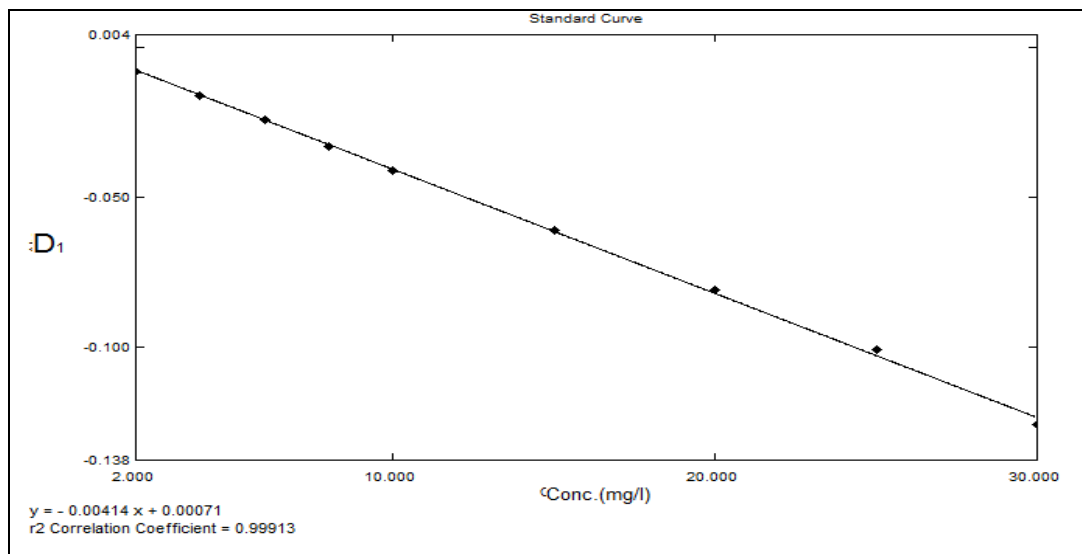


Figure (3-13) Calibration curve of 1D spectra for TMP 2-30 mg/L at $V = 301.5$ nm.

3.2.2.2. Second Derivative:

2D spectra of TMP have derived for normal spectra using ($S = 5$), with ($\Delta\lambda = 4$), as shown in figure (3-21-c). 2D spectra have two P at 250.7 and 309.2 nm, and two V at 241.7 and 290.5 nm. The wavelengths at 309.2 and 290.5 nm not be used because the 309.2 nm shifted to high value and the 290.5 nm have weak 2D value. Calibration curves were constructed for the wavelengths 250.7 and 241.7 nm, as shown in figures (3-14) and (3-15) respectively. Table (3-3) shows the linear equations, correlation coefficients and the concentration ranges for these calibration curves.

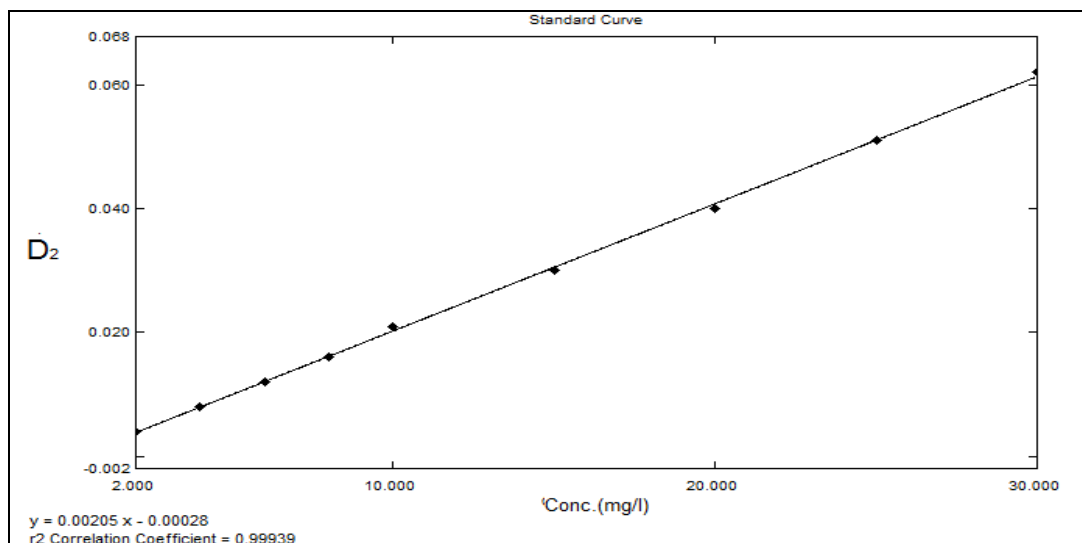


Figure (3-14) Calibration curve of 2D spectra for TMP 2-30 mg/L at $P = 250.7$ nm.

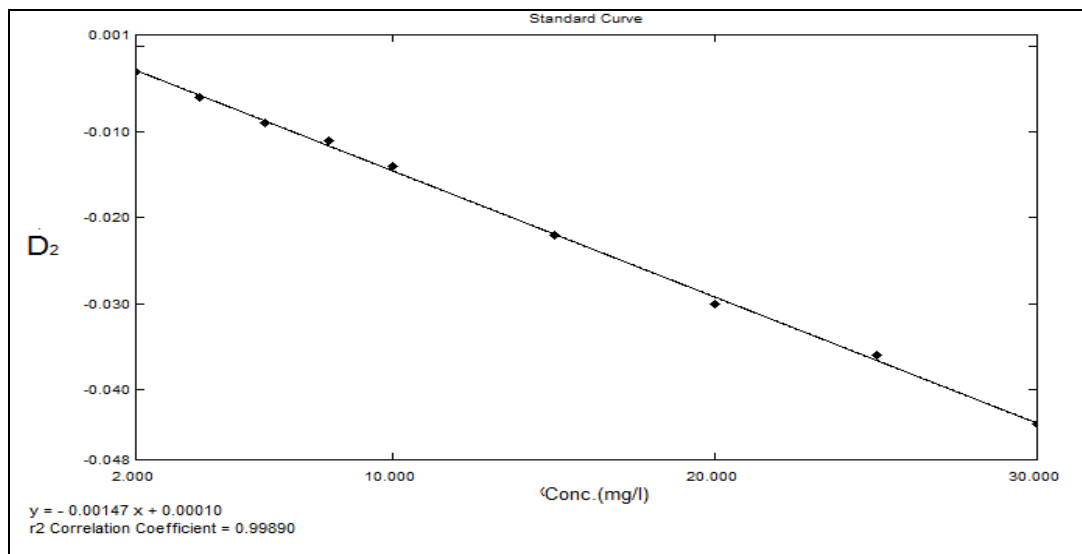


Figure (3-15) Calibration curve of 2D spectra for TMP 2-30 mg/Lat $V = 241.7$ nm.

3.2.2.3. Third Derivative:

3D spectra of TMP have derived for normal spectra using ($S = 40$), with ($\Delta\lambda = 8$). Figure (3-21-d) shows that 3D spectra have two P at 246.1 and 301.8 nm and four V at 256.2, 276.3, 286.0 and 314.6 nm. The wavelengths at 314.6, 301.8 and 276.3 nm not be used because the 314.6, 301.8 nm shifted to high value at high concentration and the 276.3 nm have weak 3D value. Calibration curves were constructed at the wavelengths 246.1, 256.2 and 286.0 nm, as shown in figures (3-16) to (3-18) respectively. The linear dynamic ranges, the linear equations and correlation coefficients for these Calibration curves are listed in table (3-3).

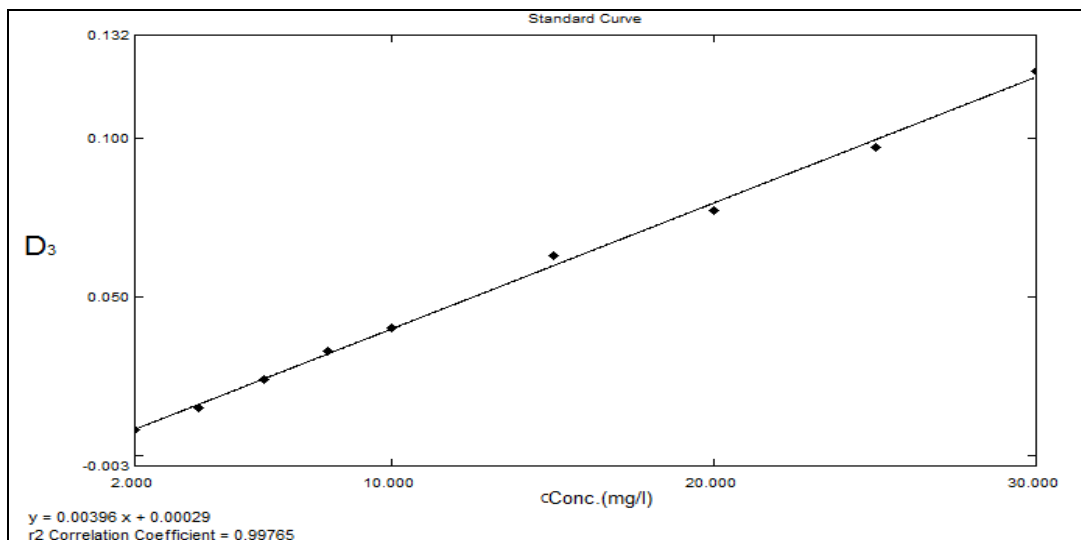


Figure (3-16) Calibration curve of 3D spectra for TMP 2-30 mg/L at P = 246.1 nm.

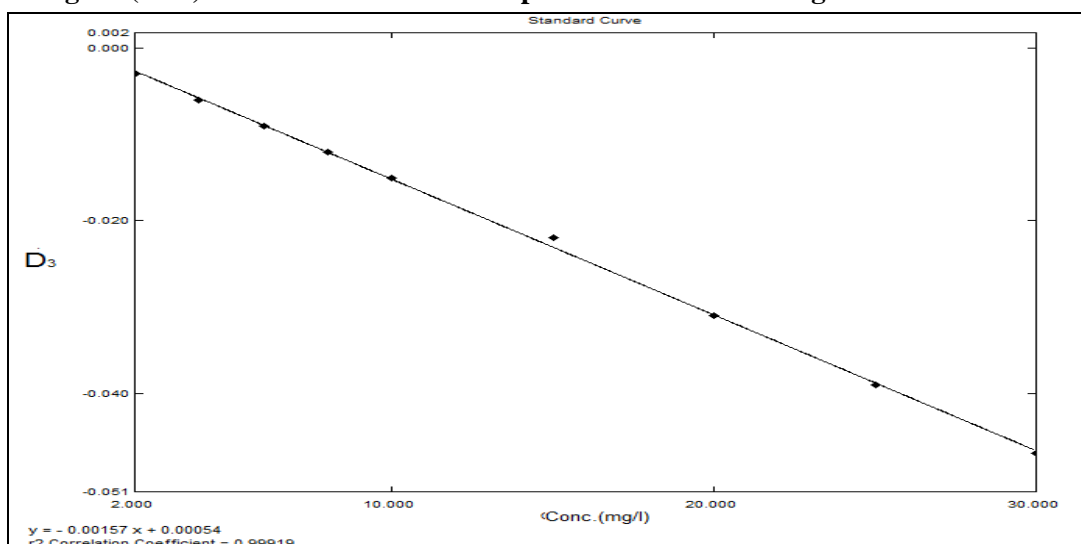


Figure (3-17) Calibration curve of 3D spectra for TMP 2-30 mg/L at V = 256.2 nm.

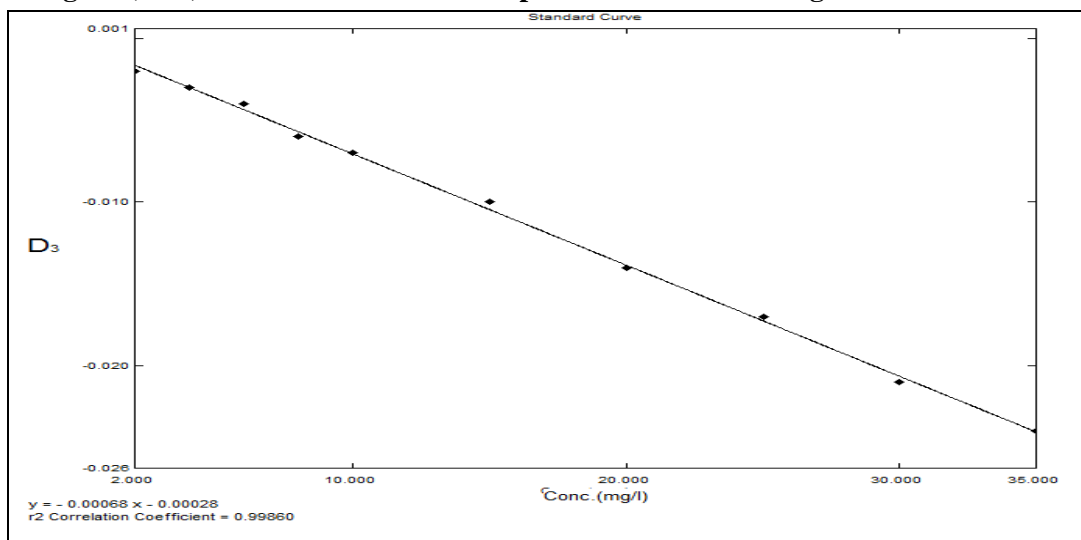


Figure (3-18) Calibration curve of 3D spectra for TMP 2-35 mg/L at V = 286.0 nm.

3.2.2.4. Fourth Derivative:

4D spectra of TMP have derived for normal spectra using ($S = 160$), with ($\Delta\lambda = 16$), as shown in figure (3-21-e). This figure shows that 4D spectra have three P at 241.0, 261.3 and 292.0 nm, and two V at 251.3 and 308.3 nm. The wavelengths at 261.3, 292.0 and 308.3 nm not be used because the 292.0, 308.3 nm shifted to high value at high concentration and the 261.3 nm have weak 4D value. Calibration curves were constructed at the wavelengths 241.0 and 251.3 nm, as shown in figures (3-19) and (3-20) respectively. The linear dynamic ranges, the linear equations and correlation coefficients for these Calibration curves are listed in table (3-3).

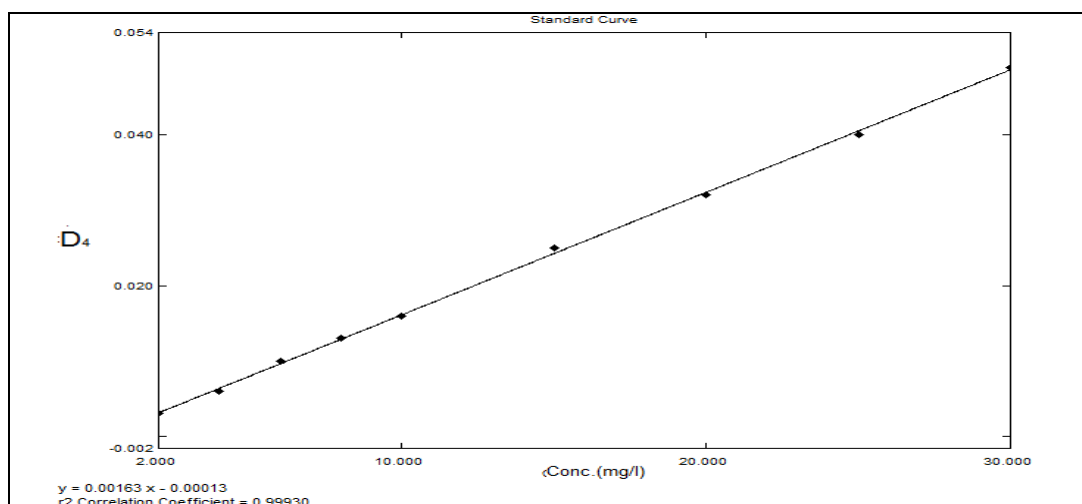


Figure (3-19) Calibration curve of 4D spectra for TMP 2-30 mg/L at P = 241.0 nm.

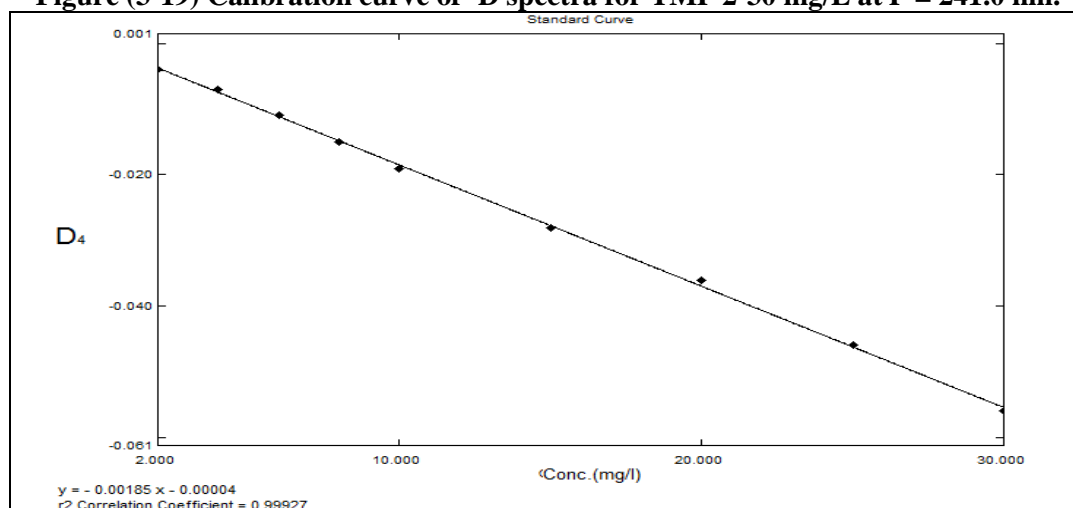


Figure (3-20) Calibration curve of 4D spectra for TMP 2-30 mg/L at V = 251.3 nm.

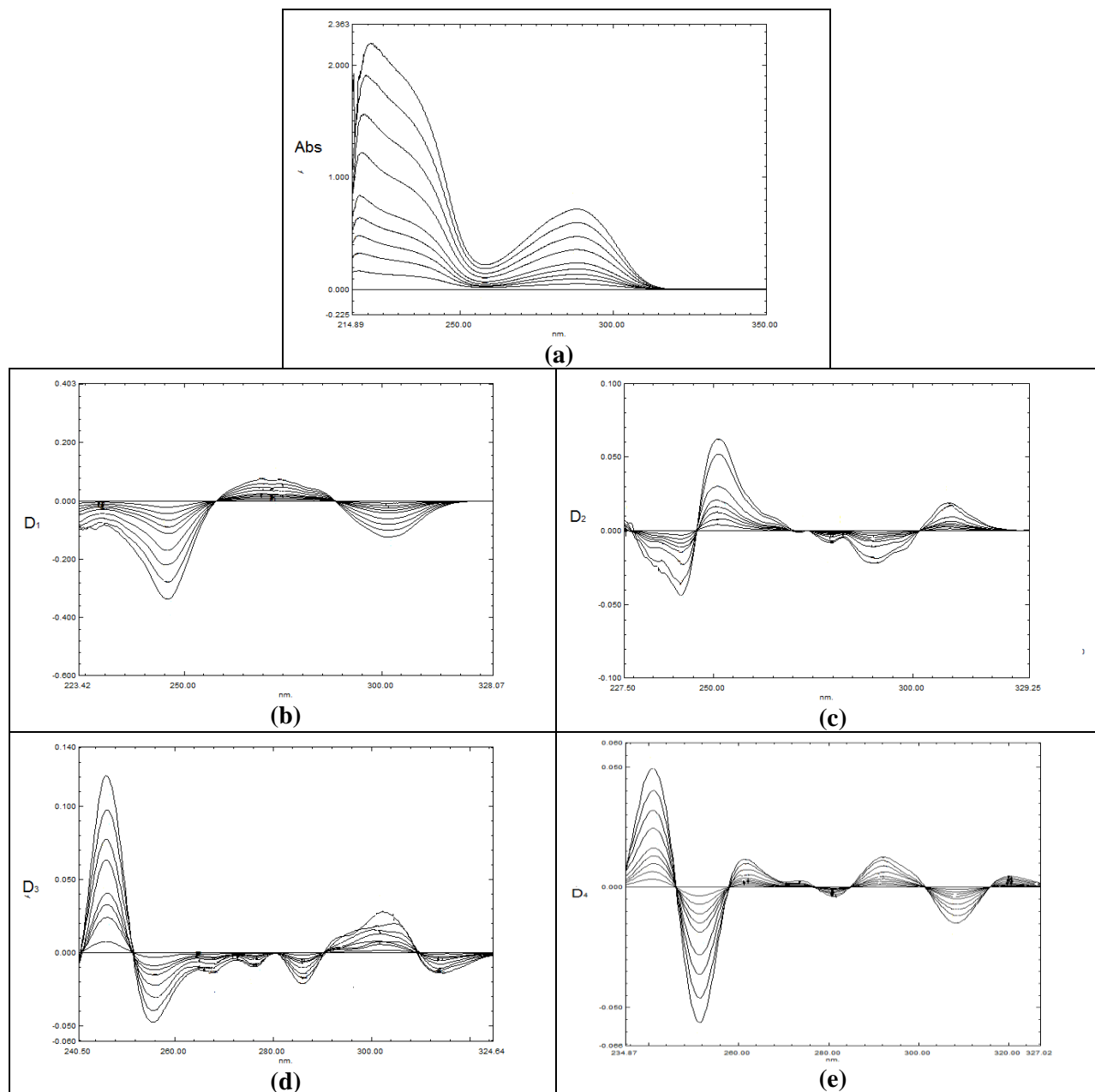


Fig. (3-21) Spectra of 2-30 mg/L TMP a- Normal spectra b- First derivative Spectra ($S=3, \lambda=2$) c- Second derivative Spectra ($S=5, \lambda=4$) d- Third derivative Spectra ($S=40, \lambda=8$) e- Fourth derivative Spectra ($S=160, \lambda=16$).

Table (3-3): The parameters obtained from the calibration curves for Normal and DS teach. of TMP.

Teach.	Conc. range mg/L	λ (nm)	Equation	r	*LOD mg/L	*LOQ mg/L
Normal	2-30	P=288.0	Y= 0.02390X-0.00280	0.9998	0.162	0.541
¹ D	2-30	P=272.2	Y= 0.00229X-0.00006	0.9997	0.540	1.799
	2-30	V=245.6	Y=-0.01127X+0.00102	-0.9998	0.289	0.963
	2-30	V=301.5	Y=-0.00414X+0.00071	-0.9995	0.430	1.435
² D	2-30	P=250.7	Y= 0.00205X-0.00028	0.9996	0.356	1.187
	2-30	V=241.7	Y=-0.00147X+0.00010	-0.9994	0.304	1.012
³ D	2-30	P=246.1	Y= 0.00396X+0.00029	0.9988	0.108	0.358
	2-30	V=256.2	Y=-0.00157X+0.00054	-0.9995	0.270	0.901
	2-35	V=286.0	Y=-0.00680X-0.00028	-0.9992	0.439	1.462
⁴ D	2-30	P=241.0	Y= 0.00163X-0.00013	0.9996	0.535	1.783
	2-30	V=251.3	Y=-0.00185X-0.00004	-0.9996	0.509	1.697

Trimethoprim can be determined using the above teach. The results for determination synthetic samples of TMP (20 mg/L) and the relative errors are listed in table (3-4).

Table (3-4): The relative error and recovery for the determination synthetic sample of 20 mg/LTMP by using normal and DS teach.

Teach.	λ (nm)	TMP found mg/L	Er %	RC %	δ_{n-1}
Normal	P=288.0	19.865	-0.68	99.33	0.119
¹ D	P=272.2	19.695	-1.53	98.48	0.053
	V=245.6	19.615	-1.93	98.08	0.044
	V=301.5	19.714	-1.43	98.57	0.022
² D	P=250.7	19.608	-1.96	98.04	0.112
	V=241.7	20.535	2.68	102.68	0.133
³ D	P=246.1	19.363	-3.19	96.82	0.043
	V=256.2	20.041	0.21	100.21	0.046
	V=286.0	20.204	1.02	101.02	0.051
⁴ D	P=241.0	19.755	-1.23	98.78	0.041
	V=251.3	19.470	-2.65	97.35	0.051

The wavelengths 246.1 nm in ³D have high relative error value and they are not be used to determine TMP.

3.3. Binary Mixture:

3.3.1. Sulphmethoxazole with Trimethoprim Mixture:

Normal spectrum cannot be used to determine each of SMX and TMP present in their mixture, due to interfering between the spectra, as shown in figure (3-34-a), therefore; DS teach. can be used in this case.

3.3.1.1. First Derivative:

First derivative tech. may be used to determine SMX only, because there is no certain wavelength suitable to determine TMP, as shown in figure (3-34-b). In figure (3-22), SMX can be determined at $\lambda = 288.0$ nm, while TMP have no contribution (zero crossing point of TMP). Calibration curves of 1D spectra for standard SMX at 288.0 nm were constructed, as shown in figures (3-23). The linear equations, correlation coefficients and concentration ranges for the calibration curve are listed in table (3-12). The results and the relative errors for the determination SMX in the presence of TMP are listed in table (3-5).

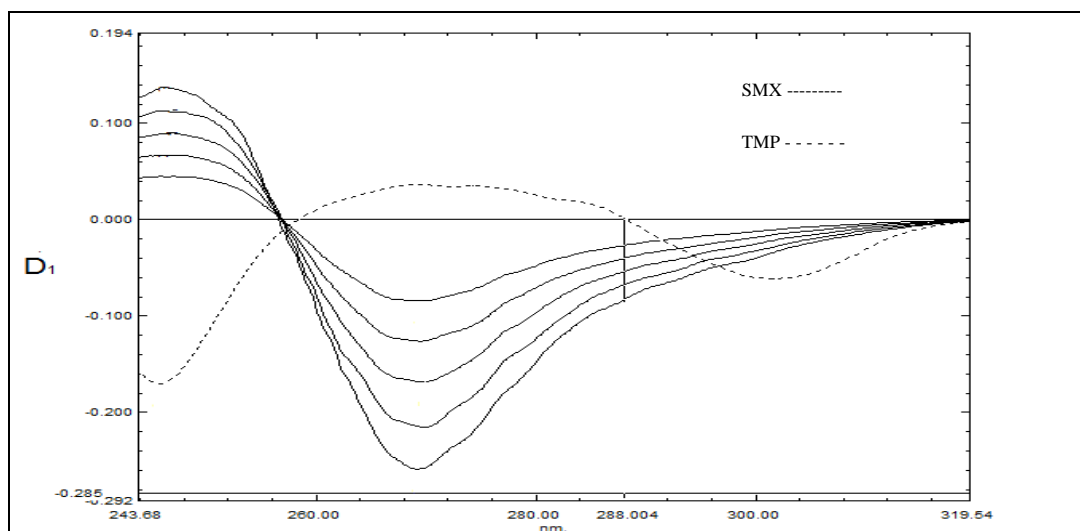


Figure (3-22) 1D spectra for(4-25) mg/L SMX and(4)mg/LTMP (zero crossing) at 288 nm.

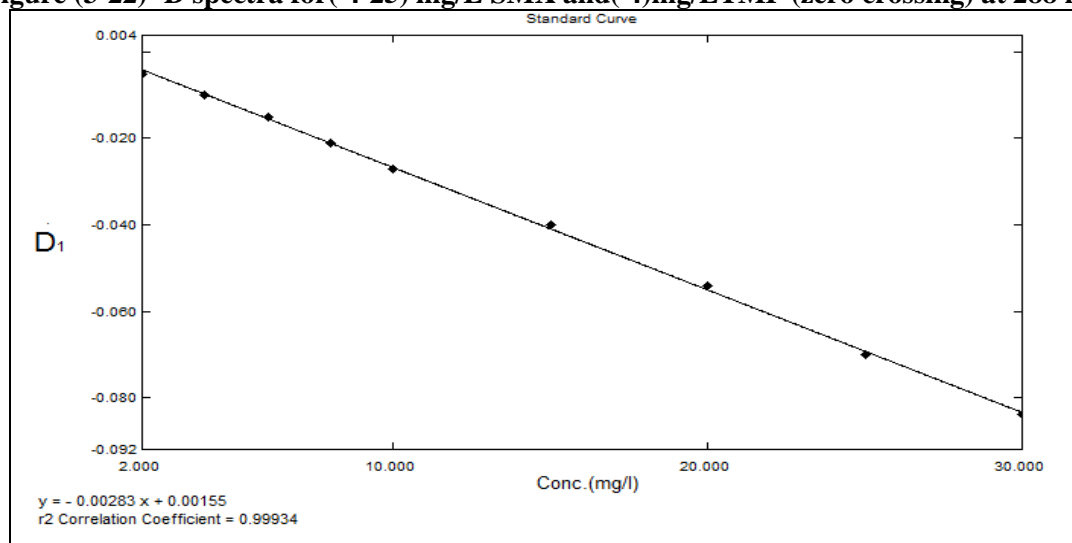


Figure (3-23) Calibration curve of 1D spectra for SMX 2-30 mg/L at $\lambda = 288$ nm.

Table (3-5): The relative error and recovery for the determination SMX in the presence of TMP at 288 nm using ¹D teach..

<i>SMX and TMP mixtures(mg/L)</i>	<i>SMX found* mg/L</i>	<i>Relative error%</i>	<i>Recovery %</i>	<i>SMX and TMP mixtures(mg/L)</i>	<i>SMX found* mg/L</i>	<i>Relative error%</i>	<i>Recovery %</i>
30 SMX+0 TMP	30.216	0.72	100.72	20 SMX+4 TMP	19.709	-1.46	98.55
20 SMX+0 TMP	19.401	-3.00	97.01	25 SMX+4 TMP	25.448	1.79	101.79
10 SMX+0 TMP	10.008	0.08	100.08	20SMX+2 TMP	20.068	0.34	100.34
4 SMX + 0 TMP	3.894	-2.65	97.35	20SMX+4 TMP	19.709	-1.46	98.55
2 SMX + 4 TMP	2.035	1.75	101.75	20SMX+6 TMP	19.709	-1.46	98.55
4 SMX + 4 TMP	3.929	-1.78	98.23	20SMX+8 TMP	20.068	0.34	100.34
6 SMX + 4 TMP	5.822	-2.97	97.03	20SMX +10TMP	20.068	0.34	100.34
8 SMX + 4 TMP	7.874	-1.58	98.43	20SMX+15 TMP	19.709	-1.46	98.55
10 SMX+4 TMP	10.026	0.26	100.26	20SMX+20 TMP	20.427	2.14	102.14
15 SMX+4 TMP	14.688	-2.08	97.92	20SMX+25 TMP	20.427	2.14	102.14

The results of table (3-5) show that SMX can be determined by ¹D teach. at $V = 288.0$ nm, when the mixture contain (0 to more than 50% ($\frac{W}{W}$) TMP) with accurate results.

3.3.1.2. Second Derivative:

Second derivative teach. cannot be used to determine each of SMX and TMP in their mixture, as shown in figure (3-34-c).

3.3.1.3. Third Derivative:

Third derivative teach. can be used to determine each of SMX and TMP in their mixture, as shown in figure (3-34-d). In the figure (3-24), SMX can be determined at $V = 251.4$ nm, while TMP have no any contribution (zero crossing point of TMP). Calibration curve of ³D spectra for standard SMX at 251.4 nm was constructed, as shown in figures (3-25). The linear equation, correlation coefficient and concentration range for the calibration curve are listed in table (3-12); on the other hand, TMP can be determined at $V = 258.6$ nm, where SMX absorbance was nil (zero crossing point of SMX), as shown in figure (3-26). The calibration curve

of 3D spectra for standard TMP at 258.6nm was constructed, as shown in figure (3-27). The linear equation, correlation coefficient and concentration range are listed in table (3-12). The results and the relative errors for the determination SMX and TMP in their mixture are listed in tables (3-6) and (3-7) respectively.

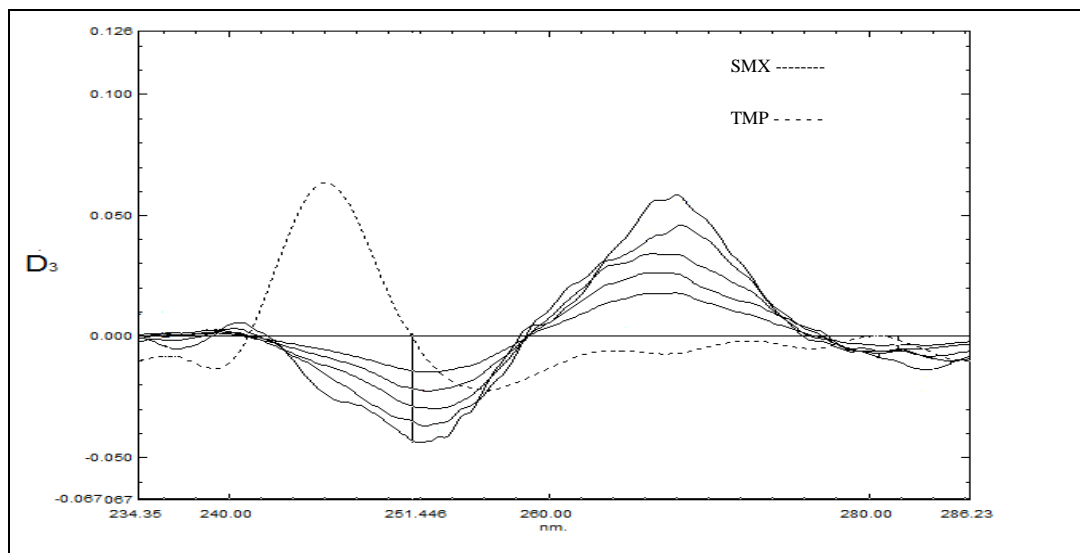


Figure (3-24) 3D spectra for (8-25) mg/L SMX and(4)mg/LTMP (zero crossing) at 251.4nm.

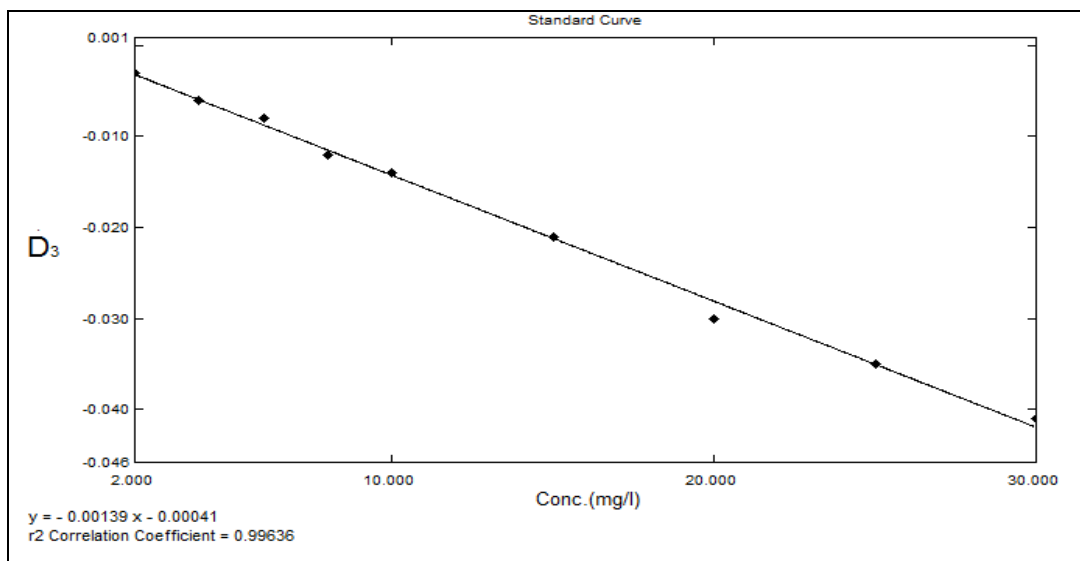


Figure (3-25) Calibration curve of 3D spectra for SMX 2-30 mg/Lat V = 251.4nm.

Table (3-6): The relative error and recovery for the determination SMX in the presence of TMP at 251.4 nm using ³D teach..

SMX and TMP mixtures (mg/L)	SMX found* mg/L	Relative error%	Recovery %	SMX and TMP mixtures (mg/L)	SMX found* mg/L	Relative error%	Recovery %
30 SMX+0 TMP	29.937	-0.21	99.79	20 SMX+4 TMP	19.621	-1.90	98.11
20 SMX+0 TMP	19.581	-2.10	97.91	25 SMX+4 TMP	24.511	-1.96	98.04
10 SMX+0 TMP	9.786	-2.14	97.86	20SMX+2TMP	20.319	1.60	101.60
4 SMX + 0 TMP	4.112	2.80	102.80	20SMX+4TMP	19.621	-1.90	98.11
2 SMX + 4 TMP	2.056	2.80	102.80	20SMX+6TMP	19.621	-1.90	98.11
4 SMX + 4 TMP	4.101	2.53	102.53	20 SMX+8 TMP	20.319	1.60	101.60
6 SMX + 4 TMP	5.849	-2.52	97.48	20 SMX+10TMP	19.621	-1.90	98.11
8 SMX + 4 TMP	8.143	1.79	101.79	20 SMX+15TMP	19.621	-1.90	98.11
10 SMX+4 TMP	9.84	-1.60	98.40	20 SMX+20TMP	20.319	1.60	101.60
15 SMX+4 TMP	14.731	-1.79	98.21	20 SMX+25TMP	20.319	1.60	101.60

The results of table (3-6) show that SMX not used to determine by ³D teach. at $\lambda = 251.4$ nm, due to the interference of TMP.

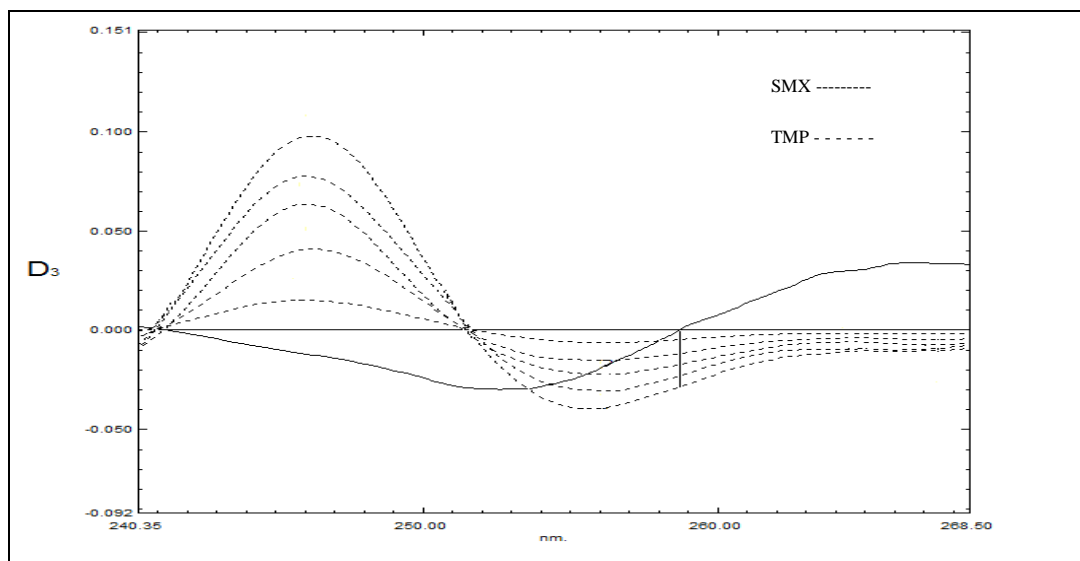


Figure (3-26) ³D spectra for (8-25) mg/L TMP and (20) mg/L SMX (zero crossing) at 258.6nm.

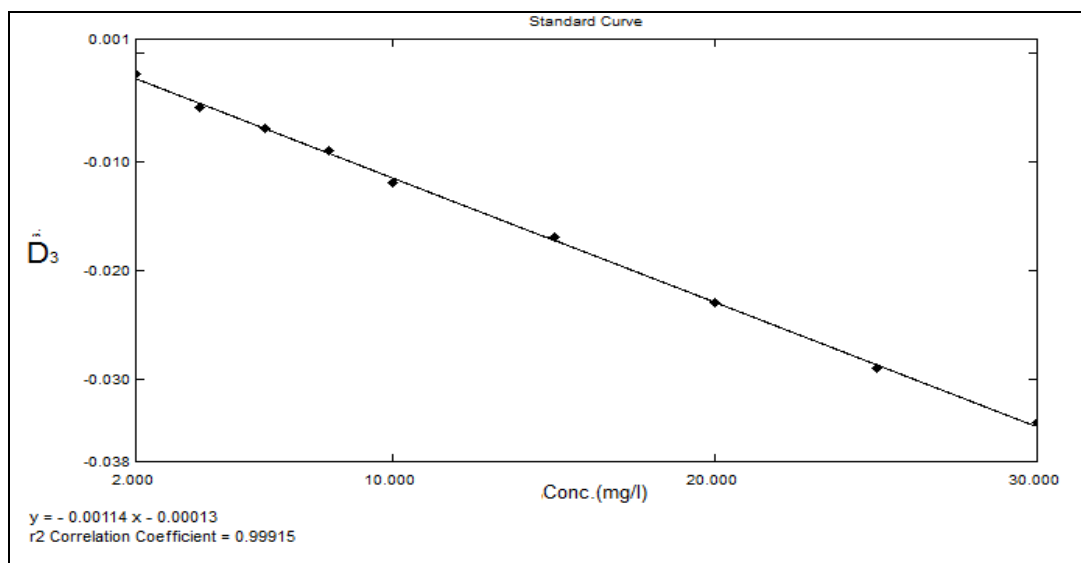


Figure (3-27) Calibration curve of 3D spectra for TMP 2-30 mg/L at $V = 258.6\text{nm}$.

Table (3-7): The relative error and recovery for the determination TMP in the presence of SMX at 258.6 nm using 3D teach.

<i>TMP and SMX mixtures (mg/L)</i>	<i>TMP found* mg/L</i>	<i>Relative error%</i>	<i>Recovery %</i>	<i>TMP and SMX mixtures (mg/L)</i>	<i>TMP found* mg/L</i>	<i>Relative error%</i>	<i>Recovery %</i>
30 TMP+0 SMX	29.537	-1.54	98.46	4 TMP +20SMX	3.942	-1.45	98.55
20 TMP+0 SMX	20.012	0.06	100.06	4 TMP +25SMX	4.031	0.77	100.78
10 TMP+0 SMX	9.736	-2.64	97.36	2 TMP+20 SMX	1.974	-1.30	98.70
4 TMP + 0 SMX	3.937	-1.58	98.43	4 TMP+20 SMX	3.942	-1.45	98.55
4 TMP + 2 SMX	4.079	1.97	101.98	6 TMP+20 SMX	6.108	1.80	101.80
4 TMP + 4 SMX	3.892	-2.70	97.30	8 TMP+20 SMX	8.36	4.50	104.50
4 TMP + 6 SMX	4.079	1.97	101.98	10TMP+20SMX	10.253	2.53	102.53
4 TMP + 8 SMX	4.079	1.97	101.98	15TMP+20SMX	14.794	-1.37	98.63
4 TMP +10SMX	3.892	-2.70	97.30	20TMP+20SMX	20.051	0.25	100.26
4 TMP +15SMX	3.892	-2.70	97.30	25TMP+20SMX	26.185	4.74	104.74

The results of table (3-7) show that TMP not used to determine by 3D teach. at $V = 258.6\text{ nm}$, due to the interference of SMX.

3.3.1.4. Fourth Derivative:

Fourth derivative teach. can be used to determine each of SMX and TMP in their mixture, as shown in figure (3-34-e). In the figure (3-28), SMX can be

determined at $V = 246.2\text{nm}$ and $p=257.8\text{ nm}$, while TMP have no any contribution (zero crossing point of TMP). The calibration curves of 4D spectra for standard SMX at 246.2 nm and 257.8 nm were constructed, as shown in figures (3-29) and (3-30) respectively. The linear equations, correlation coefficients and concentration ranges for these calibration curves are listed in table (3-12); on the other hand, TMP can be determined at $V=251.5\text{nm}$ and $P = 237.6\text{nm}$, where SMX absorbance was nil (zero crossing point of SMX), as shown in figure (3-31).

The calibration curve of 4D spectra for standard TMP at 251.5nm and 237.6nm were constructed, as shown in figures (3-32)and (3-33) respectively.

The linear equations, correlation coefficients and concentration ranges are listed in table (3-12). The results and the relative errors for the determination SMX and TMP in their mixture are listed in tables (3-8), (3-9), (3-10) and (3-11) respectively.

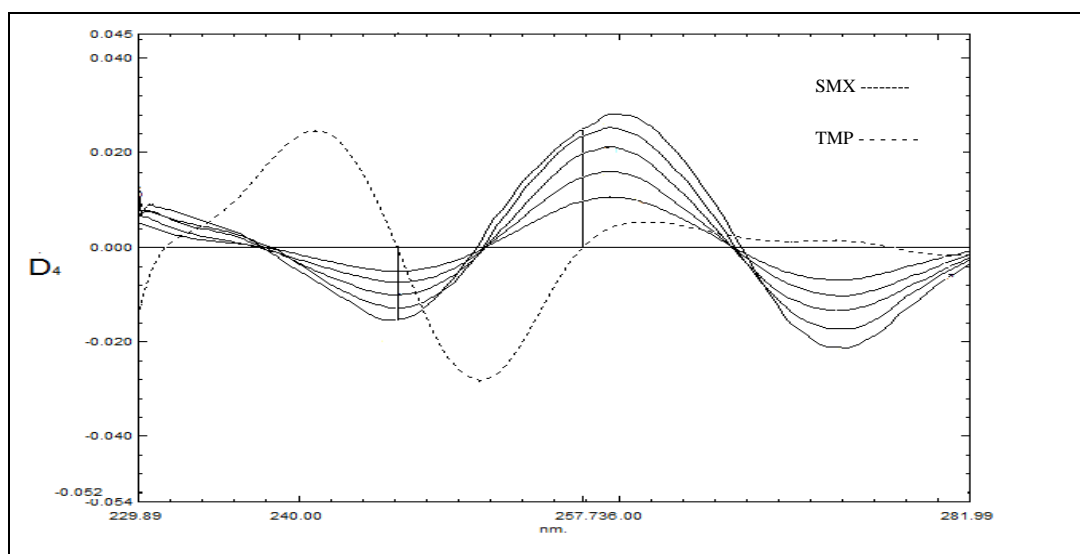


Figure (3-28) 4D spectra for (8-25) mg/L SMX and (4)mg/LTMP (zero crossing) at 246.2 and 257.8nm .

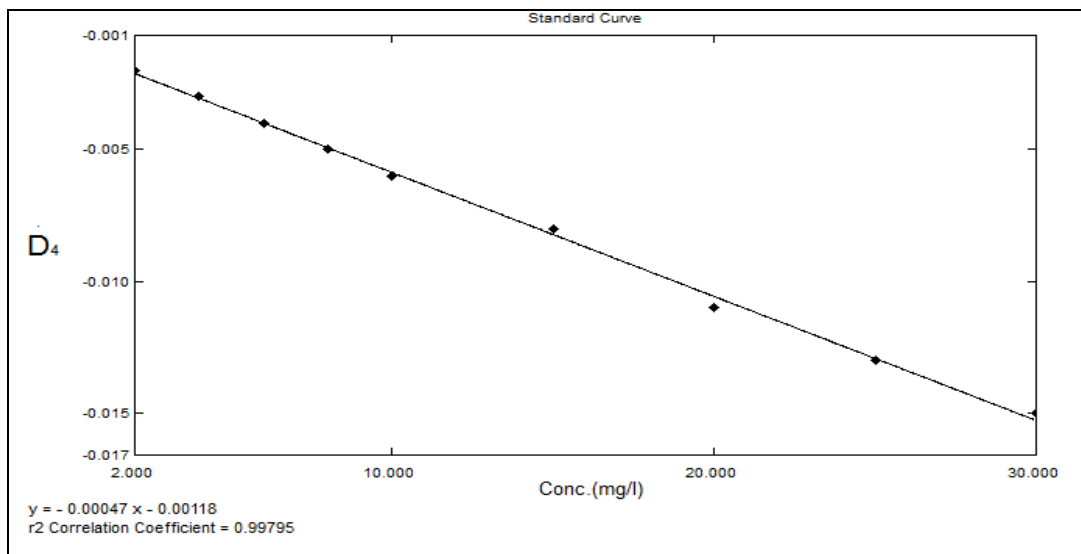


Figure (3-29) Calibration curve of 4D spectra for SMX 2-30 mg/L at V = 246.2nm.

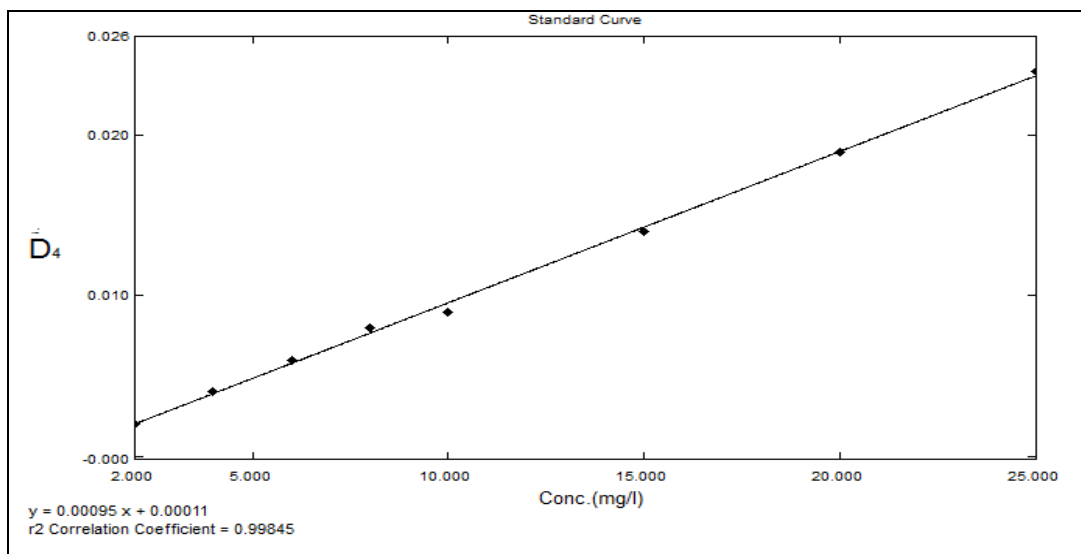


Figure (3-30) Calibration curve of 4D spectra for SMX 2-30 mg/L at P= 257.8nm.

Table (3-8) The relative error and recovery for the determination SMX in the presence of TMP at 246.2 nm using ⁴D teach.

SMX and TMP mixtures (mg/L)	SMX found* mg/L	Relative error%	Recovery %	SMX and TMP mixtures (mg/L)	SMX found* mg/L	Relative error%	Recovery %
30 SMX+0 TMP	29.762	-0.79	99.21	20 SMX+4 TMP	19.829	-0.85	99.15
20 SMX+0 TMP	19.817	-0.91	99.09	25 SMX+4 TMP	25.454	1.82	101.82
10 SMX+0 TMP	9.756	-2.44	97.56	20 SMX+2 TMP	19.829	-0.85	99.15
4 SMX + 0 TMP	3.920	-2.00	98.00	20 SMX+4 TMP	19.829	-0.85	99.15
2 SMX + 4 TMP	2.120	6.00	106.00	20 SMX+6 TMP	19.829	-0.85	99.15
4 SMX + 4 TMP	4.043	1.08	101.08	20 SMX+8 TMP	20.829	4.15	104.15
6 SMX + 4 TMP	6.210	3.50	103.50	20SMX+10 TMP	20.829	4.15	104.15
8 SMX + 4 TMP	7.956	-0.55	99.45	20SMX+15 TMP	21.841	9.21	109.21
10 SMX+4 TMP	10.568	5.68	105.68	20SMX+20 TMP	20.829	4.15	104.15
15 SMX+4 TMP	14.793	-1.38	98.62	20SMX+25 TMP	21.854	9.27	109.27

Table (3-9): The relative error and recovery for the determination SMX in the presence of TMP at 257.8 nm using ⁴D teach.

SMX and TMP mixtures (mg/L)	SMX found* mg/L	Relative error%	Recovery %	SMX and TMP mixtures (mg/L)	SMX found* mg/L	Relative error%	Recovery %
25 SMX+0 TMP	25.145	0.58	100.58	20 SMX+4 TMP	19.977	-0.11	99.89
20 SMX+0 TMP	19.869	-0.66	99.35	25 SMX+4 TMP	25.266	1.06	101.06
10 SMX+0 TMP	9.899	-1.01	98.99	20 SMX+2 TMP	19.977	-0.11	99.89
4 SMX + 0 TMP	4.085	2.13	102.13	20 SMX+4 TMP	19.977	-0.11	99.89
2 SMX + 4 TMP	1.994	-0.30	99.70	20 SMX+6 TMP	19.977	-0.11	99.89
4 SMX + 4 TMP	4.098	2.45	102.45	20 SMX+8 TMP	19.977	-0.11	99.89
6 SMX + 4 TMP	6.105	1.75	101.75	20SMX+10TMP	19.977	-0.11	99.89
8 SMX + 4 TMP	8.141	1.76	101.76	20SMX+15TMP	19.977	-0.11	99.89
10 SMX+4 TMP	9.918	-0.82	99.18	20SMX+20TMP	19.977	-0.11	99.89
15 SMX+4 TMP	14.688	-2.08	97.92	20SMX+25TMP	18.919	-5.41	94.60

The results of table (3-8) and (3-9) show that SMX can be determined with high accuracy by 4D teach. at $P = 257.8$ nm, when the mixture contain (0 to more than 50% $\left(\frac{w}{w}\right)$ TMP).

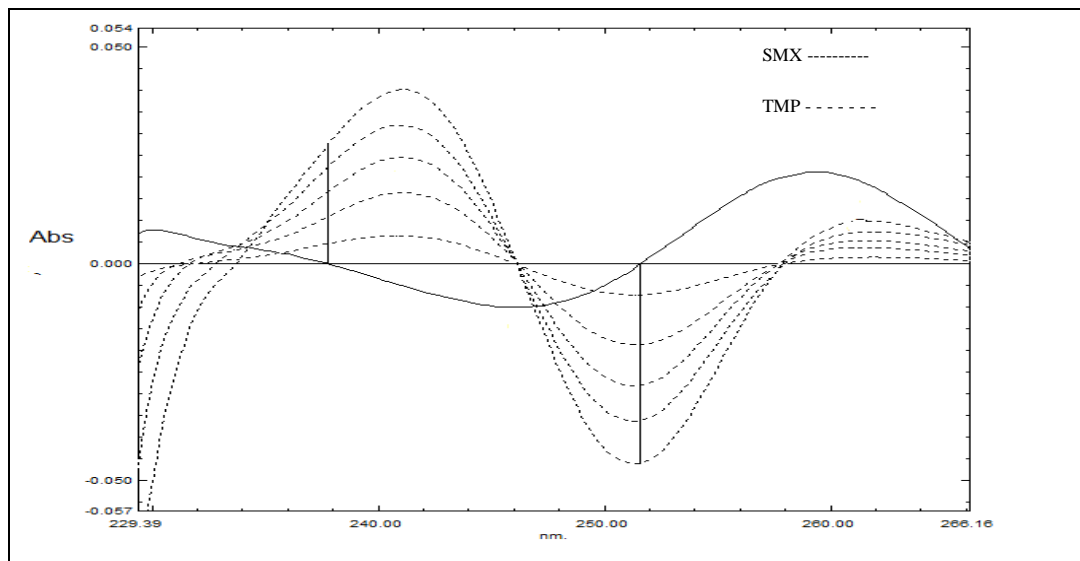


Figure (3-31) 4D spectra for (8-25) mg/L TMP and (20)mg/LSMX (zero crossing) at 251.5 and 237.6nm.

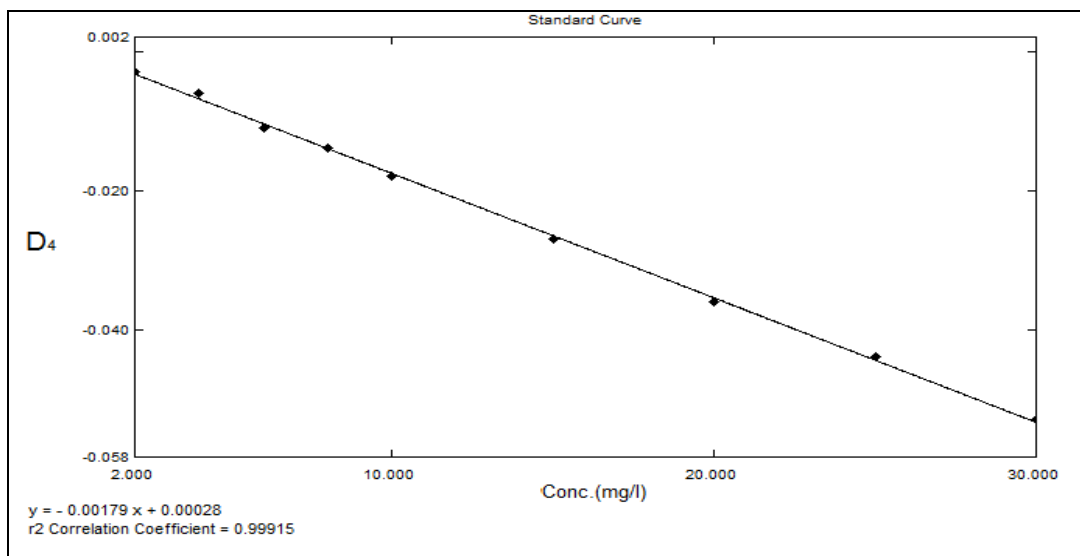


Figure (3-32) Calibration curve of 4D spectra for TMP 2-30 mg/L at $V = 251.5$ nm.

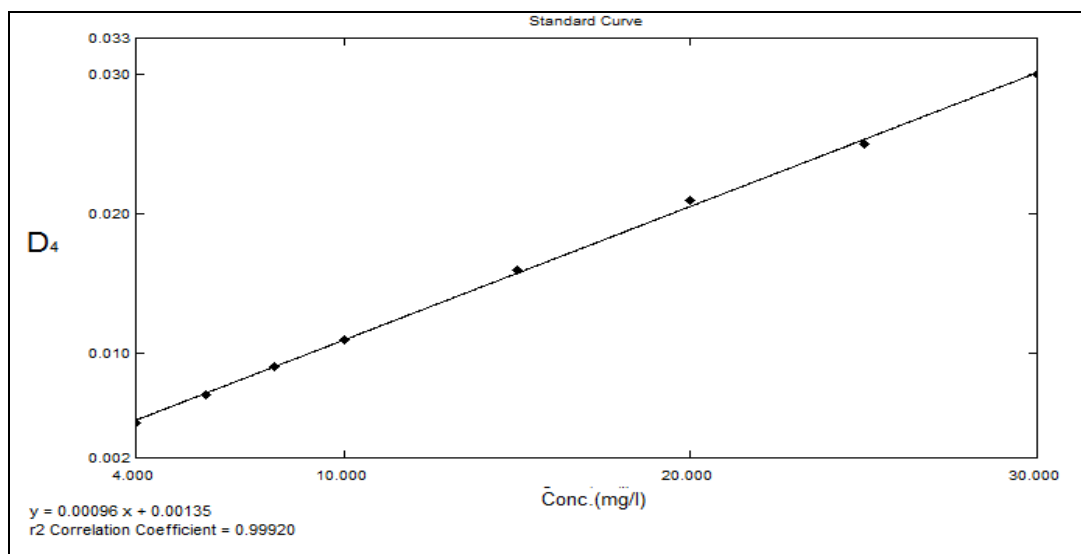


Figure (3-33) Calibration curve of 4D spectra for TMP4-30 mg/L at P= 237.6nm.

Table (3-10): The relative error and recovery for the determination TMP in the presence of SMX at 251.5 nm using 4D teach.

TMP and SMX mixtures (mg/L)	TMP found* mg/L	Relative error%	Recovery %	TMP and SMX mixtures (mg/L)	TMP found* mg/L	Relative error%	Recovery %
30 TMP+0 SMX	29.676	-1.08	98.92	4 TMP+20 SMX	4.024	0.60	100.60
20 TMP+0 SMX	19.47	-2.65	97.35	4 TMP+25 SMX	4.024	0.60	100.60
10 TMP+0 SMX	9.723	-2.77	97.23	2 TMP+20 SMX	1.946	-2.70	97.30
4 TMP + 0 SMX	3.967	-0.82	99.18	4 TMP+20 SMX	4.024	0.60	100.60
4 TMP + 2 SMX	3.996	-0.10	99.90	6 TMP+20 SMX	5.933	-1.12	98.88
4 TMP + 4 SMX	3.996	-0.10	99.90	8 TMP+20 SMX	8.099	1.24	101.24
4TMP + 6 SMX	4.024	0.60	100.60	10TMP+20SMX	10.165	1.65	101.65
4 TMP + 8 SMX	3.996	-0.10	99.90	15TMP+20SMX	15.132	0.88	100.88
4 TMP+10 SMX	4.024	0.60	100.60	20TMP+20SMX	19.687	-1.56	98.44
4 TMP+15 SMX	3.996	-0.10	99.90	25TMP+20SMX	24.885	-0.46	99.54

Table (3-11) The relative error and recovery for the determination TMP in the presence of SMX at 237.6 nm using ⁴D teach.

<i>TMP and SMX mixtures (mg/L)</i>	<i>TMP found* mg/L</i>	<i>Relative error%</i>	<i>Recovery %</i>	<i>TMP and SMX mixtures (mg/L)</i>	<i>TMP found* mg/L</i>	<i>Relative error%</i>	<i>Recovery %</i>
30 TMP+0 SMX	29.652	-1.16	98.84	4 TMP+20 SMX	3.932	-1.70	98.30
20 TMP+0 SMX	20.254	1.27	101.27	4 TMP+25 SMX	3.932	-1.70	98.30
10 TMP+0 SMX	9.886	-1.14	98.86	4 TMP+20 SMX	3.932	-1.70	98.30
4 TMP + 0 SMX	3.887	-2.83	97.18	6 TMP+20 SMX	5.974	-0.43	99.57
4 TMP + 4 SMX	3.895	-2.63	97.38	8 TMP+20 SMX	7.974	-0.32	99.68
4 TMP + 6 SMX	3.895	-2.63	97.38	10TMP+20SMX	10.059	0.59	100.59
4 TMP + 8 SMX	3.895	-2.63	97.38	15TMP+20SMX	15.271	1.81	101.81
4 TMP+10 SMX	3.895	-2.63	97.38	20TMP+20SMX	20.484	2.42	102.42
4 TMP+15 SMX	3.932	-1.70	98.30	25TMP+20SMX	24.786	-0.86	99.14

The results of table (3-10) and (3-11) show that TMP can be determined with high accuracy by ⁴D teach. at $\lambda = 251.5$ nm, when the mixture contain (0 to more than 50% ($\frac{w}{w}$) SMX).

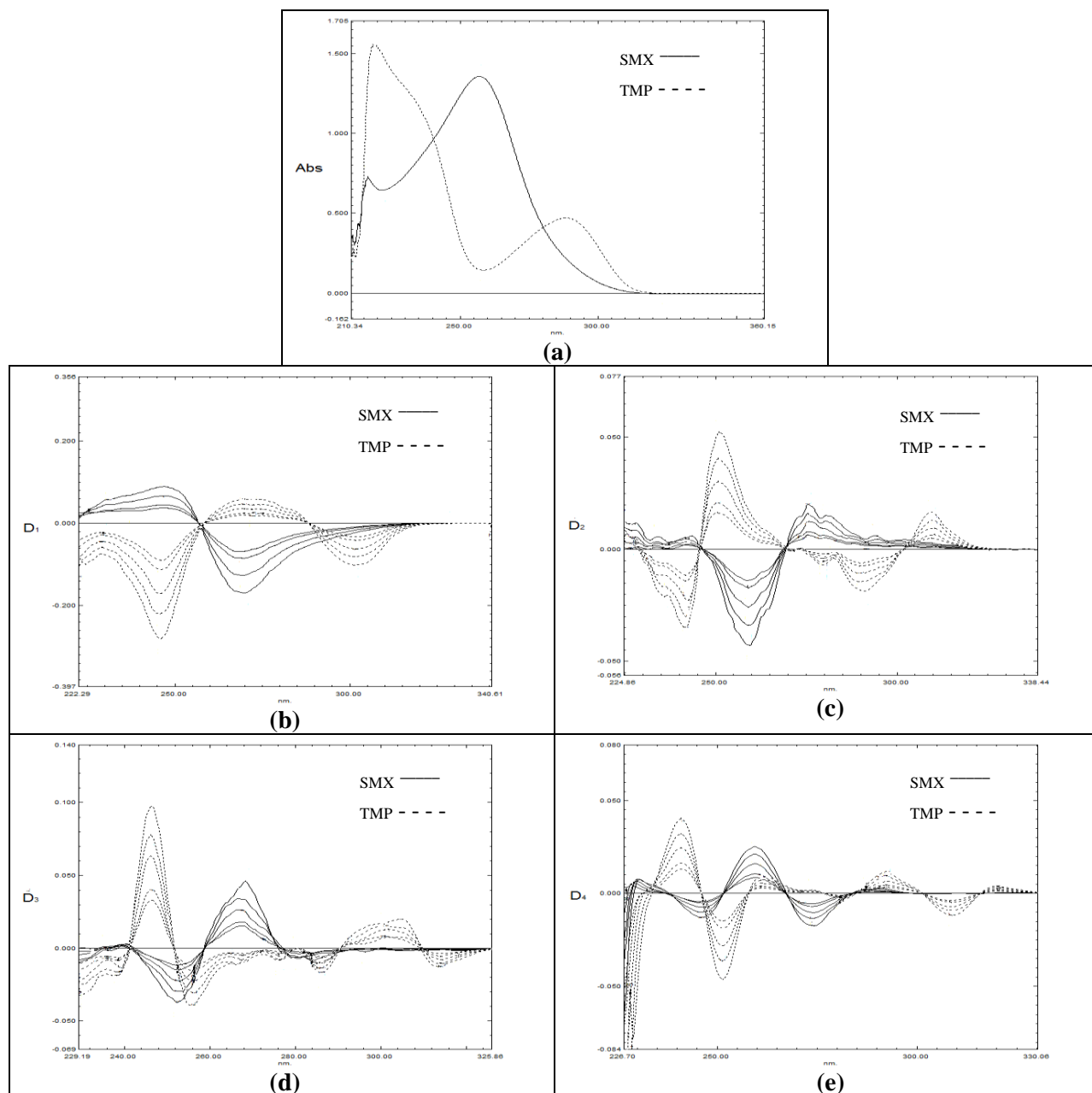


Fig. (3-34) Spectra of 8-25 mg/L SMX, 8-25 mg/L TMP a- Normal spectra of 20 mg/L for each SMX and TMP. b- First derivative spectra ($S=3, \lambda=2$) c- Second derivative spectra ($S=5, \lambda=4$) d- Third derivative spectra ($S=40, \lambda=8$) e- Fourth derivative spectra ($S=160, \lambda=16$).

Table (3-13) show that SMX can be determined in the presence of TMP by using ⁴D teach. at 257.8 nm and ¹D teach. at 288.0 nm, while TMP can be determined in the presence SMX by using ⁴D teach. at 251.5 nm.

Table (3-12) : The parameters obtained from the calibration curves for DS teach. of SMX and TMP.

Teach.		Conc. range mg/L	λ (nm)	Equation	r
SMX	¹ D	2-30	V=288	Y=-0.00283x+0.00155	0.9996
	³ D	2-30	V=251.4	Y=-0.00139x-0.00041	0.9981
	⁴ D	2-30	V=246.2	Y=-0.00047x-0.00118	0.9989
	⁴ D	2-25	P=257.8	Y= 0.00095x+0.00011	0.9992
TMP	³ D	2-30	V=258.6	Y=-0.00114x-0.00013	0.9995
	⁴ D	2-30	V=251.5	Y=-0.00179x+0.00028	0.9995
	⁴ D	4-30	P=237.6	Y= 0.00096x+0.00135	0.9995

Results for the analysis of standard drugs were compared with the British pharmacopoeia teach. ^(47, 48) using F test. As it is shown in Table (3-13), the analytical teach. was accepted according to the tabulated value of (F) is greater than the calculated value at 95% confidence limit.

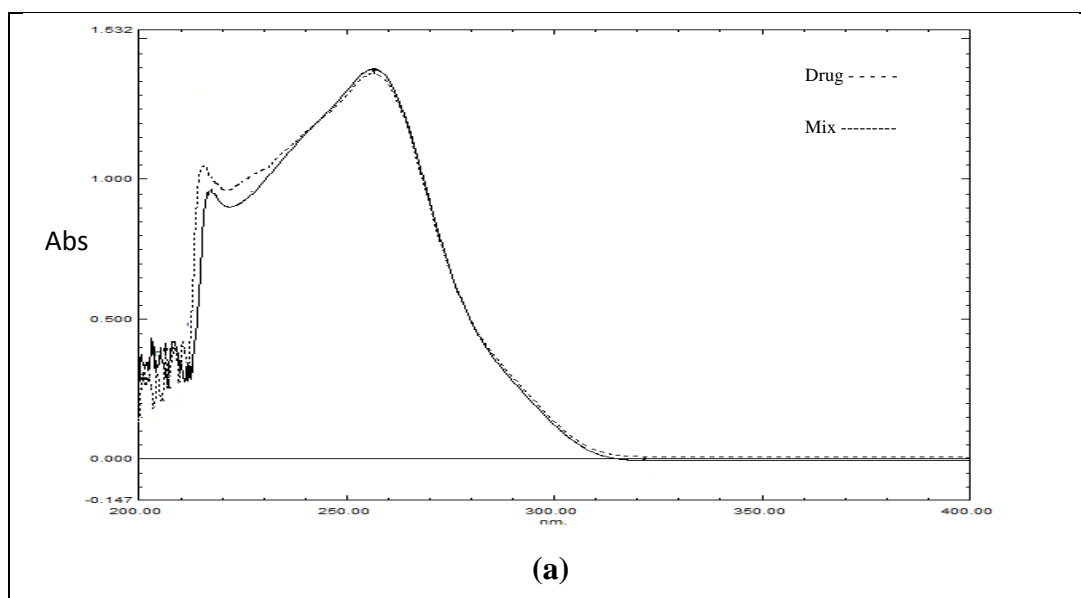
Table (3-13): Statistical data for the calibration curves that used to determine SMX and TMP in their mixture.

Drug	SMX		TMP
Teach.	⁴ D	¹ D	⁴ D
λ (nm)	P=257.8	V=288	V=251.5
Linearity range (mg/L)	2-25	2-30	2-30
R	0.9992	0.9996	0.9995
Slope	0.00095	-0.00283	-0.00179
Intercept	+0.00011	+0.00155	+0.00028
LOD (mg/L)	0.360	0.750	0.382
LOQ (mg/L)	1.200	2.499	1.275
*RSD (concentration)**	0.280	0.255	1.136
*SD	0.056	0.050	0.046
†F experimental	9.696	10.86	9.304
††F theoretical	19.34		

*n = 3. ** Concentration = 20 mg/L for SMX and 4 mg/L for TMP. †F = when the Standard deviation for SMX and TMP is (0.543 and 0.428) respectively, ††F theoretical = theoretical value at 95% confidence limit for $n_1=6, n_2=3$.

3.4. Interferences study:

To find the effect of matrix constituents on the results of determination, comparative analysis was carried out for standard solution containing active components at concentrations (20SMX+4TMP) mg/L comparable to those of the analyzed drug contain the same concentrations, they show the same normal spectra Fig.(3-35-a). While Fig.(3-35-b) show comparable between standard solution containing active components at concentrations (20SMX+4TMP) mg/L with interfering material (starch, gelatin, magnesium setrate, avecil, sucrose)at ten time greater than the concentrations of (20SMX+4TMP) mg/L.



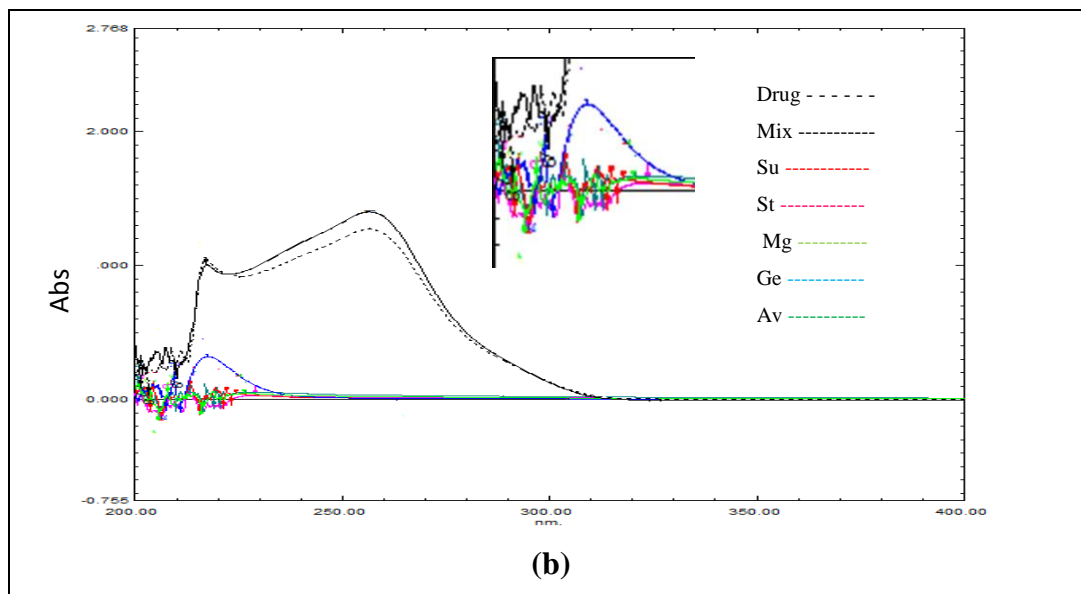


Fig. (3-35) Normal spectra for analyzed preparation (a) Mix with drug (b) Mix with (Av, Ge, Mg, St, Su)

3.5. Analysis of Pharmaceutical Samples:

3.5.1. Sulphamethaxzole with Trimethprim Mixture:

TRIMOL and METHOPRIM samples (20 mg/L) was measured by using 1D , and 4D teach.s, as shown in table (3-14) and(3-15).

Table (3-14): The relative error and recovery for the determination of Trimol sample (20 mg/LSMX + 4 mg/LTMP) by using DS teach.

Drugs	Trimol (SMX)		Trimol (TMP)
	1D	4D	4D
Teach.			
λ (nm)	V=288	P=257.8	V=251.5
Conc. found (mg/L)	18.562	20.972	3.875
Er %	-7.189	4.864	-3.12
RC %	92.811	104.864	96.88
$\mu = \bar{x} \pm (t\delta)/\sqrt{n}$	18.562 \pm 0.200	20.972 \pm 0.172	3.875 \pm 0.300
$\delta n-1$	0.161	0.139	0.241

*Each concentration represents an average of at least five measurements.

Table (3-15) The relative error and recovery for the determination of Methoprim sample (20 mg/LSMX + 4 mg/LTMP) by using DS teach.s.

Drugs	Methoprim (SMX)		Methoprim (TMP)
	¹ D	⁴ D	⁴ D
Teach.			
λ (nm)	V=288	P=257.8	V=251.5
Conc. found (mg/L)	17.844	17.880	3.209
Er %	-10.778	-10.596	-19.77
RC %	89.222	89.404	80.23
$\mu = \bar{x} \pm (t\delta)/\sqrt{n}$	17.844 \pm 0.199	17.880 \pm 0.036	3.209 \pm 0.049
δ_{n-1}	0.160	0.029	0.039

*Each concentration represents an average of at least five measurements.

Table (3-14) and (3-15) shows the results for the determination of Trimol and Methoprim (SMX+TMP mixture) by ¹D and ⁴D teach.s. The suitable teach. that gave more accurate result was the ⁴D teach. at 257.8 and 251.5 nm for SMX and TMP respectively. Table (3-16) shows a comparison between standard and commercial drug by ⁴D teach.

Table (3-16): Statistical data for the determination of (SMX + TMP) in their mixture in pure and pharmaceutical form by ⁴D teach.

SMX+TMP Mixture	SMX				TMP			
	Found mg/L $\lambda=257.8\text{nm}$	ER%	RC%	RSD %	Found mg/L $\lambda=251.5\text{nm}$	ER%	RC%	RSD%
Standard								
20SMX+4TMP	19.977	-0.11	99.89	0.280	4.024	0.60	100.6	1.136
Trimol								
20SMX+4TMP	20.972	4.86	104.86	0.663	3.875	-3.12	96.88	6.243
Methoprim								
20SMX+4TMP	17.880	-10.59	89.40	0.165	3.209	-19.77	80.23	1.241

*Each concentration represents an average of at least three measurements.

- **Part Two:**

3.6. Paracetamol:

3.6.1. Normal Spectroscopy:

Normal spectra of PAR gave a fixed absorption wavelength at 243.1 nm with molar absorptivity $1.5988 \times 10^4 \text{ L.mol}^{-1}.\text{cm}^{-1}$, as shown in figure (3-36-a). The calibration curve is linear in the concentration range of 2-30 mg/L, The LOD and LOQ were 0.102 and 0.339 mg/L respectively. The linear regression equation is $Y=0.06365x+0.01371$, with 0.99990 of the correlation coefficient, as shown in table (3-17).

3.6.2. Derivative Spectrophotometry:

The UV derivative 1D , 2D , 3D , and 4D spectra have derived for normal spectra of PAR. All peaks and valleys below than 220.0 nm gave noisy signals; therefore, they cannot be used.

3.6.2.1. Selection of Optimum Instrumental Conditions:

The scaling factor affecting only on the derivative amplitude, weak derivative amplitude needs to high scaling factor to give a good high peak, The suitable scaling factor that chosen to give good peak were 10,60,100 and 300 for 1D , 2D , 3D and 4D respectively and for the PAR and CAF. However, if the value of $\Delta\lambda$ is too large, the spectral intensity signal of the first derivative deteriorates ⁽⁴⁶⁾. The suitable $\Delta\lambda$ that optimized to give good selectivity were 2, 4, 8 and 16 for 1D , 2D , 3D and 4D respectively for the PAR, CAF.

3.6.2.2. First Derivative:

First derivative spectra of PAR have derived for normal spectra using ($S = 10$) and ($\Delta\lambda = 2$), as shown in figure (3-36-b). 1D spectra show one P at 223.5 nm and

two V at 258.6 and 289.0 nm. The calibration curves were constructed for the wavelengths 223.5, 258.6 and 289.0 nm, as shown in part one. The linear regression equations, correlation coefficients and the concentration ranges for the calibration curves are listed in table (3-17).

3.6.2.3. Second Derivative:

²D spectra of PAR have derived for normal spectra using (S = 60), with ($\Delta\lambda = 4$), as shown in figure (3-36-c). ²D spectra have two P at 268.3 and 302.4 nm, and one V at 246.6 nm. The calibration curves were constructed for the wavelengths 268.3, 302.4 and 246.6nm as shown in part one. Table (3-17) shows the linear regression equations, correlation coefficients and the concentration ranges for these calibration curves

3.6.2.4. Third Derivative:

³D spectra of PAR have derived for normal spectra using (S = 100), with ($\Delta\lambda = 8$). Figure (3-36-d) shows that ³D spectra have three P at 256.0, 289.1 and 300.0 nm and three V at 236.7, 275.1 and 306.9 nm. The wavelengths at 289.1, 300.0 and 306.9 nm cannot be used because they have weak ³D value. The 256.0 nm shifted to high value at high concentration. The calibration curves were constructed at wavelengths 236.7 and 275.1 as shown in part one. The linear dynamic ranges, the linear equations and correlation coefficients for the calibration curves are listed in table (3-17).

3.6.2.5. Fourth Derivative:

⁴D spectra of PAR have derived for normal spectra by using (S = 300), with ($\Delta\lambda = 16$), as shown in figure (3-36-e). ⁴D spectra have three P at 221.6, 246.9 and 280.8 nm, and three V at 233.5, 267.1 and 304.0 nm. The wavelength at 246.9 nm cannot be used because the 246.9 nm shifted to high value at high concentration and the wavelength 233.5 and 304.0 nm are very weak; therefore, it cannot be used.

Calibration curve was constructed at 221.6, 280.8 and 267.1 nm, as shown in part one. The linear regression equation, correlation coefficient and the concentration range are listed in table (3-17).

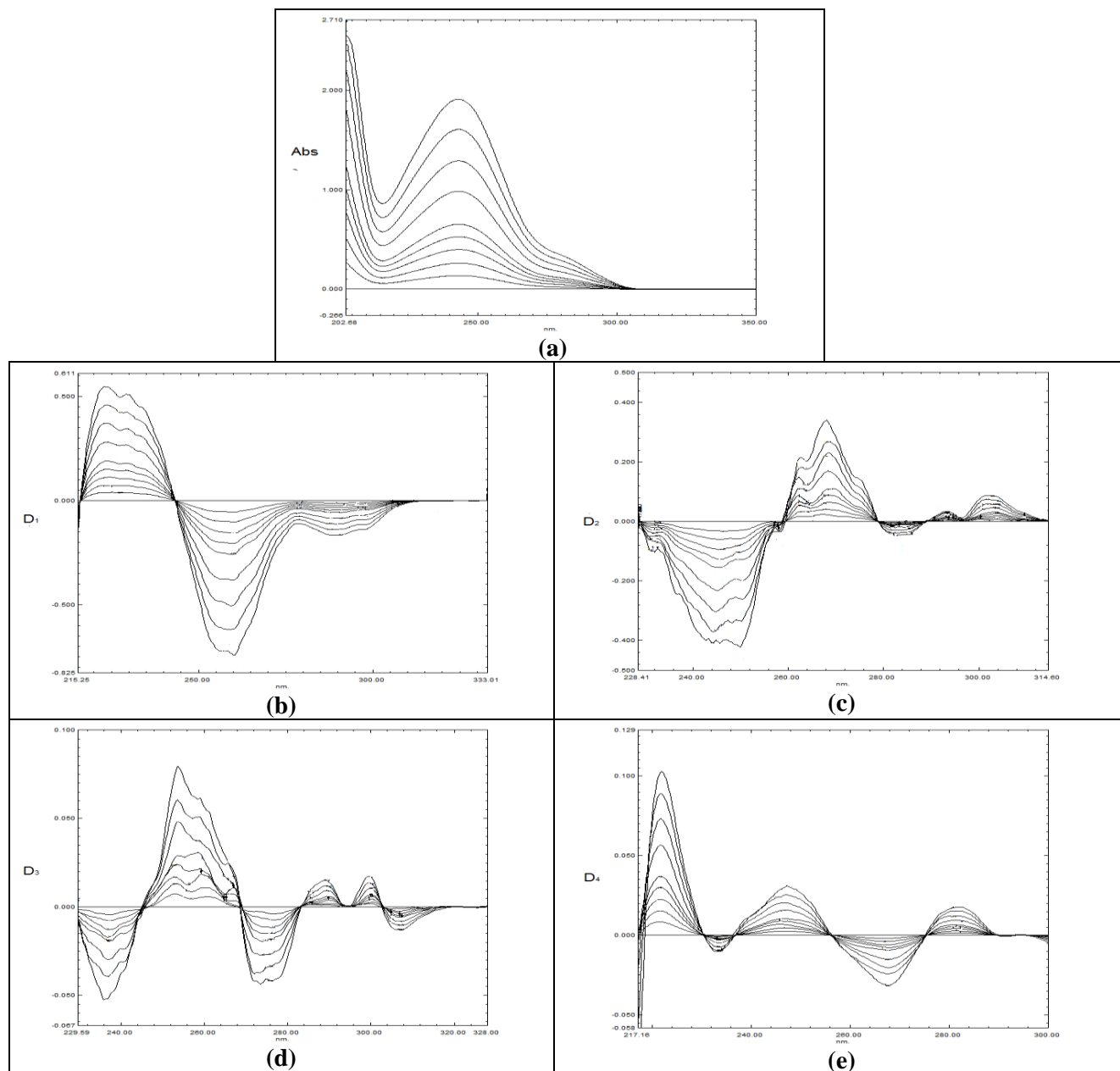


Fig. (3-36) Spectra of 2-30 mg/L PAR ,a- Normal spectra b- First derivative spectra ($S=10, \lambda=2$) c- Second derivative spectra ($S=60, \lambda=4$) d- Third derivative spectra ($S=100, \lambda=8$) e- Fourth derivative spectra ($S=300, \lambda=16$).

Table (3-17): The parameters obtained from the calibration curves for normal and DS teach. of PAR.

Teach.	Conc. range mg/L	λ (nm)	Equation	r	*LOD mg/L	*LOQ mg/L
Normal	2-30	P=243.1	Y= 0.06365X+0.01371	0.9999	0.102	0.339
¹ D	2-30	P=223.5	Y= 0.01818X+0.00389	0.9998	0.129	0.431
	2-30	V=258.6	Y=-0.02411X-0.00976	-0.9996	0.144	0.480
	2-30	V=289.0	Y=-0.00555X-0.00032	-0.9999	0.106	0.355
² D	2-30	P=268.3	Y= 0.01116X-0.00138	0.9992	0.465	1.549
	2-30	P=302.4	Y=0.00290X-0.00027	0.9994	0.484	1.614
	2-30	V=246.6	Y=-0.01314X-0.01336	-0.9992	0.424	1.414
³ D	2-30	V=236.7	Y=-0.00197X-0.00045	-0.9981	0.542	1.805
	2-25	V=275.1	Y=-0.00162X-0.00125	-0.9989	0.431	1.436
⁴ D	2-25	P=221.6	Y= 0.00356X+0.00116	0.9996	0.143	0.476
	2-25	P=280.8	Y=-0.00060X-0.00005	0.9988	0.564	1.879
	2-25	V=267.1	Y=-0.00097X-0.00006	-0.9986	0.548	1.825

Paracetamol can be determined using the above teach. The results for determination synthetic samples of PAR (20 mg/L) and the relative errors are listed in table (3-18).

Table (3-18): The relative error, recovery and standard deviation for the determination synthetic sample of 20 mg/L PAR by using normal and DS teach.

Teach.	λ (nm)	PAR found mg/L	Er %	RC %	δ_{n-1}
Normal	P=243.1	20.328	1.64	101.64	0.067
¹ D	P=223.5	20.506	2.53	102.53	0.027
	V=258.6	20.540	2.70	102.70	0.031
	V=289.0	20.109	0.54	100.54	0.088
² D	P=268.3	20.937	4.69	104.69	0.051
	P=302.4	20.212	1.06	101.06	0.044
	V=246.6	20.524	2.62	102.62	0.054
³ D	V=236.7	19.891	-0.55	99.46	0.036
	V=275.1	20.835	4.18	104.18	0.044
⁴ D	P=221.6	20.617	3.08	103.08	0.027
	P=280.8	20.56	2.80	102.80	0.040
	V=267.1	19.567	-2.17	97.84	0.030

Table (3-18) shows the wavelengths that can be used to determine PAR. The wavelength 268.3 nm in ²D, 275.1nm in ³D and 221.6 nm in ⁴D was not used are used to determine PAR due to the high relative error value.

3.7. Caffeine:

3.7.1. Normal Spectroscopy:

Normal spectra of CAF gave a fixed absorption wavelength at 273.1 nm with molar absorptivity $0.98789 \times 10^4 \text{ L.mol}^{-1}.\text{cm}^{-1}$, as shown in figure (3-37-a).

The calibration curve is linear in the concentration range of 2-30 mg/L, as shown in part one. The LOD and LOQ were 0.035 and 0.117 mg/L respectively. The linear regression equation is $Y=0.05087x+0.00650$, with 0.99995 of the correlation coefficient, as shown in table (3-19).

3.7.2. Derivative Spectrophotometry:

The UV derivative spectra 1D , 2D , 3D and 4D have derived for normal Spectra of CAF. All peaks and valleys below than 220.0 nm not be used because they gave noisy signals.

3.7.2.1. First Derivative:

1D spectra of CAF have derived for normal spectra using ($S = 10$), with ($\Delta \lambda = 2$). Figure (3-37-b) shows that 1D spectrums have one P at 260.3 nm and two V at 235.9 and 286.8 nm. Calibration curve was constructed for the wavelength 260.3, 235.9 and 286.8 nm, as shown in part one. The linear equation, correlation coefficient and the concentration range for these calibration curves are listed in table (3-19).

3.7.2.2. Second Derivative:

2D spectra of CAF have derived for normal spectra using ($S = 60$), with ($\Delta \lambda = 4$), as shown in figure (3-37-c). 2D spectra have two P at 245.3, 293.2 nm and two V at 232.5 and 275.8 nm. Calibration curves were constructed for the wavelengths 245.3, 293.2, 232.5 and 275.8 nm, as shown in part one.

Table (3-19) shows the linear equations, correlation coefficients and the concentration ranges for the calibration curves.

3.7.2.3. Third Derivative:

From the normal spectra of CAF, ³D spectra have derived using ($S = 100$), with ($\Delta \lambda = 8$). Figure (3-37-d) show that ³D spectra have two P at 238.5 and 286.4 nm and three V at 226.6, 264.2 and 300.0 nm. The wavelength at 264.2 nm cannot be used because the 264.2 nm shifted to high value at high concentration.

The calibration curves were constructed at the wavelengths 226.6, 238.5, 286.4 and 300.0 nm, as shown in part one. The linear equations, correlation coefficients and the concentration ranges for these calibration curves are listed in table (3-19).

3.7.2.4. Fourth Derivative

⁴D spectra of CAF have derived for normal spectra by using ($S = 300$), with ($\Delta \lambda = 16$), as shown in figure (3-37-e). ⁴D spectra have three P at 231.0, 280.9 and 304.0 nm, and two V at 244.3 and 292.6 nm. The wavelength at 304.0 nm is very weak; therefore, it was canceled. Calibration curves were constructed for the wavelengths at 231.0, 280.9, 244.3 and 292.6 nm, as shown in part one. Table (3-19) shows the linear equations, correlation coefficients and the concentration ranges for the calibration curves.

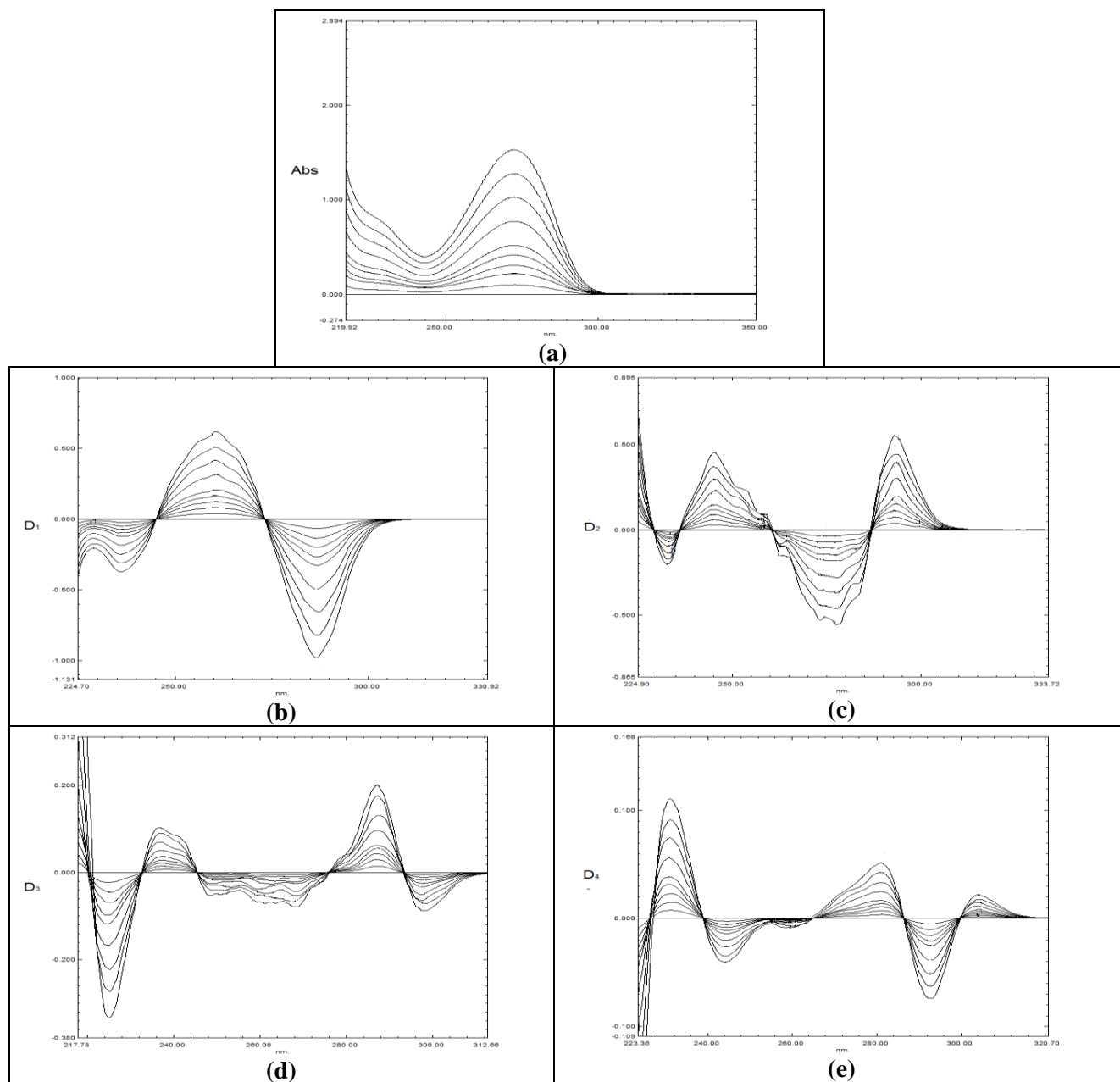


Fig. (3-37) Spectra of 2-30 mg/L CAF ,a- Normal spectra b- First derivative spectra ($S=10, \lambda=2$) c- Second derivative spectra ($S=60, \lambda=4$) d- Third derivative spectra ($S=100, \lambda=8$) e- Fourth derivative spectra ($S=300, \lambda=16$).

Table (3-19): The parameters obtained from the calibration curves for normal and DS teach. of CAF.

Teach.	Conc. range mg/L	λ (nm)	Equation	r	*LOD mg/L	*LOQ mg/L
Normal	2-30	P=273.1	Y= 0.05087X+0.00650	0.9999	0.035	0.117
¹ D	2-30	P=260.3	Y= 0.02058X+0.00106	0.9998	0.125	0.416
	2-30	V=235.9	Y=-0.01242X-0.00142	-0.9999	0.088	0.292
	2-30	V=286.8	Y=-0.03251X-0.00306	-0.9999	0.041	0.136
² D	2-30	P=245.3	Y= 0.01500X-0.00155	0.9997	0.136	0.452
	2-30	P=293.2	Y=0.01813X+0.00847	0.9980	0.283	0.944
	2-30	V=232.5	Y=0.00691X+0.00214	-0.9992	0.477	1.591
	2-30	V=275.8	Y=0.01779X-0.00284	-0.9993	0.312	1.040
³ D	2-30	V=226.6	Y=-0.00993X-0.00247	-0.9996	0.174	0.580
	2-30	P=238.5	Y=-0.00314X+0.00159	0.9989	0.279	0.929
	2-30	P=286.4	Y=0.00668X-0.00093	0.9983	0.383	1.278
	2-30	V=300.0	Y=-0.00259X+0.00023	-0.9991	0.536	1.788
⁴ D	2-30	P=231.0	Y= 0.00367X+0.00075	0.9996	0.153	0.511
	2-30	P=280.9	Y=0.00169X+0.00012	0.9993	0.302	1.007
	2-30	V=244.3	Y=-0.00133X-0.00032	-0.9987	0.557	1.856
	2-30	V=292.6	Y=-0.00251X-0.00051	-0.9995	0.200	0.666

Caffeine can be determined using the above teach. The results for determination synthetic samples of CAF (20 mg/L) and the relative errors are listed in table (3-20).

Table (3-20) The relative error, recovery and standard deviation for the determination synthetic sample of 20 mg/LCAF by using normal and DS teach..

Teach.	λ (nm)	CAF found mg/L	Er %	RC %	δ_{n-1}
Normal	P=273.1	20.213	1.06	101.07	0.037
¹ D	P=260.3	20.207	1.04	101.03	0.033
	V=235.9	19.992	-0.04	99.96	0.044
	V=286.8	20.064	0.32	100.32	0.040
² D	P=245.3	20.197	0.98	100.99	0.030
	P=293.2	21.098	5.49	105.49	0.055
	V=232.5	20.148	0.74	100.74	0.035
	V=275.8	20.702	3.51	103.51	0.027
³ D	V=226.6	20.292	1.46	101.46	0.031
	P=238.5	19.581	-2.10	97.91	0.045
	P=286.4	18.959	-5.21	94.80	0.055
	V=300.0	19.377	-3.12	96.89	0.044
⁴ D	P=231.0	20.238	1.19	101.19	0.031
	P=280.9	19.444	-2.78	97.22	0.028
	V=244.3	19.244	-3.78	96.22	0.028
	V=292.6	20.5	2.50	102.50	0.025

Table (3-20) shows the wavelengths that can be used to determine CAF. The wavelength 293.2, 275.8 nm in ²D and 286.4, 300.0nm in ³D and 244.3nm in ⁴D not be used to determine CAF due to the high relative error value.

3.8. Binary Mixture:

3.8.1. Paracetamol with Caffeine Mixture:

The zero order spectra of standard PAR and CAF were found to be overlapped making the determination unthinkable, as shown in figure (3-44-a).

3.8.1.1. First Derivative:

First derivative tech. can be used to determine PAR only, because there is no suitable wavelength to determine CAF, as shown in figure (3-44-b). In figure (3-38), PAR can be determined at $\lambda = 273.6$ nm, while CAF have no any contribution; Calibration curve of 1D spectra for standard PAR at 273.6 nm was constructed, as shown in part one. The linear equation, correlation coefficient and concentration range for this calibration curve are listed in table (3-29). The results and the relative errors for the determination of PAR in the mixture are listed in tables (3-21).

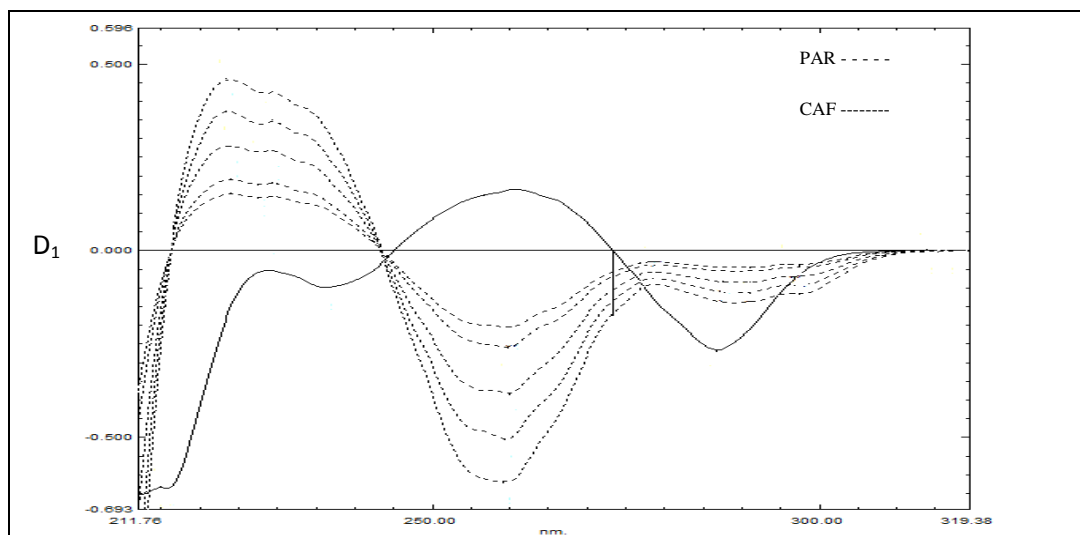


Figure (3-38) 1D spectra for (8-25) mg/L PAR and (8) mg/L CAF (zero crossing) at 273.6nm.

Table (3-21) The relative error and recovery for the determination PAR in the presence of CAF at 273.6 nm using ¹D teach.

<i>PAR and CAF mixtures (mg/L)</i>	<i>PAR found* mg/L</i>	<i>Relative error%</i>	<i>Recovery %</i>	<i>PAR and CAF mixtures (mg/L)</i>	<i>PAR found* mg/L</i>	<i>Relative error%</i>	<i>Recovery %</i>
30PAR+ 0 CAF	30.187	0.62	100.62	20PAR+20 CAF	21.337	6.69	106.69
20PAR+ 0 CAF	19.63	-1.85	98.15	20PAR+25 CAF	22.579	12.90	112.90
10PAR+ 0 CAF	10.159	1.59	101.59	2 PAR +3 CAF	2.086	4.30	104.30
4 PAR + 0 CAF	3.949	-1.28	98.73	4 PAR +3 CAF	4.104	2.60	102.60
20PAR+ 2 CAF	20.716	3.58	103.58	6 PAR +3 CAF	6.123	2.05	102.05
20 PAR+ 4 CAF	20.406	2.03	102.03	8 PAR +3 CAF	8.141	1.76	101.76
20PAR + 6 CAF	20.251	1.26	101.26	10 PAR+3 CAF	10.187	1.87	101.87
20PAR+ 8 CAF	21.027	5.14	105.14	15 PAR+3 CAF	15.438	2.92	102.92
20PAR+10 CAF	21.027	5.14	105.14	20 PAR+3 CAF	20.406	2.03	102.03
20PAR+15 CAF	21.493	7.46	107.47	25 PAR+3 CAF	25.219	0.88	100.88

3.8.1.2. Second Derivative:

Second derivative teach. can be used to determine CAF only in their mixtures, as shown in figure (3-44-c). PAR not be determined; on the other hand, CAF can be determined at P = 223.7 and V=278.8 nm, where PAR absorbance was nil (zero crossing point of PAR), as shown in figure (3-39). Calibration curve of ²D spectra for standard CAF at 223.7 and 278.8 nm were constructed, as shown in part one. The linear equation, correlation coefficient, and concentration range for the calibration curves are listed in table (3-29). The results and the relative errors for the determination of CAF in their mixtures are listed in tables (3-22) and (3-23) .

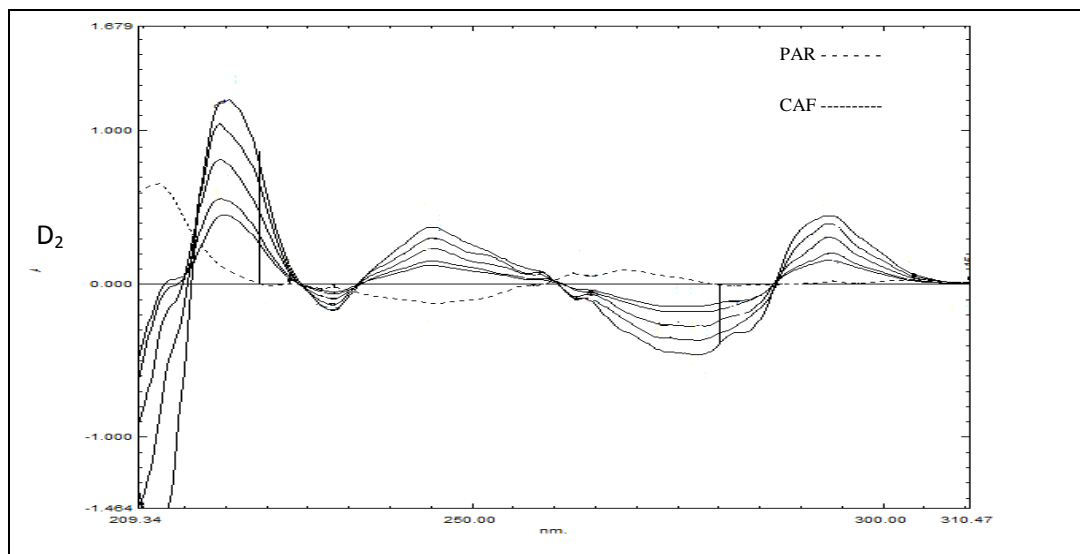


Figure (3-39) 2D spectra for (8-25) mg/L CAF and (8) mg/L PAR (zero crossing) at 223.7 and 278.8 nm

Table (3-22): The relative error and recovery for the determination CAF in the presence of PAR at 223.7 nm using 2D teach.

PAR and CAF mixtures (mg/L)	CAF found* mg/L	Relative error%	Recovery %	PAR and CAF mixtures (mg/L)	CAF found* mg/L	Relative error%	Recovery %
0 PAR+ 30 CAF	29.944	-0.19	99.81	20PAR +20 CAF	20.445	2.23	102.23
0 PAR+ 20 CAF	19.832	-0.84	99.16	20PAR +25 CAF	24.888	-0.45	99.55
0 PAR+ 10 CAF	9.894	-1.06	98.94	2 PAR +3 CAF	2.821	-5.97	94.03
0 PAR + 4 CAF	4.078	1.95	101.95	4 PAR +3 CAF	2.909	-3.03	96.97
20PAR + 2 CAF	1.869	-6.55	93.45	6 PAR +3 CAF	2.821	-5.97	94.03
20PAR + 4 CAF	4.136	3.40	103.40	8 PAR +3 CAF	2.997	-0.10	99.90
20PAR + 6 CAF	6.562	9.37	109.37	10 PAR+3 CAF	2.997	-0.10	99.90
20PAR + 8 CAF	8.257	3.21	103.21	15 PAR+3 CAF	3.172	5.73	105.73
20PAR +10CAF	10.391	3.91	103.91	20 PAR+3 CAF	2.88	-4.00	96.00
20PAR +15CAF	15.857	5.71	105.71	25 PAR+3 CAF	2.792	-6.93	93.07

Table (3-23): The relative error and recovery for the determination CAF in the presence of PAR at 278.8 nm using ²D teach.

<i>PAR and CAF mixtures (mg/L)</i>	<i>CAF found* mg/L</i>	<i>Relative error%</i>	<i>Recovery %</i>	<i>PAR and CAF mixtures (mg/L)</i>	<i>CAF found* mg/L</i>	<i>Relative error%</i>	<i>Recovery %</i>
0 PAR+ 30 CAF	30.137	0.46	100.46	20PAR +20 CAF	19.832	-0.84	99.16
0 PAR + 20CAF	19.665	-1.68	98.33	20PAR +25 CAF	24.846	-0.62	99.38
0 PAR + 10CAF	9.861	-1.39	98.61	2 PAR +3 CAF	2.954	-1.53	98.47
0 PAR + 4 CAF	4.012	0.30	100.30	4 PAR +3 CAF	3.121	4.03	104.03
20PAR + 2CAF	2.063	3.15	103.15	6 PAR +3 CAF	2.954	-1.53	98.47
20PAR + 4CAF	4.124	3.10	103.10	8 PAR +3 CAF	3.065	2.17	102.17
20PAR + 6 CAF	6.185	3.08	103.08	10 PAR+3 CAF	3.121	4.03	104.03
20PAR + 8 CAF	7.856	-1.80	98.20	15 PAR+3 CAF	2.954	-1.53	98.47
20PAR +10CAF	10.195	1.95	101.95	20 PAR+3 CAF	3.065	2.17	102.17

3.8.1.3. Third Derivative:

Third derivative teach. can be used to determine each of PAR and CAF in their mixtures, as shown in figure (3-44-d). In figure (3-40), PAR can be determined at $V = 275.8$ nm, while CAF have no any contribution. Calibration curve of ³D spectra for standard PAR at 275.8 nm was constructed, as shown in part one. The linear equation, correlation coefficient and concentration range for the calibration curve are listed in table (3-29); on the other hand, CAF can be determined at $V=268.6$ nm, where PAR absorbance was nil (zero crossing point of PAR), as shown in figure (3-41). The calibration curve of ³D spectra for standard CAF at 268.6 nm was constructed, as shown in part one. The linear equation, correlation coefficient, and concentration range for the calibration curve are listed in table (3-29). The results and the relative errors for the determination of PAR and CAF in their mixtures are listed in tables (3-24) and (3-25) respectively.

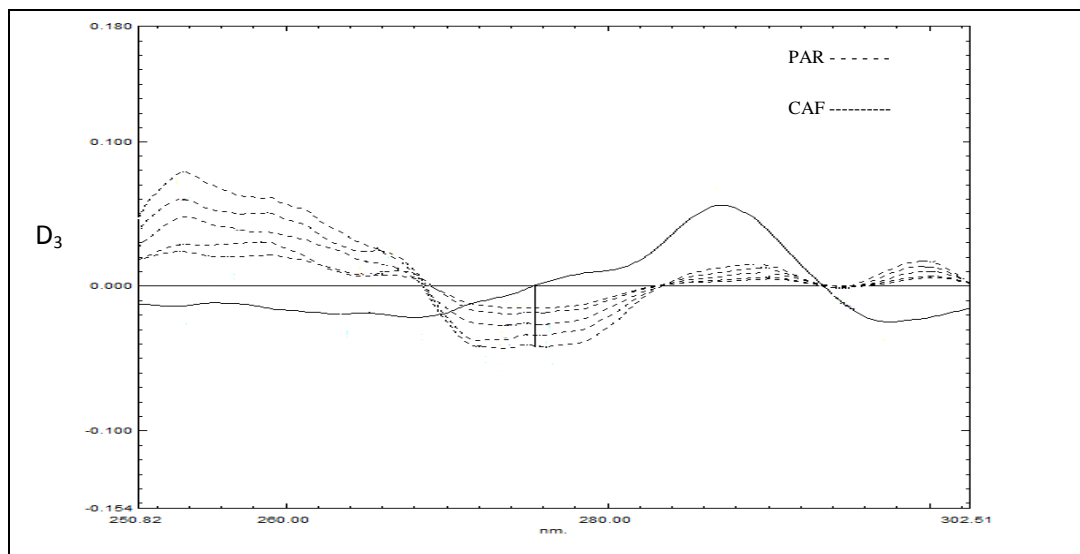


Figure (3-40) ³D spectra for (8-25) mg/L PAR and(8)mg/L CAF (zero crossing) at 275.8 nm.

Table (3-24): The relative error and recovery for the determination PAR in the presence of CAF at 275.8 nm using ³D teach.

<i>PAR and CAF mixtures (mg/L)</i>	<i>PAR found* mg/L</i>	<i>Relative error%</i>	<i>Recovery %</i>	<i>PAR and CAF mixtures (mg/L)</i>	<i>PAR found* mg/L</i>	<i>Relative error%</i>	<i>Recovery %</i>
30PAR+ 0 CAF	29.955	-0.15	99.85	20PAR +20 CAF	20.219	1.10	101.10
20PAR + 0 CAF	20.194	0.97	100.97	20PAR +25 CAF	20.194	0.97	100.97
10PAR + 0 CAF	10.041	0.41	100.41	2 PAR +3 CAF	1.974	-1.30	98.70
4 PAR + 0 CAF	3.997	-0.08	99.93	4 PAR +3 CAF	4.054	1.35	101.35
20PAR + 2 CAF	20.219	1.10	101.10	6 PAR +3 CAF	6.026	0.43	100.43
20PAR + 4 CAF	20.219	1.10	101.10	8 PAR +3 CAF	8.154	1.93	101.93
20PAR + 6 CAF	20.194	0.97	100.97	10 PAR+3 CAF	10.181	1.81	101.81
20PAR + 8 CAF	20.194	0.97	100.97	15 PAR+3 CAF	15.213	1.42	101.42
20PAR +10CAF	19.568	-2.16	97.84	20 PAR+3 CAF	20.219	1.10	101.10
20PAR +15CAF	20.194	0.97	100.97	25 PAR+3 CAF	25.152	0.61	100.61

The results of table (3-24) show that PAR can be determined with high accuracy by ³D teach. at $V = 275.8$ nm, when the mixture contain (0 to more than 50 % ($\frac{W}{W}$))CAF.

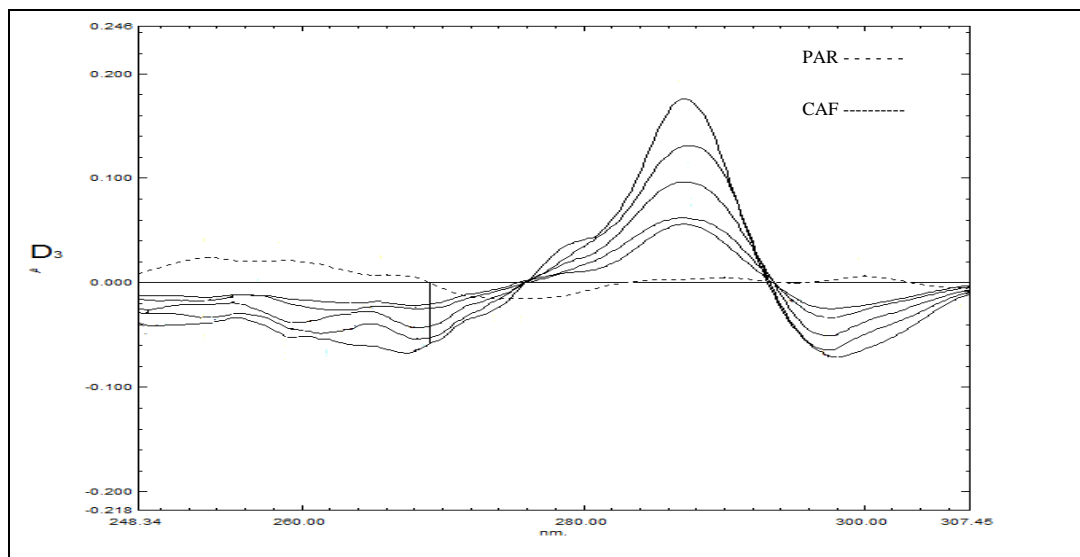


Figure (3-41) ³D spectra for(8-25) mg/L CAF and(8)mg/L PAR (zero crossing) at 268.6nm.

Table (3-25): The relative error and recovery for the determination CAF in the presence of PAR at 268.6 nm using ³D teach..

<i>PAR and CAF mixtures (mg/L)</i>	<i>CAF found* mg/L</i>	<i>Relative error%</i>	<i>Recovery %</i>	<i>PAR and CAF mixtures (mg/L)</i>	<i>CAF found* mg/L</i>	<i>Relative error%</i>	<i>Recovery %</i>
0 PAR+ 30 CAF	30.179	0.60	100.60	20PAR +20 CAF	21.395	6.98	106.98
0 PAR + 20CAF	20.632	3.16	103.16	20PAR +25CAF	24.832	-0.67	99.33
0 PAR + 10CAF	9.557	-4.43	95.57	2 PAR +3 CAF	3.447	14.90	114.90
0 PAR + 4 CAF	3.829	-4.28	95.73	4 PAR +3 CAF	3.065	2.17	102.17
20PAR + 2 CAF	2.123	6.15	106.15	6 PAR +3 CAF	3.065	2.17	102.17
20PAR + 4 CAF	4.284	7.10	107.10	8 PAR +3 CAF	3.447	14.90	114.90
20PAR + 6 CAF	6.502	8.37	108.37	10 PAR+3 CAF	3.447	14.90	114.90
20PAR + 8 CAF	8.087	1.09	101.09	15 PAR+3 CAF	3.447	14.90	114.90
20PAR +10CAF	10.848	8.48	108.48	20 PAR+3 CAF	3.447	14.90	114.90
20PAR +15CAF	15.667	4.45	104.45	25 PAR+3 CAF	3.447	14.90	114.90

3.8.1.4. Fourth Derivative

Fourth derivative tech. can be used to determine each of PAR and CAF in their mixtures, as shown in figure (3-44-e). In figure (3-42), PAR can be determined at $\lambda = 264.8$ nm, while CAF have no any contribution. Calibration curve of 4D spectra for standard PAR at 264.8 nm was constructed, as shown in part one. The linear equation, correlation coefficient and concentration range for the calibration curve are listed in table (3-29); on the other hand, CAF can be determined at $\lambda = 230.4$ and $\lambda = 294.7$ nm, where PAR absorbance was nil (zero crossing point of PAR), as shown in figure (3-43). Calibration curve of 4D spectra for standard CAF at 230.4 and 290.7 nm were constructed, as shown in part one. The linear equation, correlation coefficient, and concentration range for the calibration curves are listed in table (3-29).

The results and the relative errors for the determination of PAR and CAF in their mixtures are listed in tables (3-26), (3-27) and (3-28) respectively.

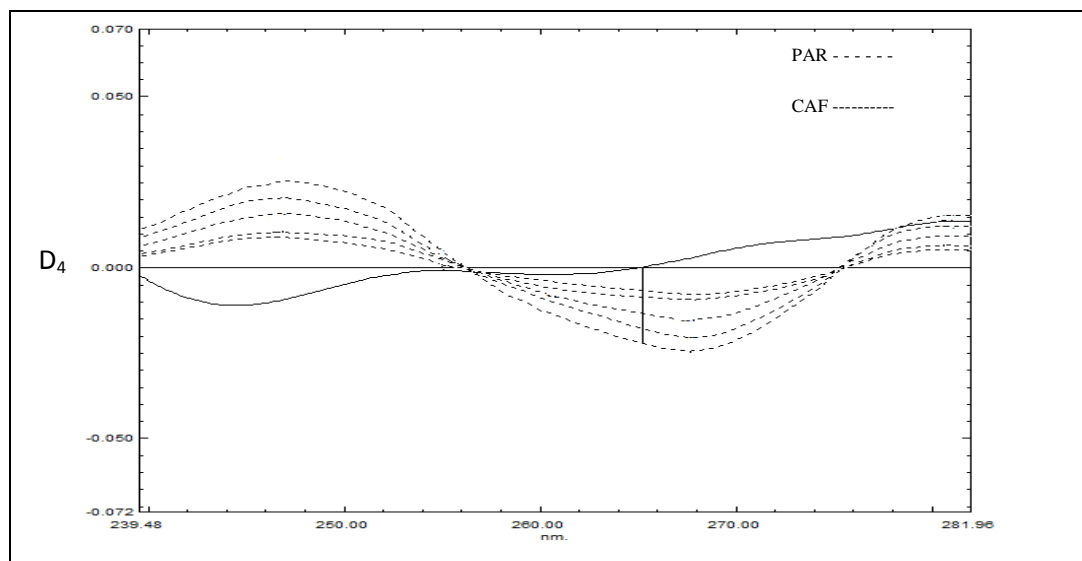


Figure (3-42) 4D spectra for (8-25) mg/L PAR and (8) mg/L CAF (zero crossing) at 264.8nm.

Table (3-26): The relative error and recovery for the determination PAR in the presence of CAF at 264.8 nm using ⁴D teach..

PAR and CAF mixtures (mg/L)	PAR found* mg/L	Relative error%	Recovery %	PAR and CAF mixtures (mg/L)	PAR found* mg/L	Relative error%	Recovery %
30 PAR+ 0 CAF	30.691	2.30	102.30	20PAR +20 CAF	22.65	13.25	113.25
20PAR + 0 CAF	19.204	-3.98	96.02	20PAR +25 CAF	21.502	7.51	107.51
10PAR + 0 CAF	10.015	0.15	100.15	2 PAR +3 CAF	1.995	-0.25	99.75
4 PAR + 0 CAF	4.204	5.10	105.10	4 PAR +3 CAF	4.272	6.80	106.80
20PAR + 2 CAF	20.353	1.77	101.77	6 PAR +3 CAF	6.569	9.48	109.48
20PAR + 4 CAF	21.502	7.51	107.51	8 PAR +3 CAF	8.866	10.83	110.83
20PAR + 6 CAF	20.353	1.77	101.77	10 PAR+3 CAF	11.164	11.64	111.64
20PAR + 8 CAF	21.502	7.51	107.51	15 PAR+3 CAF	15.758	5.05	105.05
20PAR +10CAF	22.65	13.25	113.25	20 PAR+3 CAF	21.502	7.51	107.51
20PAR +15CAF	22.65	13.25	113.25	25 PAR+3 CAF	24.948	-0.21	99.79

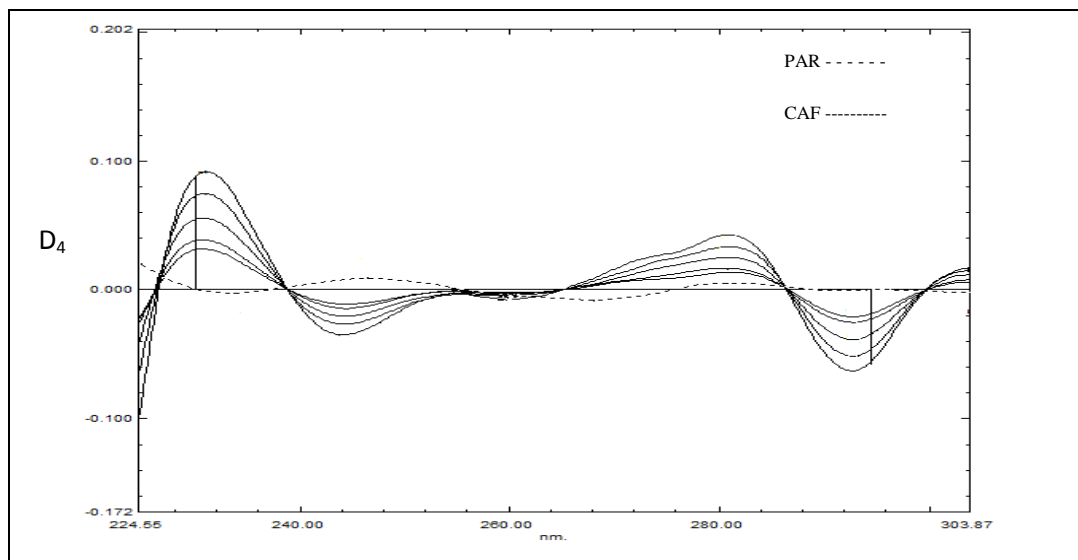


Figure (3-43) ⁴D spectra for (8-25) mg/L CAF and (8) mg/L PAR (zero crossing) at 230.4 and 294.7nm.

Table (3-27): The relative error and recovery for the determination CAF in the presence of PAR at 230.4 nm using ⁴D teach..

<i>PAR and CAF mixtures (mg/L)</i>	<i>CAF found* mg/L</i>	<i>Relative error%</i>	<i>Recovery %</i>	<i>PAR and CAF mixtures (mg/L)</i>	<i>CAF found* mg/L</i>	<i>Relative error%</i>	<i>Recovery %</i>
0 PAR+ 30 CAF	29.931	-0.23	99.77	20PAR +20 CAF	20.195	0.98	100.98
0 PAR+ 20 CAF	19.082	-4.59	95.41	20PAR +25 CAF	24.646	-1.42	98.58
0 PAR+ 10 CAF	9.902	-0.98	99.02	2 PAR +3 CAF	2.948	-1.73	98.27
0 PAR + 4 CAF	3.783	-5.43	94.58	4 PAR +3 CAF	2.948	-1.73	98.27
20PAR + 2 CAF	2.192	9.60	109.60	6 PAR +3 CAF	2.948	-1.73	98.27
20PAR + 4 CAF	4.339	8.48	108.48	8 PAR +3 CAF	2.948	-1.73	98.27
20PAR + 6 CAF	6.286	4.77	104.77	10 PAR+3 CAF	2.948	-1.73	98.27
20PAR + 8 CAF	8.512	6.40	106.40	15 PAR+3 CAF	3.226	7.53	107.53
20PAR +10CAF	10.181	1.81	101.81	20 PAR+3 CAF	3.226	7.53	107.53
20PAR +15CAF	15.188	1.25	101.25	25 PAR+3 CAF	3.226	7.53	107.53

Table (3-28): The relative error and recovery for the determination CAF in the presence of PAR at 294.7 nm using ⁴D teach..

<i>PAR and CAF mixtures (mg/L)</i>	<i>CAF found* mg/L</i>	<i>Relative error%</i>	<i>Recovery %</i>	<i>PAR and CAF mixtures (mg/L)</i>	<i>CAF found* mg/L</i>	<i>Relative error%</i>	<i>Recovery %</i>
0 PAR+ 30 CAF	29.95	-0.17	99.83	20PAR +20 CAF	20.222	1.11	101.11
0 PAR+ 20 CAF	20.158	0.79	100.79	20PAR +25 CAF	25.233	0.93	100.93
0 PAR+ 10 CAF	9.971	-0.29	99.71	2 PAR +3 CAF	3.001	0.03	100.03
0 PAR + 4 CAF	3.93	-1.75	98.25	4 PAR +3 CAF	3.001	0.03	100.03
20PAR + 2 CAF	2.012	0.60	100.60	6 PAR +3 CAF	3.001	0.03	100.03
20PAR + 4 CAF	4.095	2.37	102.38	8 PAR +3 CAF	3.001	0.03	100.03
20PAR + 6 CAF	6.054	0.90	100.90	10 PAR+3 CAF	3.001	0.03	100.03
20PAR + 8 CAF	8.177	2.21	102.21	15 PAR+3 CAF	3.001	0.03	100.03
20PAR+10 CAF	10.035	0.35	100.35	20 PAR+3 CAF	3.001	0.03	100.03
20PAR+15 CAF	15.011	0.07	100.07	25 PAR+3 CAF	3.001	0.03	100.03

The results of table (3-28) show that CAF can be determined with high accuracy by ⁴D teach. at $V = 294.4$ nm, when the mixture contain (0 to more than 50% ($\frac{W}{W}$) PAR).

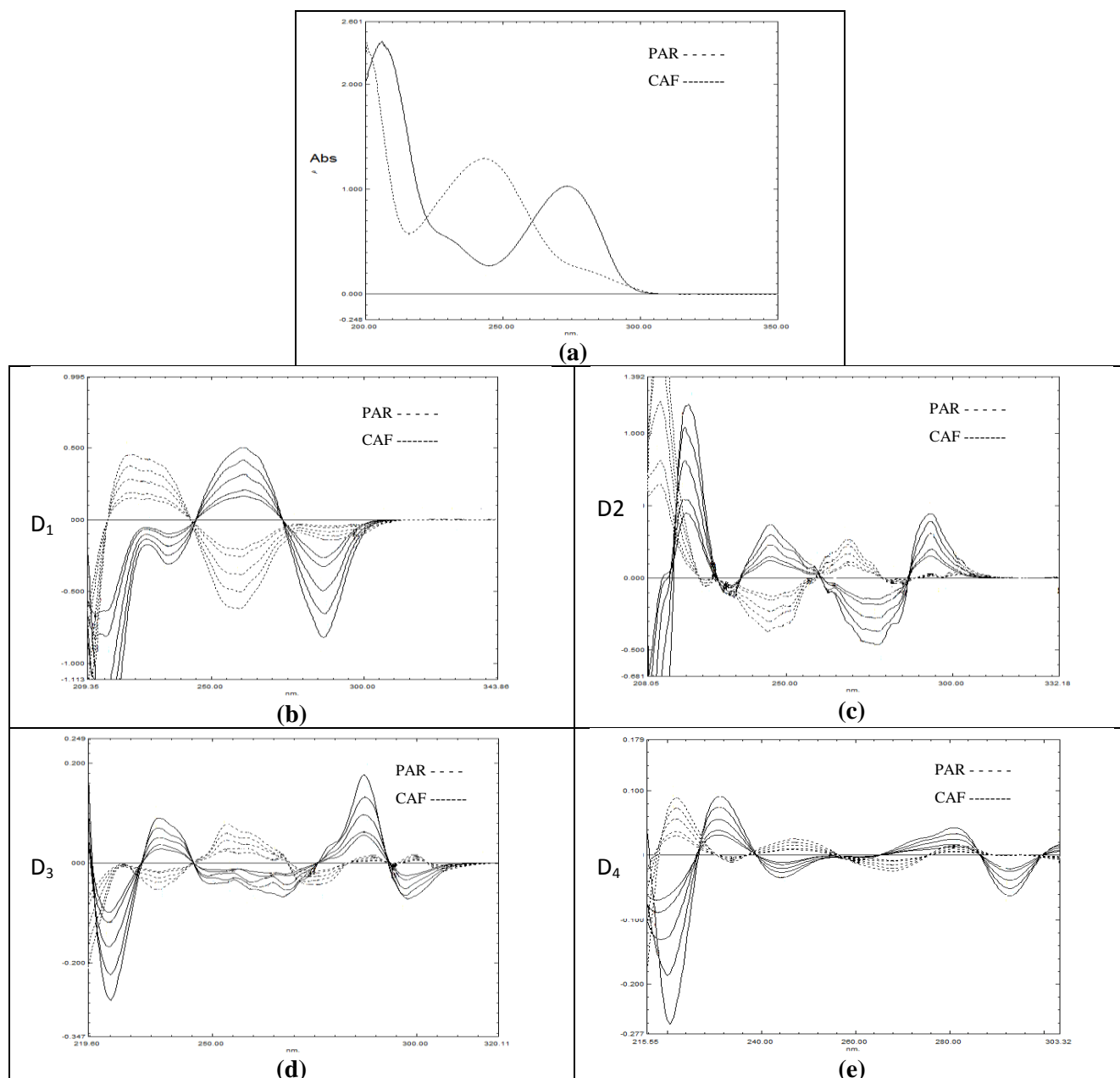


Fig. (3-44) Spectra of 8-25 mg/L PAR 8-25 mg/LCAF a- Normal spectra of 20 mg/Lfor each PAR and CAF. b- First derivative spectra ($S=10, \lambda=2$) c- Second derivative spectra ($S=60, \lambda=4$) d- Third derivative spectra ($S=100, \lambda=8$) e- Fourth derivative spectra ($S=300, \lambda=16$).

Table (3-29): The parameters obtained from the calibration curves for DS teach. of PAR and CAF.

Teach.		Conc. range mg/L	λ (nm)	Equation	r
PAR	¹ D	2-30	V=273.6	Y=-0.00644x-0.00156	-0.9998
	³ D	2-35	V=275.8	Y=-0.00160x-0.00173	-0.9987
	⁴ D	2-30	V=264.8	Y=-0.00087x-0.00028	-0.9988
CAF	² D	2-30	P=223.7	Y= 0.03421x+0.01148	0.9996
	² D	2-30	V=278.8	Y=-0.01795x+0.00203	-0.9998
	³ D	2-30	V=268.6	Y=-0.00262x+0.00003	-0.9970
	⁴ D	2-30	P=230.4	Y= 0.00359x+0.00140	0.9995
	⁴ D	2-35	V=294.7	Y=-0.00215x-0.00054	-0.9995

Table (3-30) show that PAR can be determined in the presence of CAF by using ³D teach. at 275.8 nm, while CAF can be determined in the presence PAR by using ⁴D teach. at 294.7 nm.

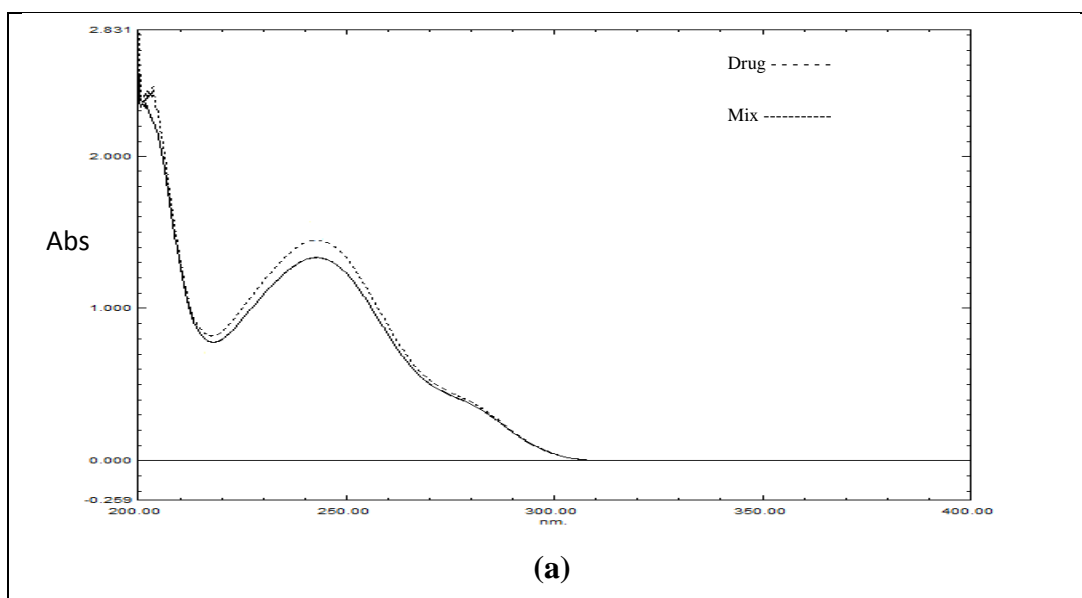
Table (3-30) Statistical data for the calibration curves that used to determine PAR and CAF in their mixture.

Drug	PAR	CAF
Teach.	³ D	⁴ D
λ (nm)	V=275.8	V=294.7
Linearity range (mg/L)	2-35	2-35
r	0.9987	0.9995
Slope	-0.00160	-0.00215
Intercept	-0.00173	-0.00054
LOD (mg/L)	0.445	0.162
LOQ (mg/L)	1.482	0.541
*RSD (concentration)**	0.222	0.130
*SD	0.045	0.004

*n = 3. ** Concentration = 20 mg/L for PAR and 3 mg/L for CAF.

3.9. Interferences study:

To find an effect of matrix constituents on the results of determination, comparative analysis was carried out for standard solution containing active components at concentrations (20PAR+3CAF) mg/L comparable to those of the analyzed drug contain the same concentration, they show the same normal spectra Fig.(3-45-a). while Fig.(3-45-b)show comparers between standard solution containing active components at concentrations (20PAR+3CAF) mg/L with interfering material (starch, gelatin, magnesium setrate, avecil, sucrose)at ten time of concentrations (20PAR+3CAF) mg/L.



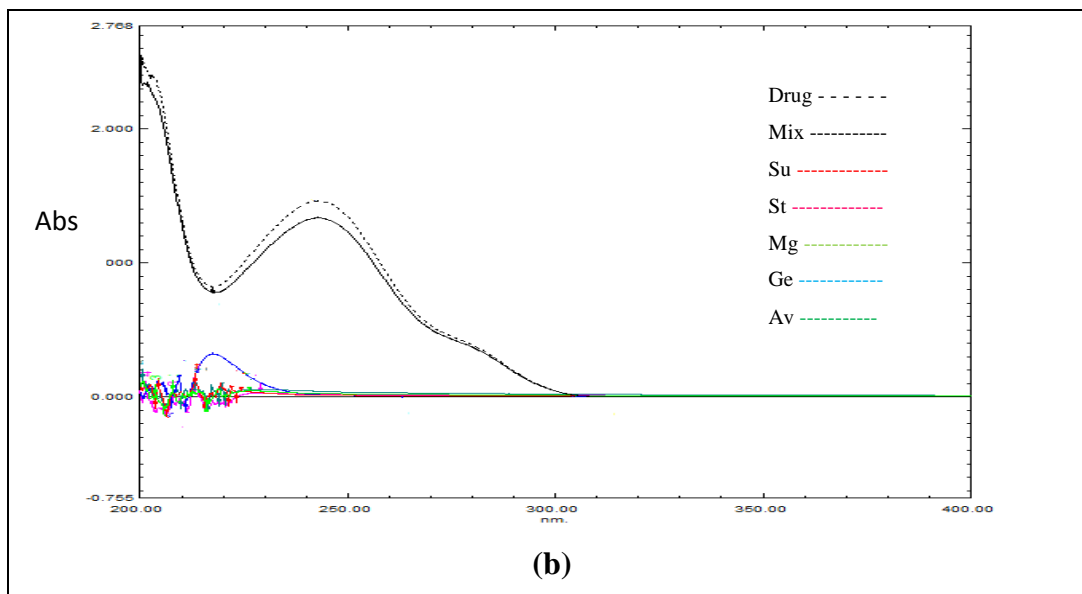


Fig. (3-45) Normal spectra for analyzed preparation (a)Mix with drug (b)Mix with drug with interferes (Av,Ge,Mg,St,Su)

3.10. Analysis of Pharmaceutical Samples:

3.10.1. Paracetamol with Caffeine Mixture:

(PANADOL EXTRA-PAR500, CAF65) sample was measured by using ^3D , and ^4D teach., as shown in table (3-31).

Table (3-31) The relative error and recovery for the determination of Panadol extra sample (20 mg/LPAR + 3mg/LCAF) by using DS teach.

Drugs	Panadol extra (PAR)	Panadol extra (CAF)
Teach.	^3D	^4D
λ (nm)	V=275.8	V=294.7
Conc. found (mg/L)	20.444	3.094
Er %	2.220	3.133
RC %	102.220	103.133
$\mu = \bar{x} \pm (t\delta)/\sqrt{n}$	20.444 \pm 0.426	3.094 \pm 0.259
$\delta n-1$	0.342	0.208

*Each concentration represents an average of at least five measurements.

Table (3-32): Statistical data for the determination of (PAR + CAF) in their mixture in pure and pharmaceutical form by ³D for PAR & ⁴D for CAF.

PAR+CAF Mixture	PAR				CAF			
	Found mg/L $\lambda=275.8\text{nm}$	ER%	RC%	RSD %	Found mg/L $\lambda=294.7\text{nm}$	ER%	RC%	RSD %
Standard								
20PAR+3CAF	20.219	1.09	101.09	0.222	3.001	0.03	100.03	0.130
Panadol Extra								
20PAR+3CAF	20.444	2.22	102.22	1.674	3.094	3.13	103.13	6.721

*Each concentration represents an average of at least three measurements.

- **Part Three:**

3.11. Hyoscine-n-butyl bromide:

3.11.1. Normal Spectroscopy

Normal UV spectra of HYO shows have no any specific wavelength, as shown in figure (3-46-a).

3.11.2. Derivative Spectrophotometry:

The UV derivative spectra 1D , 2D , 3D and 4D have derived for normal spectra of HYO.

3.11.2.1. Selection of Optimum Instrumental Conditions:

The scaling factor affecting only on the derivative amplitude, weak derivative amplitude needs to high scaling factor to give a good high peak, The suitable scaling factor that chosen to give good peak were 6, 25, 75 and 150 for 1D , 2D , 3D and 4D respectively and for the PAR and HYO. However, if the value of $\Delta\lambda$ is too large, the spectral intensity signal of the first derivative deteriorates, ⁽⁴⁶⁾. The suitable $\Delta\lambda$ that optimized to give good selectivity were 2, 4, 8 and 16 for 1D , 2D , 3D and 4D respectively for the PAR and HYO.

3.11.2.2. First Derivative:

1D spectra of HYO have derived for normal spectra using ($S = 6$), with ($\Delta\lambda=2$). Figure (3-46-b) shows that 1D spectra have one V at 209.2 nm. The calibration curve was constructed for the wavelength 209.2 nm, as shown in part one. The linear equation, correlation coefficient and the concentration range for the calibration curve are listed in table (3-33).

3.11.2.3. Second Derivative:

²D spectra of HYO have derived for normal spectra using ($S = 25$), with ($\Delta\lambda=4$), as shown in figure (3-46-c). ²D spectra have two P at 213.7 and 220.3 nm. The calibration curves were constructed for the wavelengths 213.7 and 220.3 nm, as shown in part one. Table (3-33) shows the linear equations, correlation coefficients and the concentration ranges for the calibration curves.

3.11.2.4. Third Derivative:

From the normal spectra of HYO, ³D spectra have derived using ($S = 75$), with ($\Delta\lambda = 8$). Fig.(3-46-d) show that ³D spectra have one P at 210.5 nm and one V at 216.6 nm. The calibration curves were constructed at the wavelengths 210.5 and 216.6 nm, as shown in part one.

The linear equations, correlation coefficients and the concentration ranges for the two calibration curves are listed in table (3-33).

3.11.2.5. Fourth Derivative:

⁴D spectra of HYO have derived for normal spectra by using ($S = 150$), with ($\Delta\lambda = 16$), as shown in figure (3-46-e). ⁴D spectra have one P at 223.0 nm, and one V at 215.1 nm. The calibration curves were constructed for the wavelengths at 223.0 and 215.1 nm, as shown in part one. Table (3-33) shows the linear equations, correlation coefficients and the concentration ranges for the calibration curves.

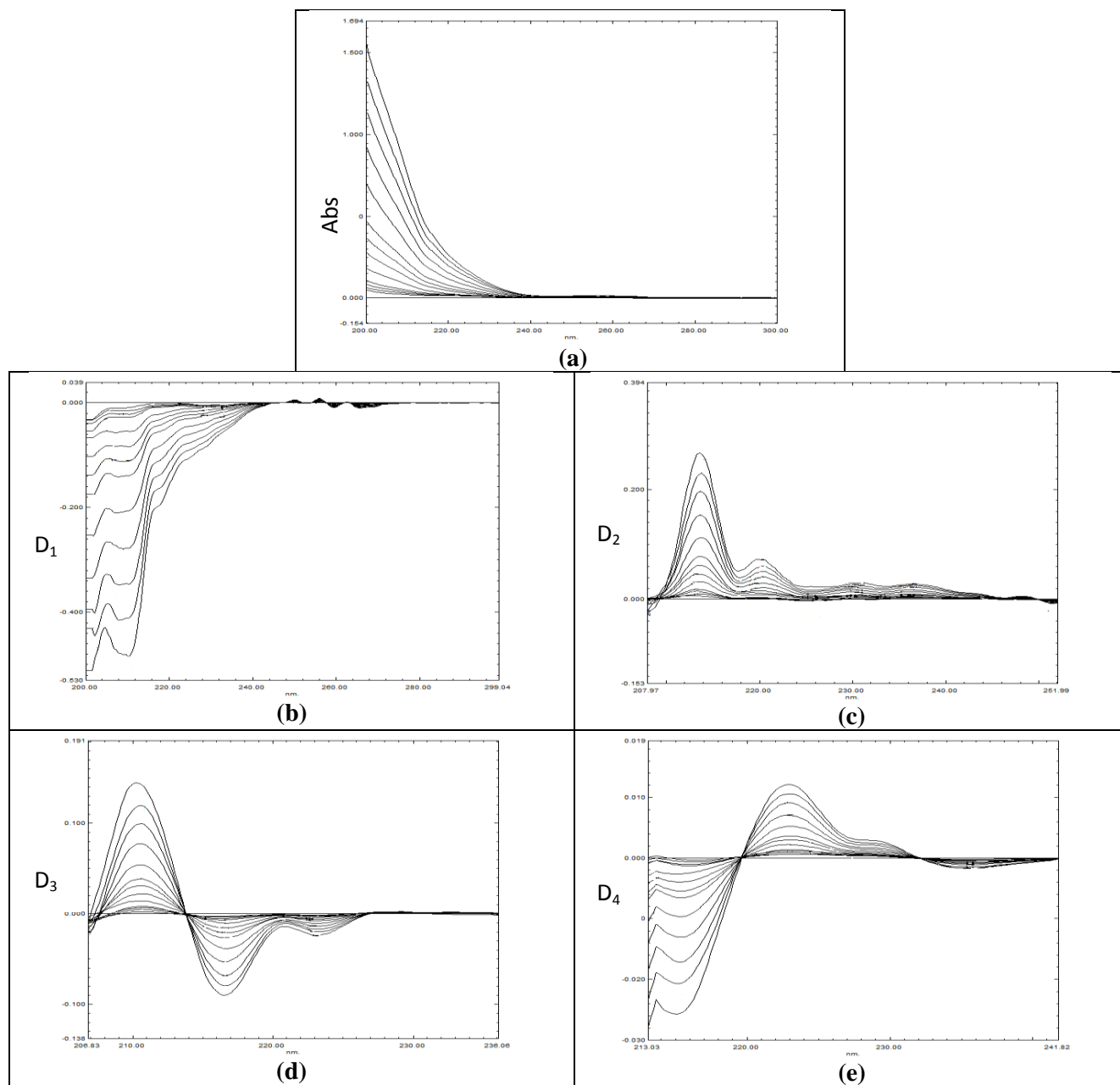


Fig. (3-46) Spectra of 0.5-35 mg/L HYO ,a- Normal spectra b- First derivative spectra ($S=6,\lambda=2$) c- Second derivative spectra ($S=25,\lambda=4$) d- Third derivative spectra ($S=75,\lambda=8$) e- Fourth derivative spectra ($S=150,\lambda=16$).

Table (3-33) The parameters obtained from the calibration curves for DS teach. of HYO.

Teach.	Conc. range mg/L	λ (nm)	Equation	r	*LOD mg/L	*LOQ mg/L
¹ D	0.5-35	V=209.2	Y=-0.01374X-0.00150	-0.9999	0.033	0.109
² D	0.5-35	P=213.7	Y= 0.00758X+0.00129	0.9998	0.111	0.369
	0.5-35	P=220.3	Y= 0.00206X-0.00099	0.9996	0.118	0.393
³ D	0.5-35	P=210.5	Y=-0.00402X-0.00126	0.9989	0.189	0.629
	0.5-35	V=216.6	Y=-0.00259X-0.00094	-0.9992	0.436	1.452
⁴ D	4-35	P=223.0	Y= 0.00036X-0.00004	0.9966	0.557	1.856
	2-30	V=215.1	Y=-0.00070X+0.00040	-0.9982	0.481	1.602

Hyoscine can be determined using the above teach. The results for determination synthetic samples of HYO (20 mg/L) and the relative errors are listed in table (3-34).

Table (3-34): The relative error and recovery for the determination synthetic sample of 20 mg/LHYO by using DS teach..

Teach.	λ (nm)	HYO found mg/L	Er %	RC %	δ_{n-1}
¹ D	V=209.2	20.191	0.95	100.95	0.030
² D	P=213.7	20.004	0.02	100.02	0.023
	P=220.3	19.935	-0.32	99.69	0.041
³ D	P=210.5	19.460	-2.70	97.30	0.029
	V=216.6	20.074	0.37	100.37	0.043
⁴ D	P=223.0	19.813	-0.94	99.06	0.021
	V=215.1	19.236	-3.82	96.18	0.038

3.12. Binary Mixture:

3.12.1. Paracetamol with Hyoscine Mixture:

The zero order spectra of standard PAR and HYO were found to be overlapped making the determination unthinkable, as shown in figure (3-52-a).

3.12.1.1. First Derivative:

First derivative tech. can be used to determine each of PAR and HYO in their mixtures, as shown in figure (3-52-b). In figure (3-47), PAR can be determined at $\lambda = 257.5$ and $\lambda = 297.4$ nm, while HYO have no any contribution. Calibration curve of 1D spectra for standard PAR at 257.5 and 297.4 nm were constructed, as shown in part one. The linear equation, correlation coefficient and concentration range for the calibration curves are listed in table (3-45); on the other hand, HYO can be determined at $\lambda = 215.9$ nm, where PAR absorbance was nil (zero crossing point of PAR), as shown in figure (3-48). Calibration curve of 1D spectra for standard HYO at 215.9 nm were constructed, as shown in part one. The linear equation, correlation coefficient, and concentration range for the calibration curve are listed in table (3-45). The results and the relative errors for the determination of PAR and CAF in their mixtures are listed in tables (3-35), (3-36) and (3-37) respectively.

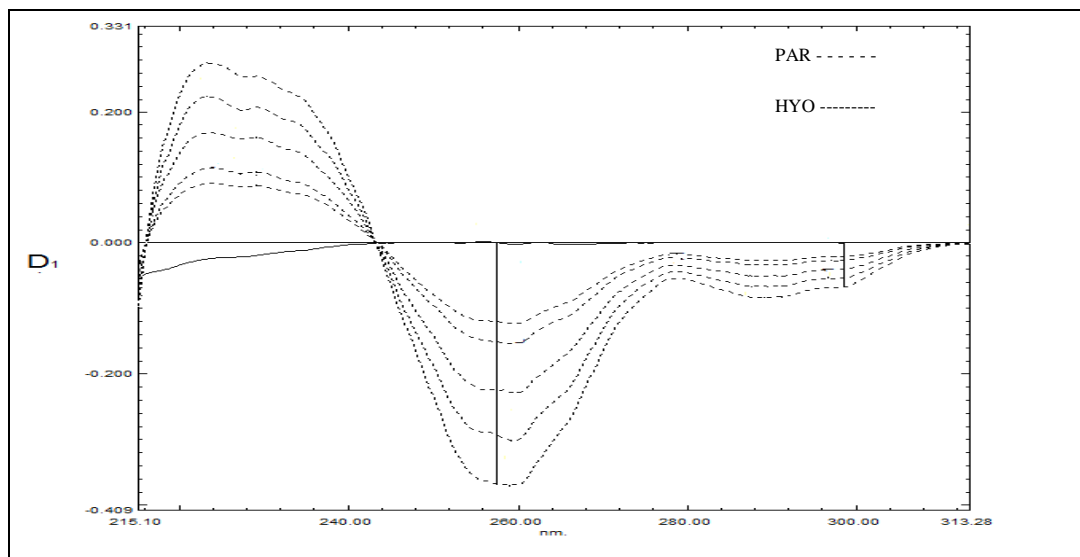


Figure (3-47) ¹D spectra for (8-25) mg/L PAR and (8)mg/L HYO (zero crossing) at 257.5 and 297.4nm.

Table (3-35): The relative error and recovery for the determination PAR in the presence of HYO at 257.5 nm using ¹D teach.

<i>PAR and HYO mixtures (mg/L)</i>	<i>PAR found* mg/L</i>	<i>Relative error%</i>	<i>Recovery %</i>	<i>PAR and HYO mixtures(mg/L)</i>	<i>PAR found* mg/L</i>	<i>Relative error%</i>	<i>Recovery %</i>
30PAR+ 0 HYO	29.639	-1.20	98.80	25PAR+15 HYO	27.75	11.00	111.00
20PAR+ 0 HYO	20.195	0.98	100.98	25PAR+20 HYO	27.68	10.72	110.72
10PAR+ 0 HYO	10.191	1.91	101.91	25PAR+25 HYO	27.75	11.00	111.00
4 PAR + 0 HYO	3.755	-6.13	93.88	2 PAR+0.5 HYO	2.006	0.30	100.30
25PAR+0.5HYO	27.47	9.88	109.88	4 PAR+0.5 HYO	4.245	6.13	106.13
25PAR+ 1 HYO	27.61	10.44	110.44	6 PAR+0.5 HYO	6.553	9.22	109.22
25PAR + 2 HYO	27.401	9.60	109.60	8 PAR+0.5 HYO	8.792	9.90	109.90
25PAR +4 HYO	27.47	9.88	109.88	10PAR+0.5HYO	10.89	8.90	108.90
25PAR +6 HYO	27.61	10.44	110.44	15PAR+0.5HYO	16.697	11.31	111.31
25PAR +8 HYO	27.261	9.04	109.04	20PAR+0.5HYO	21.524	7.62	107.62
25PAR+ 10HYO	22.084	-11.66	88.34	25PAR+0.5HYO	27.47	9.88	109.88

Table (3-36): The relative error and recovery for the determination PAR in the presence of HYO at 297.4 nm using ¹D teach.

PAR and HYO mixtures (mg/L)	PAR found* mg/L	Relative error%	Recovery %	PAR and HYO mixtures (mg/L)	PAR found* mg/L	Relative error%	Recovery %
30 PAR+ 0 HYO	30.433	1.44	101.44	25 PAR+15HYO	24.809	-0.76	99.24
20PAR + 0 HYO	19.922	-0.39	99.61	25 PAR+20HYO	24.809	-0.76	99.24
10PAR + 0 HYO	9.873	-1.27	98.73	25PAR +25HYO	24.809	-0.76	99.24
4 PAR + 0 HYO	3.974	-0.65	99.35	2 PAR +0.5HYO	2.031	1.55	101.55
25PAR+0.5HYO	25.171	0.68	100.68	4PAR +0.5 HYO	4.036	0.90	100.90
25PAR+ 1 HYO	24.809	-0.76	99.24	6 PAR +0.5HYO	6.111	1.85	101.85
25PAR + 2 HYO	25.171	0.68	100.68	8PAR +0.5 HYO	8.186	2.33	102.33
25 PAR +4 HYO	25.809	3.24	103.24	10PAR+0.5HYO	10.298	2.98	102.98
25PAR +6 HYO	24.446	-2.22	97.78	15PAR+0.5HYO	15.297	1.98	101.98
25PAR +8 HYO	24.446	-2.22	97.78	20PAR+0.5HYO	20.009	0.05	100.05
25PAR+10 HYO	24.809	-0.76	99.24	25PAR+0.5HYO	25.171	0.68	100.68

The results of table (3-36) show that PAR can be determined with high accuracy by ¹D teach. at $\lambda = 297.4$ nm, when the mixture contain (0 to 50% ($\frac{W}{W}$) HYO).

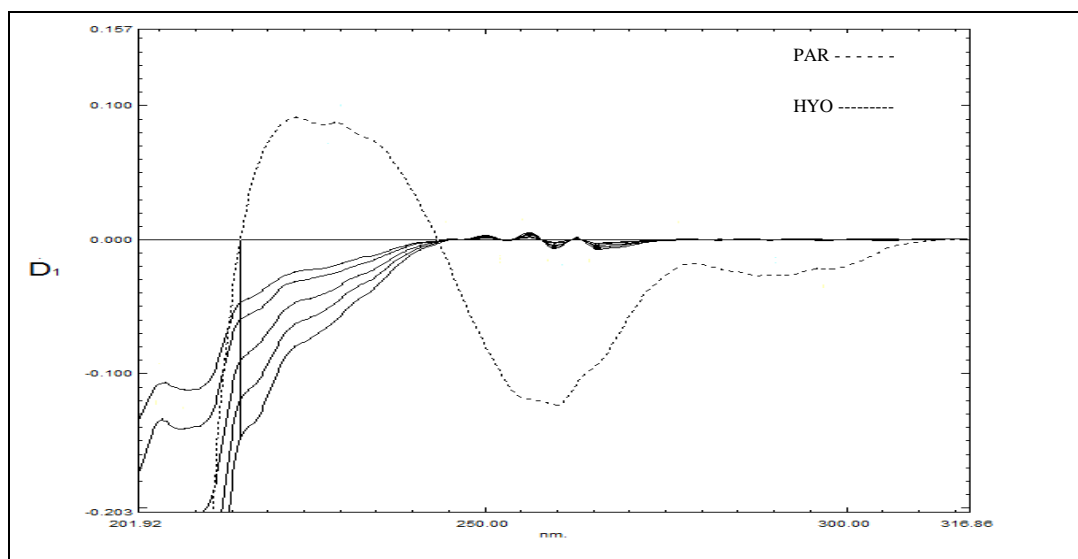


Figure (3-48) ¹D spectra for (8-25) mg/LHYO and (8)mg/L PAR (zero crossing) at 215.9nm.

Table (3-37): The relative error and recovery for the determination HYO in the presence of PAR at 215.9 nm using ¹D teach.

PAR and HYO mixtures (mg/L)	HYO found* mg/L	Relative error%	Recovery %	PAR and HYO mixtures (mg/L)	HYO found* mg/L	Relative error%	Recovery %
0 PAR+ 30 HYO	29.519	-1.60	98.40	25PAR +15HYO	15.387	2.58	102.58
0 PAR+ 20 HYO	20.281	1.40	101.41	25PAR +20HYO	20.402	2.01	102.01
0 PAR+ 10 HYO	10.103	1.03	101.03	25PAR +25HYO	25.126	0.504	100.504
0 PAR+ 4 HYO	4.056	1.40	101.40	2 PAR +0.5HYO	0.486	-2.80	97.20
25PAR+0.5HYO	0.506	1.20	101.20	4 PAR +0.5HYO	0.486	-2.80	97.20
25PAR+ 1 HYO	1.014	1.40	101.40	6 PAR +0.5HYO	0.512	2.40	102.40
25PAR + 2 HYO	2.023	1.15	101.15	8 PAR +0.5HYO	0.506	1.20	101.20
25PAR +4 HYO	4.118	2.95	102.95	10PAR+0.5HYO	0.512	2.40	102.40
25PAR +6 HYO	6.206	3.43	103.43	15PAR+0.5HYO	0.512	2.40	102.40
25PAR +8 HYO	8.143	1.79	101.79	20PAR+0.5HYO	0.512	2.40	102.40
25PAR+10 HYO	10.256	2.56	102.56	25PAR+0.5HYO	0.506	1.20	101.20

The results of table (3-37) show that HYO can be determined with high accuracy by ¹D teach. at $V = 215.9$ nm, when the mixture contain (0 to more than 50% ($\frac{W}{W}$) PAR).

3.12.1.2. Second Derivative:

Second derivative teach. can be used to determine PAR only, because there is no suitable wavelength to determine HYO, as shown in figure (3-52-c). In figure (3-49), PAR can be determined at $V = 245.4$, $P = 268.2$ and $P = 303.5$ nm, while HYO have no any contribution; The calibration curve of ²D spectra for standard PAR at 245.4, 268.2 and 303.5 nm was constructed, as shown in part one. The linear equation, correlation coefficient and concentration range for those calibration curves are listed in table (3-45).

The results and the relative errors for the determination of PAR in the mixture are listed in tables (3-38) to (3-40) respectively.

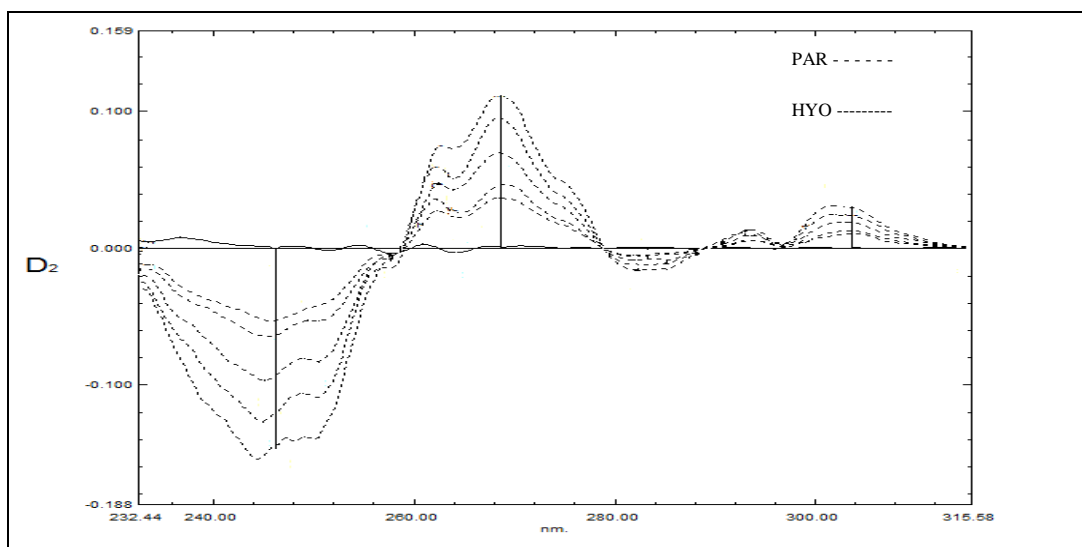


Figure (3-49) 2D spectra for (8-25) mg/L PAR and (8) mg/L HYO (zero crossing) at 245.5, 268.2 and 303.5nm.

Table (3-38): The relative error and recovery for the determination PAR in the presence of HYO at 245.4 nm using 2D teach.

PAR and HYO mixtures (mg/L)	PAR found* mg/L	Relative error%	Recovery %	PAR and HYO mixtures (mg/L)	PAR found* mg/L	Relative error%	Recovery %
25 PAR+ 0 HYO	23.984	-4.06	95.94	25PAR+15 HYO	24.656	-1.38	98.62
20PAR + 0 HYO	20.118	0.59	100.59	25PAR+20 HYO	24.656	-1.38	98.62
10PAR + 0 HYO	9.863	-1.37	98.63	25PAR+25 HYO	24.152	-3.39	96.61
4 PAR + 0 HYO	3.643	-8.93	91.08	2 PAR +0.5HYO	1.896	-5.20	94.80
25PAR+0.5HYO	24.825	-0.70	99.30	4 PAR +0.5HYO	3.834	-4.15	95.85
25PAR + 1 HYO	25.497	1.99	101.99	6 PAR +0.5HYO	5.997	-0.05	99.95
25PAR + 2 HYO	27.01	8.04	108.04	8 PAR +0.5HYO	8.35	4.38	104.38
25PAR + 4 HYO	26.337	5.35	105.35	10PAR+0.5HYO	10.199	1.99	101.99
25PAR + 6 HYO	26.169	4.68	104.68	15PAR+0.5HYO	15.411	2.74	102.74
25PAR + 8 HYO	24.993	-0.03	99.97	20PAR+0.5HYO	20.286	1.43	101.43
25PAR+ 10HYO	26.842	7.37	107.37	25PAR+0.5HYO	24.825	-0.70	99.30

Table (3-39): The relative error and recovery for the determination PAR in the presence of HYO at 268.2 nm using ²D teach.

<i>PAR and HYO mixtures (mg/L)</i>	<i>PAR found* mg/L</i>	<i>Relative error%</i>	<i>Recovery %</i>	<i>PAR and HYO mixtures (mg/L)</i>	<i>PAR found* mg/L</i>	<i>Relative error%</i>	<i>Recovery %</i>
30 PAR+ 0 HYO	30.015	0.05	100.05	25PAR+15 HYO	23.714	-5.14	94.86
20PAR + 0 HYO	20.02	0.10	100.10	25PAR+20 HYO	23.062	-7.75	92.25
10PAR + 0 HYO	9.807	-1.93	98.07	25PAR+25 HYO	23.062	-7.75	92.25
4 PAR + 0 HYO	3.723	-6.93	93.08	2 PAR +0.5HYO	2.419	20.95	120.95
25PAR+0.5HYO	25.017	0.07	100.07	4 PAR +0.5HYO	4.592	14.80	114.80
25PAR + 1 HYO	23.931	-4.28	95.72	6 PAR +0.5HYO	6.113	1.88	101.88
25PAR + 2 HYO	23.496	-6.02	93.98	8 PAR +0.5HYO	8.124	1.55	101.55
25PAR + 4 HYO	23.496	-6.02	93.98	10PAR+0.5HYO	9.985	-0.15	99.85
25PAR + 6 HYO	24.366	-2.54	97.46	15PAR+0.5HYO	15.239	1.59	101.59
25PAR + 8 HYO	24.148	-3.41	96.59	20PAR+0.5HYO	20.889	4.45	104.45
25PAR+ 10HYO	24.800	-0.80	99.20	25PAR+0.5HYO	25.017	0.07	100.07

Table (3-40): The relative error and recovery for the determination PAR in the presence of HYO at 303.5 nm using ²D teach..

<i>PAR and HYO mixtures (mg/L)</i>	<i>PAR found* mg/L</i>	<i>Relative error%</i>	<i>Recovery %</i>	<i>PAR and HYO mixtures (mg/L)</i>	<i>PAR found* mg/L</i>	<i>Relative error%</i>	<i>Recovery %</i>
25 PAR+ 0 HYO	29.648	-1.17	98.83	25PAR+15 HYO	25.055	0.22	100.22
20PAR + 0 HYO	19.542	-2.29	97.71	25PAR+20 HYO	25.055	0.22	100.22
10PAR + 0 HYO	10.155	1.55	101.55	25PAR+25 HYO	24.136	-3.46	96.54
4 PAR + 0 HYO	3.924	-1.90	98.10	2 PAR +0.5HYO	2.032	1.60	101.60
25PAR+0.5HYO	25.055	0.22	100.22	4 PAR +0.5HYO	4.087	2.17	102.18
25PAR + 1 HYO	25.055	0.22	100.22	6 PAR +0.5HYO	5.924	-1.27	98.73
25PAR + 2 HYO	25.973	3.89	103.89	8 PAR +0.5HYO	8.162	2.03	102.03
25PAR + 4 HYO	25.055	0.22	100.22	10PAR+0.5HYO	10.218	2.18	102.18
25PAR + 6 HYO	25.055	0.22	100.22	15PAR+0.5HYO	15.211	1.41	101.41
25PAR + 8 HYO	24.136	-3.46	96.54	20PAR+0.5HYO	19.705	-1.48	98.53
25PAR+ 10HYO	24.136	-3.46	96.54	25PAR+0.5HYO	25.055	0.22	100.22

The results of table (3-40) show that PAR can be determined with high accuracy by 3D teach. at $P = 303.5$ nm, when the mixture contain (0 to 50% ($\frac{W}{W}$)HYO).

3.12.1.3. *Third Derivative:*

Third derivative teach. can be used to determine PAR only, because there is no suitable wavelength to determine HYO, as shown in figure (3-52-d). In figure (3-50), PAR can be determined at $V = 237.1$, $V=214.0$ nm, while HYO have no any contribution; The calibration curve of 3D spectra for standard PAR at 237.1, and 214.0 nm was constructed, as shown in part one .The linear equation, correlation coefficient and concentration range for those calibration curves are listed in table (3-45). The results and the relative errors for the determination of PAR in the mixture are listed in tables (3-41) and (3-42).

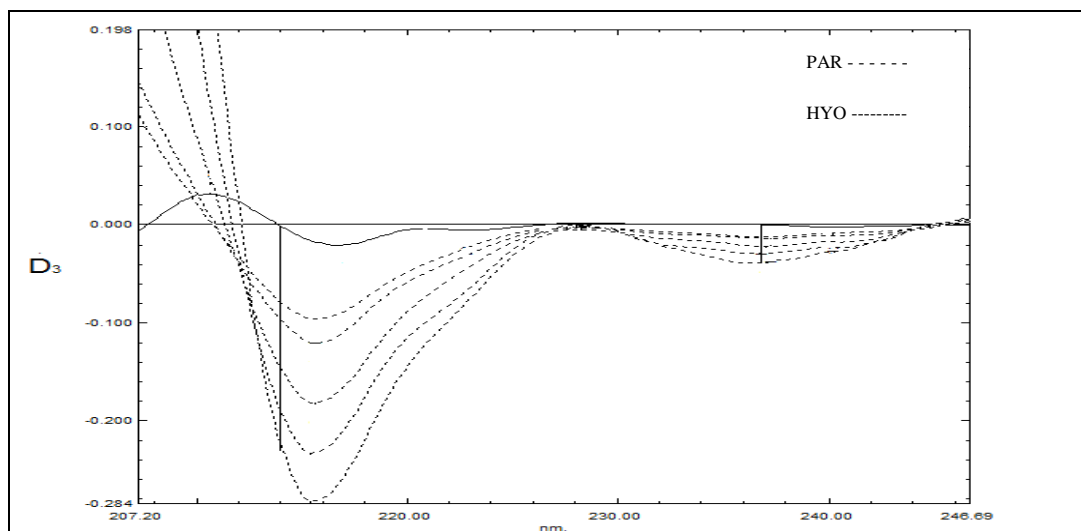


Figure (3-50) 3D spectra for (8-25) mg/LPAR and (8) mg/L HYO (zero crossing) at 237.1 and 214.0nm.

Table (3-41): The relative error and recovery for the determination PAR in the presence of HYO at 237.1 nm using ³D teach.

<i>PAR and HYO mixtures (mg/L)</i>	<i>PAR found* mg/L</i>	<i>Relative error%</i>	<i>Recovery %</i>	<i>PAR and HYO mixtures (mg/L)</i>	<i>PAR found* mg/L</i>	<i>Relative error%</i>	<i>Recovery %</i>
25 PAR+ 0 HYO	28.969	-3.44	96.56	25PAR+15 HYO	29.649	18.60	118.60
20PAR + 0 HYO	18.765	-6.18	93.83	25PAR+20 HYO	29.649	18.60	118.60
10PAR + 0 HYO	9.242	-7.58	92.42	25PAR+25 HYO	28.289	13.156	113.156
4 PAR + 0 HYO	3.799	-5.03	94.98	2 PAR +0.5HYO	2.239	11.95	111.95
25PAR+0.5HYO	26.928	7.71	107.71	4 PAR +0.5HYO	3.845	-3.88	96.13
25PAR + 1 HYO	28.969	15.88	115.88	6 PAR +0.5HYO	6.701	11.68	111.68
25PAR + 2 HYO	26.248	4.99	104.99	8 PAR +0.5HYO	8.742	9.28	109.28
25PAR + 4 HYO	24.207	-3.17	96.83	10PAR+0.5HYO	9.922	-0.78	99.22
25PAR + 6 HYO	27.609	10.44	110.44	15PAR+0.5HYO	14.684	-2.11	97.89
25PAR + 8 HYO	25.568	2.27	102.27	20PAR+0.5HYO	20.126	0.63	100.63
25PAR+ 10HYO	29.649	18.60	118.60	25PAR+0.5HYO	26.248	4.99	104.99

Table (3-42): The relative error and recovery for the determination PAR in the presence of HYO at 214.0 nm using ³D teach.

<i>PAR and HYO mixtures (mg/L)</i>	<i>PAR found* mg/L</i>	<i>Relative error%</i>	<i>Recovery %</i>	<i>PAR and HYO mixtures (mg/L)</i>	<i>PAR found* mg/L</i>	<i>Relative error%</i>	<i>Recovery %</i>
25 PAR+ 0 HYO	24.26	-2.96	97.04	25PAR+15 HYO	21.073	-15.71	84.29
20PAR + 0 HYO	19.204	-3.98	96.02	25PAR+20 HYO	21.292	-14.83	85.17
10PAR + 0 HYO	10.082	0.82	100.82	25PAR+25 HYO	21.292	-14.83	85.17
4 PAR + 0 HYO	3.818	-4.55	95.45	2 PAR +0.5HYO	1.943	-2.85	97.15
25PAR+0.5HYO	23.710	-5.16	94.84	4 PAR +0.5HYO	3.987	-0.32	99.68
25PAR + 1 HYO	23.710	-5.16	94.84	6 PAR +0.5HYO	6.126	2.10	102.10
25PAR + 2 HYO	21.292	-14.83	85.17	8 PAR +0.5HYO	8.434	5.42	105.43
25PAR + 4 HYO	21.073	-15.71	84.29	10PAR+0.5HYO	10.192	1.92	101.92
25PAR + 6 HYO	23.710	-5.16	94.84	15PAR+0.5HYO	15.577	3.85	103.85
25PAR + 8 HYO	21.073	-15.71	84.29	20PAR+0.5HYO	20.523	2.62	102.62
25PAR+ 10HYO	21.292	-14.83	85.17	25PAR+0.5HYO	24.501	-2.00	98.00

3.12.1.4. Fourth Derivative:

Fourth derivative tech. can be used to determine PAR only, because there is no suitable wavelength to determine HYO, as shown in figure (3-52-e). In figure (3-51), PAR can be determined at $P = 219.7$, $V = 266.3$ nm, while HYO have no any contribution; The calibration curve of 4D spectra for standard PAR at 219.7, and 266.3 nm was constructed, as shown in part one. The linear equation, correlation coefficient and concentration range for those calibration curves are listed in table (3-45). The results and the relative errors for the determination of PAR in the mixture are listed in tables (3-43) and (3-44).

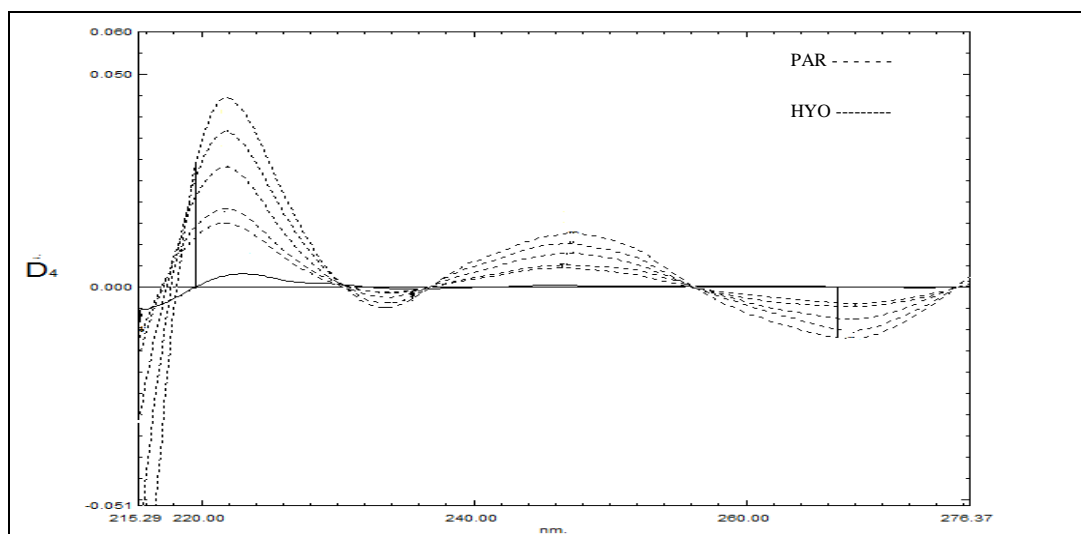


Figure (3-51) 4D spectra for (8-25) mg/L PAR and (8)mg/L HYO (zero crossing) at 219.7 and 266.3nm.

Table (3-43): The relative error and recovery for the determination PAR in the presence of HYO at 219.7 nm using ⁴D teach..

<i>PAR and HYO mixtures (mg/L)</i>	<i>PAR found* mg/L</i>	<i>Relative error%</i>	<i>Recovery %</i>	<i>PAR and HYO mixtures (mg/L)</i>	<i>PAR found* mg/L</i>	<i>Relative error%</i>	<i>Recovery %</i>
20 PAR+ 0 HYO	19.429	-2.86	97.15	25PAR+15 HYO	20.168	-19.33	80.67
15PAR + 0 HYO	15.731	4.87	104.87	25PAR+20 HYO	20.908	-16.37	83.63
4 PAR + 0 HYO	3.897	-2.58	97.43	2 PAR +0.5HYO	1.765	-11.75	88.25
25PAR+0.5HYO	20.168	-19.33	80.67	4 PAR +0.5HYO	3.954	-1.15	98.85
25PAR + 1 HYO	20.908	-16.37	83.63	6 PAR +0.5HYO	6.221	3.68	103.68
25PAR + 2 HYO	20.168	-19.33	80.67	8 PAR +0.5HYO	8.411	5.14	105.14
25PAR + 4 HYO	20.908	-16.37	83.63	10PAR+0.5HYO	9.965	-0.35	99.65
25PAR + 6 HYO	20.168	-19.33	80.67	15PAR+0.5HYO	15.731	4.87	104.87
25PAR + 8 HYO	20.168	-19.33	80.67	20PAR+0.5HYO	19.65	-1.75	98.25
25PAR+ 10HYO	20.908	-16.37	83.63	25PAR+0.5HYO	20.168	-19.33	80.67

Table (3-44): The relative error and recovery for the determination PAR in the presence of HYO at 266.3 nm using ⁴D teach.

<i>PAR and HYO mixtures (mg/L)</i>	<i>PAR found* mg/L</i>	<i>Relative error%</i>	<i>Recovery %</i>	<i>PAR and HYO mixtures (mg/L)</i>	<i>PAR found* mg/L</i>	<i>Relative error%</i>	<i>Recovery %</i>
30 PAR+ 0 HYO	30.238	0.79	100.79	25PAR+15 HYO	26.449	5.80	105.80
20PAR + 0 HYO	20.127	0.63	100.64	25PAR+20 HYO	26.449	5.80	105.80
10PAR + 0 HYO	10.092	0.92	100.92	25PAR+25 HYO	26.449	5.80	105.80
4 PAR + 0 HYO	3.973	-0.68	99.33	2 PAR +0.5HYO	2.026	1.30	101.30
25PAR+0.5HYO	24.414	-2.34	97.66	4 PAR +0.5HYO	4.062	1.55	101.55
25PAR + 1 HYO	26.449	5.80	105.80	6 PAR +0.5HYO	6.097	1.62	101.62
25PAR + 2 HYO	26.449	5.80	105.80	8 PAR +0.5HYO	8.132	1.65	101.65
25PAR + 4 HYO	24.414	-2.34	97.66	10PAR+0.5HYO	10.167	1.67	101.67
25PAR + 6 HYO	26.449	5.80	105.80	15PAR+0.5HYO	15.273	1.82	101.82
25PAR + 8 HYO	24.414	-2.34	97.66	20PAR+0.5HYO	20.344	1.72	101.72
25PAR+ 10HYO	24.414	-2.34	97.66	25PAR+0.5HYO	24.414	-2.34	97.66

Table (3-44) shows that PAR can be determined in the presence of HYO by using 1D teach. At 297.4 nm and 2D teach. at 303.5nm, while HYO can be determined in the presence PAR by using 1D teaches. At 215.9 nm.

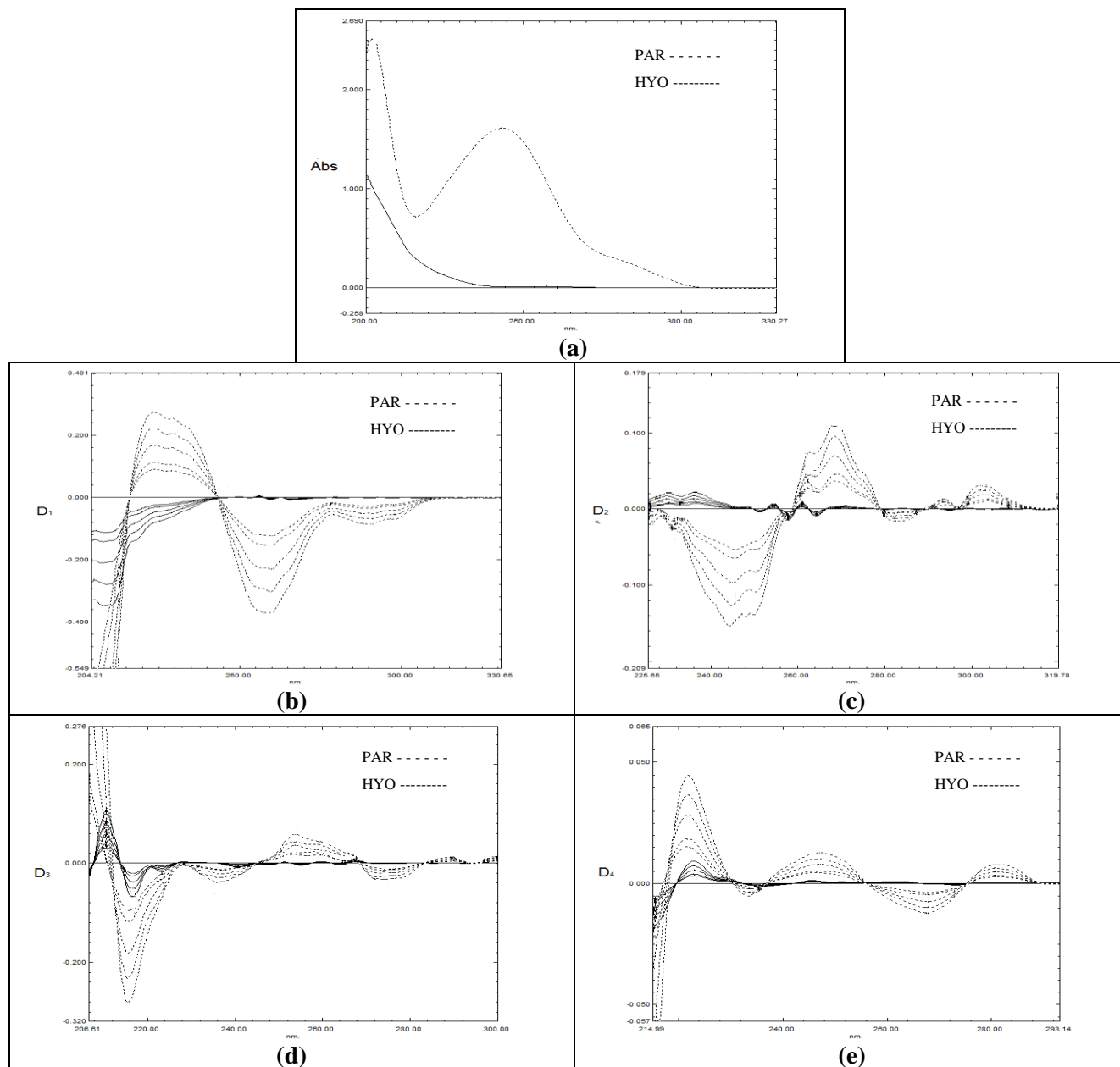


Fig. (3-52) Spectra of 8-25 mg/L PAR 8-25 mg/LHYO a- Normal spectra of 25 mg/L for each PAR and HYO. b- First derivative spectra ($S=6\lambda=2$) c- Second derivative spectra ($S=25,\lambda=4$) d- Third derivative spectra ($S=75,\lambda=8$) e- Fourth derivative spectra ($S=150,\lambda=16$)

Table (3-45): The parameters obtained from the calibration curves for DS teach. of PAR and HYO.

Teach.		Conc. range mg/L	λ (nm)	Equation	r
PAR	¹ D	2-30	V=257.5	Y=-0.01439×-0.00542	-0.9996
	¹ D	2-30	V=297.4	Y=-0.00278×+0.00012	-0.9998
	² D	2-25	V=245.4	Y=-0.00595×-0.00333	-0.9985
	² D	2-30	P=268.2	Y= 0.00468×-0.00091	0.9990
	² D	2-30	P=303.5	Y= 0.00111×+0.00151	0.9987
	³ D	2-35	V=237.1	Y=-0.00145×-0.00041	-0.9983
	³ D	2-25	V=214.0	Y=-0.00910×-0.00626	-0.9986
	⁴ D	2-20	P=219.7	Y= 0.00135×+0.00073	0.9976
	⁴ D	2-30	V=266.3	Y=-0.00049×-0.00000	-0.9991
HYO	¹ D	2-25	V=215.9	Y=-0.00602×+0.00111	-0.9997

Table (3-46) Statistical data for the calibration curves that used to determine PAR and HYO in their mixture.

Drug	PAR		HYO
Teach.	¹ D	² D	¹ D
λ (nm)	V=297.4	P=303.5	V=215.9
Linearity range (mg/L)	2-30	2-30	2-25
r	0.9998	0.9987	0.9997
Slope	-0.00278	0.00111	-0.00602
Intercept	+0.00012	+0.00151	+0.00111
LOD (mg/L)	0.081	0.250	0.091
LOQ (mg/L)	0.269	0.832	0.302
*RSD (concentration)**	0.107	0.400	0.342
*SD	0.027	0.100	0.002

*n = 3. ** Concentration = 25 mg/L for PAR and 0.5 mg/L for HYO

3.13. Interferences study:

To find an effect of matrix constituents on the results of determination, comparative analysis was carried out for standard solution containing active components at concentrations (25PAR+0.5HYO) mg/L comparable to those of the analyzed drug contain the same concentration, they show the same normal spectra Fig.(3-53-a).while Fig.(3-53-b)show comparable between standard solution containing active components at concentrations (25PAR+0.5HYO) mg/L with interfering material (Titanium dioxide)at ten time of concentrations (25PAR+0.5HYO) mg/L.

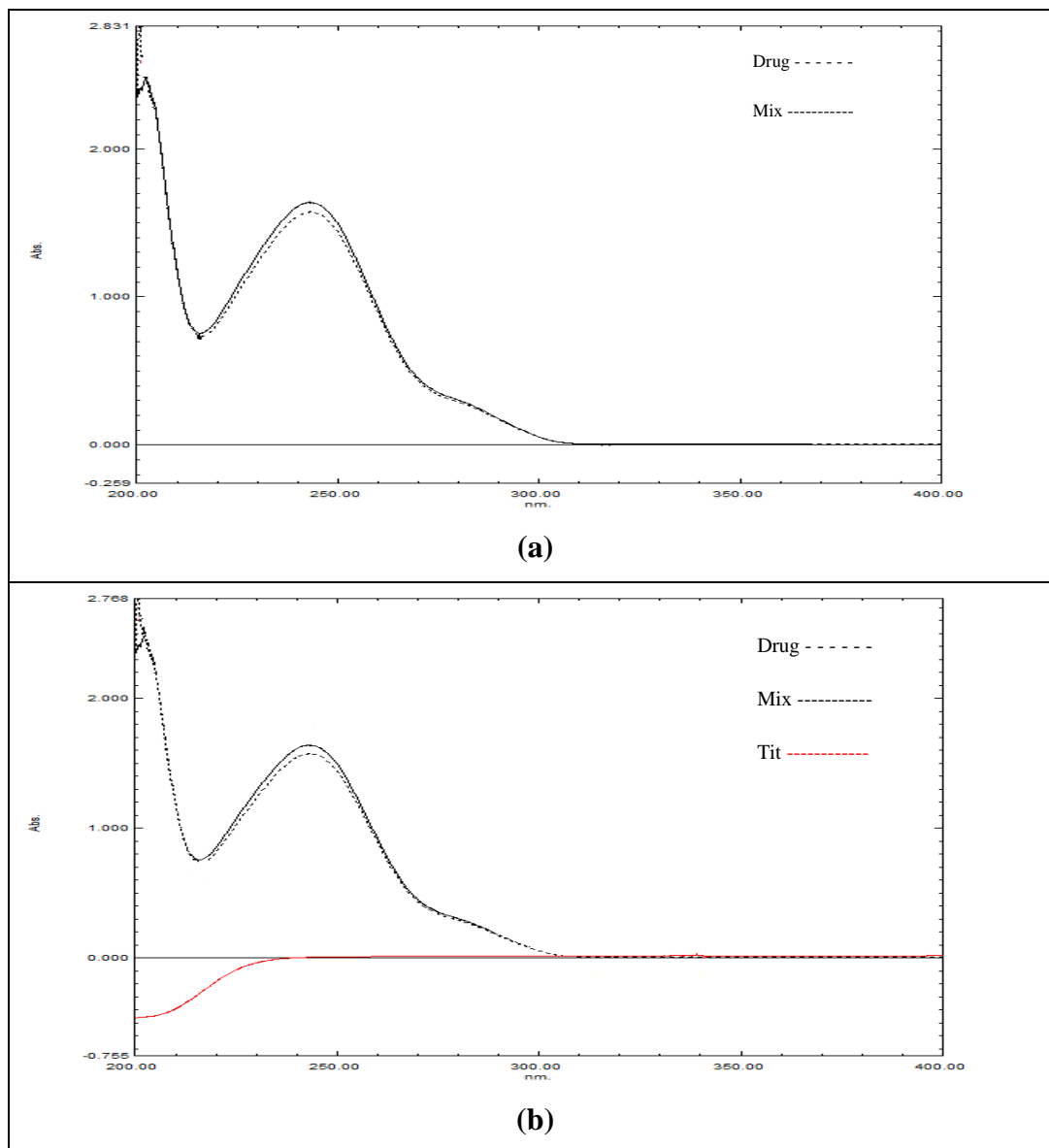


Fig. (3-53) Normal spectra for analyzed preparation.(a)Mix with drug (b)Mix with Tit.

3.14. Analysis of Pharmaceutical Samples:

3.14.1. Paracetamol with Hyoscine Mixture:

SPAZMOTIC PLUS sample (25 mg/L) was measured by using 1D , and 2D teach., as shown in table (3-47).

Table (3-47): The relative error and recovery for the determination of Spazmotic plus sample (25 mg/LPAR + 0.5 mg/LHYO) by using DS teach.

Drugs	Spazmotic plus (PAR)	
	¹ D	² D
Teach.		
λ (nm)	V=297.4	P=303.5
Conc. found (mg/L)	26.426	23.768
Er %	5.704	-4.926
RC %	105.704	95.073
$\mu = \bar{x} \pm (t\delta)/\sqrt{n}$	26.426 \pm 0.056	23.768 \pm 0.626
$\delta n-1$	0.045	0.503

*Each concentration represents an average of at least five measurements.

Table (3-47) shows the results for the determination of Spazmotic plus (PAR) by ¹D and ²D teach. The suitable teach. That gave more accurate result was the ²D teach. at 303.5 nm for PAR. While HYO cannot be determining by using direct teach. Therefore standard additions teach. (SAM) used to determine it as shown in Fig. (3-54). Table (3-48) shows the comparing between standard and commercial drug by ²D for PAR and ¹D for HYO.

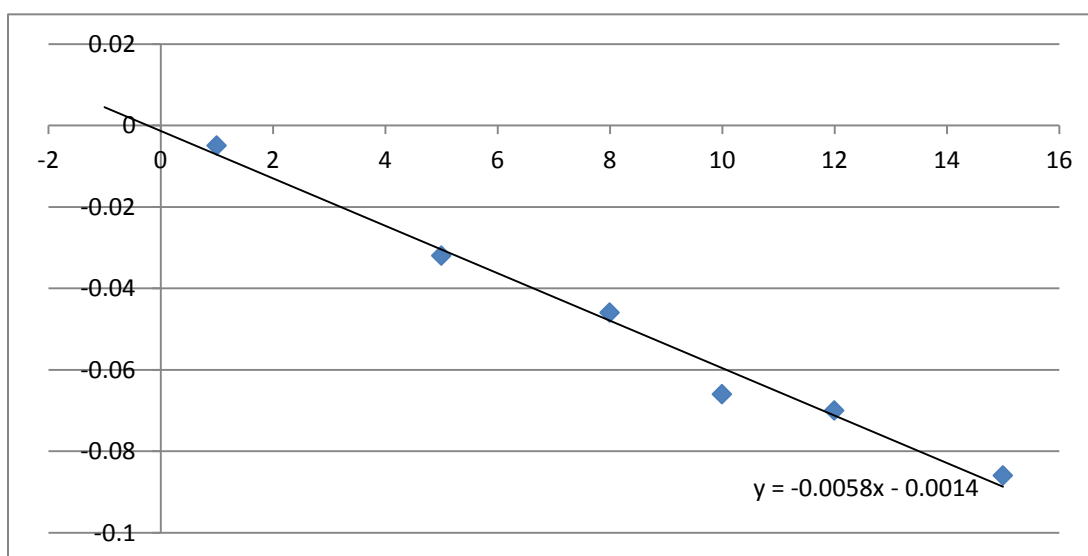


Fig. (3-54) Calibration curves for standard additions teach. (SAM) for HYO by using ¹D teach. at V=215.9nm.

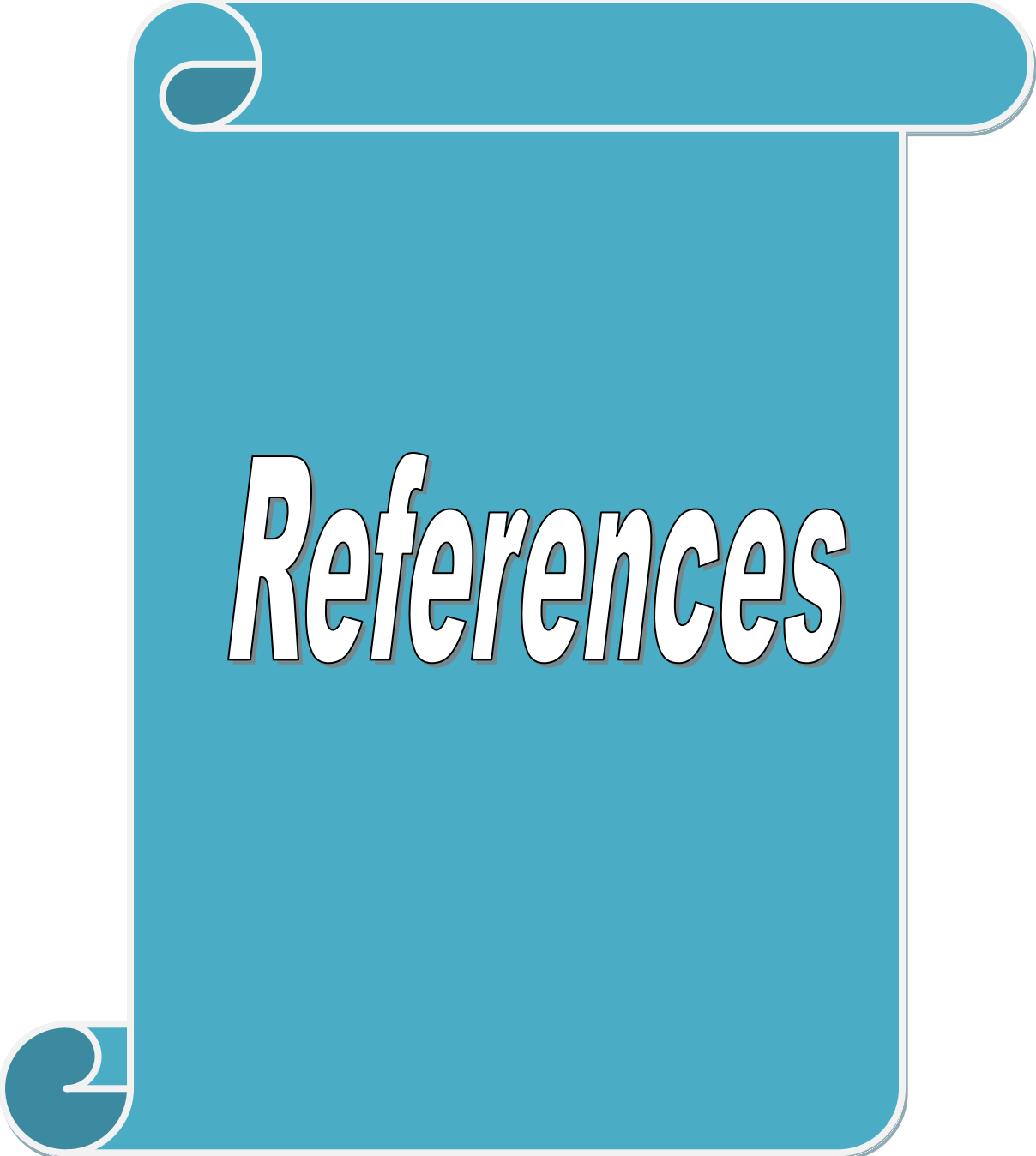
Table (3-48): Statistical data for the determination of (PAR + HYO) in their mixture in pure and pharmaceutical form by 2D for PAR and 1D for HYO.

PAR+HYO Mixture	PAR				HYO			
	Found mg/L $\lambda=303.5\text{nm}$	ER%	RC%	RSD %	Found mg/L $\lambda=215.9\text{nm}$	ER%	RC%	RSD%
Standard								
25PAR+0.5HYO	25.055	0.22	100.22	0.552	0.506	1.20	101.20	0.342
Spazmotic plus								
25PAR+0.5HYO	23.768	-4.92	95.07	2.117	0.505	0.93	100.93	7.779

*Each concentration represents an average of at least three measurements.

Conclusions

A fast and accurate teach. for determining sulphamethoxazole and trimethoprim, paracetamol and caffeine, paracetamol and hyoscine-n-butyl bromide was developed by using derivative spectrophotometry. The advantages of this teach. is that both constituents can be determined directly in a single sample without the need to be separated. It was also found that D^4, D^1 and D^4 is used for determining sulphamethoxazole and trimethoprim, while D^3 and D^4 is used for determining paracetamol and caffeine, then D^1 and D^1, D^2 is used for determining hyoscine-n-butyl bromide and paracetamol in tablets respectively .



References

References:

- 1- J.W. Robinson, E.M. Frame and G.M. Frame, "Undergraduate Instrumental Analysis", *Marcel Dekker New York*, 6th Edition, pp. 76-79, 2005.
- 2- S.E. Braslavsky, K.N. Houk and J. W. Verhoeven, "Glossary of terms used in photochemistry", *IUPAC*, 3rd Edition, pp. 15-16, 2005.
- 3- J.T.H. Roos, "Deviations from Beer's law and precision in atomic absorption spectrophotometry", *Spectrochimica Acta Part B: Atomic Spectroscopy*, Vol. 25, No. 10, pp. 539-544, 1970.
- 4- K. Buijs and M.J. Maurice, "Some considerations on apparent deviations from lambert-beer's law", *Analytica Chimica Acta*, Vol. 47, No. 3, pp. 469-474, 1969.
- 5- M. Pollard, C. Batt, B. Stern and S.M. Young, "Analytical Chemistry in Archaeology", *Cambridge University Press*, pp. 70-71, 2007.
- 6- J. Kenkel, "Analytical Chemistry for Technicians" *CRC Press, LLC*, 3rd Edition, pp. 205-215, 2003.
- 7- Y. Kostov and G. Rao, "Low-cost optical instrumentation for biomedical measurements", *Rev. Sci. Instrum.*, Vol. 71, No. 12, pp. 4361-4374, 2000.
- 8- C. Vandecasteele and C. B. Block, "Modern Methods for Trace Element Determination", *John Wiley & Sons.*, pp. 86-89, 1997.
- 9- R. Daniel, P. Nostell and A. Roos, "Single-beam integrating sphere spectrophotometer for reflectance and transmittance measurements versus angle of incidence in the solar wavelength range on diffuse and specular samples", *Rev. Sci. Instrum.*, Vol. 70, No. 5, pp. 2481-2494, 1999.
- 10- W. Gong, M. Mowlem, M. Kraft and H. Morgan, "A Simple, Low-Cost Double Beam Spectrophotometer for Colorimetric Detection of Nitrite in Seawater", *IEEE Sens. J.*, Vol. 9, No. 7, pp. 862-869, 2009.

References

- 11- Y. Haemisch, T. Frach, C. Degenhardt and A. Thon, “Fully Digital Arrays of Silicon Photomultipliers (dSiPM) – a Scalable Alternative to Vacuum Photomultiplier Tubes (PMT)”, *Physics Procedia*, Vol. 37, pp. 1546-1560, 2012.
- 12- L. León, J.J. Maraver, J. Carbajo and J.D. Mozo, “Simple and multi-configurational flow-cell detector for UV–vis spectroelectrochemical measurements in commercial instruments”, *Sensors and Actuators B: Chemical*, Vol. 186, pp. 263-269, 2013.
- 13- M. A. Osman, I. H. Suffet and S. D. Faust, “Pesticides Identification at the Residue Level”, *Am. Chem. Soc.*, Ch. 7, pp. 95-118, 1971.
- 14- D. A. Skoog and D. M. West, “Principles of Instrumental analysis”, *Saunders College Publishing*, 6th Edition, 1985.
- 15- M. Maleque, M.R. Hasan, F. Hossen and S. Safi, “Development and validation of a simple UV spectrophotometric method for the determination of levofloxacin both in bulk and marketed dosage formulations”, *J. Pharm. Anal.*, Vol. 6, No. 2, pp. 454-457, 2012.
- 16- I. pasha, F. Rehman, T. Mohammed, Y. Sanjyothi and S. Kumar, “New visible spectrophotometric methods for the determination of ampicillin trihydrate in bulk drug and their formulations”, *Int. j. pharm.& Ind. Res.*, Vol. 2, No. 1, pp. 47-50, 2012.
- 17- M.Q. Al-Abachi and H. Hadi, “A developed spectrophotometric determination of amoxicillin forms via charge-transfer reaction with metol”, *JNUS*, Vol. 10, No. 2, pp. 1-6, 2007.
- 18- Y.H. Muhamad, “A Simple Spectrophotometric Assay of Sildenafil in Pure and Pharmaceutical Preparations”, *JNUS*, Vol. 15, No. 1, pp. 18-24, 2012.

References

- 19- A.S. Al-Ayash, "A new sensitive spectrophotometric method for the determination of adrenaline in pharmaceutical preparations", *JNUS*, Vol. 11, No. 3, pp.46-54, 2008.
- 20- S.S. Abed, "Determination of macro amount of paracetamol in pharmaceutical preparations by molecular spectrophotometric method", *JNUS*, Vol. 12, No. 2, pp. 46-53, 2009.
- 21- A.Z.M. Hussein, "Spectrophotometric Determination of Ascorbic acid in Aqueous Solutions and in Pharmaceuticals formulations", *JNUS*, Vol. 16, No. 3, pp. 65-71, 2013.
- 22- N.R. Ahmad, "Facial visible spectrophotometric determination of metformin hydrochloride in glucosam tablets and industrial waste water: Application to content uniformity testing", *Iraq J. Pharm.*, Vol. 12, No. 1, pp. 75-86, 2012.
- 23- K.N. Prashanth, K. Basavaiah and C.M. Xavier, "Development and validation of UV-spectrophotometric methods for the determination of sumatriptan succinate in bulk and pharmaceutical dosage form and its degradation behavior under varied stress conditions", *JAAUBAS*, Vol. 15, No. 1, pp. 43-52, 2014.
- 24- J. D. Morrison, "Studies of Ionization Efficiency. Part III. The Detection and Interpretation of Fine Structure", *J. Chem. Phys.*, Vol. 21, No. 10, pp. 1767-1771, 1953.
- 25- T. C. O'Haver, "Derivative and Wavelength Modulation Spectrometry", *Anal. Chem.*, Vol. 51, No. 1, pp. 91A-100A, 1979.
- 26- C.B. Ojeda, F.S. Rojas and J.M. Pavon, "Recent developments in derivative ultraviolet/visible absorption spectrophotometry", *Talanta*, Vol. 42, No. 9, pp. 1195-1214, 1995.

References

- 27- A.Y. El-Sayed and N.A. El-Salem, "Recent developments of derivative spectrophotometry and their analytical applications", *Anal. Sci.*, Vol. 21, No. 1, pp. 595-614, 2005.
- 28- G.V. Popovic, L.B. Pfenndt and V.M. Stefanovic, "Analytical application of derivative spectrophotometry", *J. Serb. Chem. Soc.*, Vol. 65, No. 7, pp. 457-472, 2000.
- 29- T.C. O'Haver, "Potential Clinical Applications of Derivative and Wavelength Modulation Spectrometry", *Clin. Chem.*, Vol. 25, No. 9, pp. 1548-1553, 1979.
- 30- J.R. Morrey, "On determining spectral peak positions from composite spectra with a digital computer", *Anal. Chem.*, Vol. 40, No. 6, pp. 905-914, 1968.
- 31- B.E. Barker and M.F. Fox, "Computer resolution of overlapping electronic absorption bands", *Chem. Soc. Rev.*, Vol. 9, No. 2, pp. 143-184, 1980.
- 32- T.C. O'Haver and G. L. Green, "Numerical error analysis of derivative spectrometry for the quantitative analysis of mixtures", *Anal. Chem.*, Vol. 48, No. 2, pp. 312-318, 1976.
- 33- T.R. Griffiths and K. King, "Some aspects of the scope and limitations of derivative spectroscopy", *Anal. Chim. Acta*, Vol. 143, No. 1, pp. 163-176, 1982.
- 34- T.C. O'Haver and T. Begley, "Signal-to-noise ratio in higher order derivative spectrometry", *Anal. Chem.*, Vol. 53, No. 12, pp. 1876-1878, 1981.
- 35- K.H. Al-Saidi, S.Abdlaziz and S. Semer, "Simultaneous determination of Amiloride hydrochloride and Hydrochlorothiazide in pharmaceuticals by derivative spectrophotometry", *JNUS*, Vol. 13, No. 4, pp. 52-61, 2010.

References

- 36- K.H. Al-Saidi, N.S. Nassory and S.A. Maki, “ Spectrophotometric determination of binary mixture of some β -lactam antibiotics”, *JNUS*, Vol. 12, No. 3, pp. 33-44, 2009.
- 37- P.R. Joshi, S.J. Parmar and B.A. Patel, “Spectrophotometric Simultaneous Determination of Salbutamol Sulfate and Ketotifen Fumarate in Combined Tablet Dosage Form by First-Order Derivative Spectroscopy Method”, *Int. J. Spec.*, Vol. 2013, pp. 1-6, 2013.
- 38- V.D. Hoang, D.T. Ly, N.H. Tho and H.M. Nguyen, “UV Spectrophotometric Simultaneous Determination of Paracetamol and Ibuprofen in Combined Tablets by Derivative and Wavelet Transforms”, *Sci. W. J.*, Vol. 2014, pp. 1-13, 2014.
- 39- M. Attimarad, “Simultaneous determination of ofloxacin and fleroxate hydrochloride by first-and ratio first-derivative UV spectrophotometry”, *J. Iran. Chem. Soc.*, Vol. 9, No. 4, pp. 551-557, 2012.
- 40- K.H. Al-Saidi and S.S. Abdul-Ameer, “Simultaneous determination of amoxicillin and potassium clavulanate antibiotics in pharmaceutical sample using derivative spectrophotometric method”, *J. Biotech. Res. Cent.*, Vol. 5, No. 3, pp. 49-60, 2011.
- 41- K.H. Al-Saidi and R.A. Hammza, “Spectrophotometric Determination of Promethazine Hydrochloride and Paracetamol in Pharmaceutical Tablets”, *JNUS*, Vol. 17, No. 1, pp. 14-23, 2014.
- 42- H.R. Pouretedal, P. Sononi, M.H. Keshavarz and A. Semnani, “Simultaneous determination of cobalt and iron using first derivative spectrophotometric and H-point standard addition methods in micellar media”, *Chem.*, Vol. 18, No. 3, pp. 22-35, 2009.

References

- 43- R. Rohilla and U. Gupta, "Simultaneous Determination of Cobalt (II) and Nickel(II) By First Order Derivative Spectrophotometry in Micellar Media", *E. J. Chem.*, Vol. 9, No. 3, pp. 1357-1363, 2012.
- 44- M.B. Tehrani and E. Souri, "Third Derivative Spectrophotometric Method for Simultaneous Determination of Copper and Nickel Using 6-(2-Naphthyl)-2, 3-dihydro-1,2,4- triazine-3-thione", *E. J. Chem.*, Vol. 8, No. 2, pp. 587-593, 2011.
- 45- M.H. Abdel-Hay, A.A. Gazy, E.M. Hassan and T.S. Belal, "Derivative and Derivative Ratio Spectrophotometric Analysis of Antihypertensive Ternary Mixture of Amiloride Hydrochloride, Hydrochlorothiazide and Timolol Maleate", *J. Chin. Chem. Soc.*, Vol. 55, No. 1, pp. 971-978, 2008.
- 46- British Pharmacopoeia, "Medicinal and pharmaceutical Substances", published by (MHRA), Vol. 1 & 2, pp. 5729, 6201, 4548, 4549, 2009.
- 47- L.S. Goodman and A. Gilman, "Pharmacological Basis of Therapeutics", MacMillan. New York, Toronto, London, p. 1115, 1975.
- 48- R. Jose, M. Maximiliano, H. Marcela, M. Adriana and C. Juan, "simultaneous determination of trimethoprim and sulphamethoxazole in immediate-release oral dosage forms by first order derivative spectroscopy: application to dissolution studies", *Int. J. Pharm. & Pharm. Sci.*, Vol. 5, No. 4, pp. 505-510, 2013.
- 49- S. Balyejjusa, R.O. Adome and D. Musoke, "Spectrophotometric determination of sulphamethoxazole and trimethoprim (co-trimoxazole) in binary mixtures and in tablets", *African Health Sciences*, Vol. 2, No. 2, pp. 56-62, 2002.
- 50- M.R. Sohrabi, M. Fathabadi and A.H. Nouri " Simultaneous spectrophotometric determination of sulfamethoxazole and trimethoprim in

References

- pharmaceutical preparations by using multivariate calibration methods”
,Journal of Applied Chemical Researches, Vol. 3, No. 12, pp. 48-52, 2010.
- 51- F. Shamsa and L. Amani, ” Determination of Sulfamethoxazole and Trimethoprim in Pharmaceuticals by Visible and UV Spectrophotometry”,
Iranian Journal of Pharmaceutical Research, Vol. 1, pp. 31-36, 2006.
- 52- H. Amini and A. Ahmadiani, “Rapid and simultaneous determination of sulfamethoxazole and trimethoprim in human plasma by high-performance liquid chromatography”, *Journal of Pharmaceutical and Biomedical Analysis*, Vol. 43, No. 3, pp. 1146-1150, 2007.
- 53- E. Sayar, S. Sahin, S. Cevheroqlu and A.A. Hincal, “Development and validation of an HPLC method for simultaneous determination of trimethoprim and sulfamethoxazole in human plasma”,*Eur. J. Drug metab pharmacokinet.*, Vol. 35, No. (1-2), pp. 41-46, 2010.
- 54- I.S.d. Silva, D.T.R. Vidal, C.L. Lago and L. Angne,”Fast simultaneous determination of trimethoprim and sulphamethoxazole by capillary zone electrophoresis with capacitively coupled contactless conductivity detection”, *Journal of Separation Science*, Vol. 36, No. 8, pp. 1405-1409, 2013.
- 55- L.S. Andrade, R.C. Rocha-Filho, Q.B. Cass and O. Fatibello-Filho,”Simultaneous Differential Pulse Voltammetric Determination of Sulphamethoxazole and Trimethoprim on a Boron-Doped Diamond Electrode”,*Electroanalysis*, Vol. 21, No. 13, pp.1475-1480, 2009.
- 56- D. Eedal, “A comparative study of the ratio spectra derivative spectrophotometry, Vierordt's method and high-performance liquid chromatography applied to the simultaneous analysis of caffeine and paracetamol in tablets”, *J. Pharm. & Biomed. Anal.*, Vol. 21, No. 4, pp. 723-730, 1999.
- 57- M.K. Rajesh and G.S. Singh, “Stability-Indicating RP-HPLC Method for Analysis of Paracetamol and Tramadol in a Pharmaceutical Dosage Form”,
E J. Chem., Vol. 9, No. 3, pp. 1347-1356, 2012.

References

- 58- R.S. Satoskar, S.D. Bhandarkar and S.S. Ainapare, "Pharmacology and pharmacotherapeutics", Popular prakashan, Mumbai, 16th edition, p. 164, 1999.
- 59- A. Nehlig, J.L. Daval and G. Debry, "Caffeine and the central nervous system: mechanisms of action, biochemical, metabolic and psychostimulant effects", *Brain Res. Rev.*, Vol. 17, No. 2, pp. 139-170, 1992.
- 60- V. Vichare, P. Mujgond, V. Tambe and S.N. Dhole," Simultaneous Spectrophotometric determination of Paracetamol and Caffeine in Tablet Formulation", *International Journal of Pharm Tech Research*, Vol. 2, No. 4, pp. 2512-2516, 2010.
- 61- H. Tavallali and M. Sheikha," Simultaneous kinetic determination of Paracetamol and Caffeine using Cu(II)-neocuproine in presents of dodecyl sulfate by H-point standard addition method", *Indian Journal of chimistry*, Vol.48A, pp. 812-816, 2009.
- 62- B. Tsvetkova, B. Kostova, I. Pencheva, A. Zlatkov, D.Rachev and P.Peikov," Validated LC Method for Simultaneous Analysis of Paracetamol and Caffeine in Model Tablet Formulation", *International Journal of Pharmacy and Pharmaceutical Sciences*, Vol. 4, No. 4, pp. 680-684, 2012.
- 63- R. Chandra¹, K. Dutt Sharma," Quantitative determination of Paracetamol and Caffeine from Formulated Tablets by Reversed Phase-HPLC Sepaprtion Technique", *International Journal of Chromatographic Science*, Vol. 3, No. 2, pp. 31-34, 2013.
- 64- V.K. REDASANI, A.P. GORLE, R.A. BADHAN, P.S. JAIN and S.J. SURANA," Simultaneous determination of Chlorpheniramine Maleate, Phenylephrine Hydrochloride, Paracetamol and Caffeine in Pharmaceutical Preparation by RP-HPLC", *Chemical Industry & Chemical Engineering Quarterly*, Vol. 19, No. 1, pp. 57-65, 2013.

References

- 65- M. Levent," HPLC Method for the Analysis of Paracetamol, Caffeine and Dipyrone", *Turk J Chem*, Vol. 26, pp. 521-528, 2002.
- 66- B.C.Lourencao, R.A.Medeiros, R.C.Rocha-Filoh, L.H.Mazo and O.Fatibello-Filoh,"Simultaneous Voltammetric determination of Paracetamol and Caffeine in Pharmaceutical Formulation using boron-doped diamond electrode", *talanta*, Vol. 12, , 2008.
- 67- S. Mueller, G.N. Tytgat, L.G. Paulo, E.M. Quigley, J. Bubeck and H. Peil, "Placebo- and paracetamol-controlled study on the efficacy and tolerability of hyoscine butylbromide in the treatment of patients with recurrent crampy abdominal pain", *Aliment Pharmacol. Ther.*, Vol. 23, pp. 1741-1748, 2005.
- 68- B.V. Elsevier," Spectrophotometric determination of paracetamol and hyoscine N-butyl bromide in film-coated tablets", *Scientia Pharmaceutica*, Vol. 64, No. 2, pp. 173-183, 1996.
- 69- N.W. Ali, M. Gamal and M.Abdelkawy," Simultaneous Determination of Hyoscine NButyl Bromide and Paracetamol by RP-TLC Spectrodensitometric Method", *British Journal of Pharmaceutical Research*, Vol. 3, No. 3, pp. 472-484, 2013.
- 70- P. Poulou and M. Panderi," Determination of hyoscine n-butylbromide, lidocaine hydrochloride, and paracetamol in injection forms using solid-phase extraction, high-performance liquid chromatography, and UV-Vis spectrophotometry", *Journal of Liquid Chromatography and Related Technologies*, Vol. 22, No. 7, pp. 1055-1068, 1999.
- 71- N.W. Ali , M.Gamal and M. Abdelkawy," Simultaneous determination of hyoscine N-butyl bromide and paracetamol in their binary mixture by RP-HPLC method", *British Journal of Pharmaceutical Research*, Vol. 3, No. 3, pp. 472-484, 2013.

1- Standard Deviation (δ_{n-1})

$$\delta_{n-1} = \sqrt{\frac{\sum (X_i - \bar{X})^2}{N-1}}$$

Where:

X_i = concentration of individual deviations.

\bar{X} = Mean of concentration.

N = no. of measurements.

2- Relative Standard Deviation (RSD%)

$$\text{RSD}\% = \frac{\delta_{n-1}}{\bar{X}} \times 100$$

3- Relative Error ($E_{\text{rel.}}\%$)

$$\text{Error} = \bar{X} - \mu$$

$$E_{\text{rel.}}\% = \frac{\text{Error}}{\mu} \times 100$$

Where:

$E_{\text{rel.}}\%$; Error relative between the results average (\bar{X}) and the true value (μ).

4- Recovery (Rec.%)

$$\text{Recovery (Rec.) \%} = \frac{\mu - E}{\mu} \times 100$$

5- Limit of detection (LOD)

$$\text{LOD} = \frac{3\delta_{n-1}X}{\bar{X}}$$

6- Limit of quantification (LOQ)

$$\text{LOQ} = \frac{10\delta_{n-1}X}{\bar{X}}$$

7- F-test

$$F = \frac{S_a^2}{S_b^2}$$

Where:

S_a , S_b are the standard deviations for first and second methods respectively, ($S_a > S_b$).

1- Sulphamethoxazole (SMX) , Trimethoprim (TMP):(normal)

Conc.of (SMX) (Mg/l)	Abs at P=256.7nm	Conc.of (TMP) (Mg/l)	Abs at P=288.0nm
2	0.127	2	0.051
4	0.261	4	0.096
6	0.398	6	0.136
8	0.538	8	0.183
10	0.676	10	0.237
15	1.012	15	0.355
20	1.356	20	0.472
25	1.717	25	0.596
30	2.054	30	0.717

2- Paracetamol(PAR) , Caffeine(CAF):(normal)

Conc.of (PAR) (Mg/l)	Abs at P=243.1nm	Conc.of (CAF) (Mg/l)	Abs at P=273.1nm
2	0.135	2	0.100
4	0.259	4	0.218
6	0.397	6	0.307
8	0.525	8	0.415
10	0.652	10	0.517
15	0.984	15	0.773
20	1.291	20	1.026
25	1.608	25	1.277
30	1.910	30	1.530

3- Paracetamol(PAR) , Hyoscine-n-butyl bromide(HYO):(normal)

Conc.of (PAR) (Mg/l)	Abs at P=243.1nm	Conc.of (HYO) (Mg/l)	<i>(HYO) cannot determanie in normal teah.</i>
2	0.135	2	
4	0.259	4	
6	0.397	6	
8	0.525	8	
10	0.652	10	
15	0.984	15	
20	1.291	20	
25	1.608	25	
30	1.910	30	

المُلخَص

في هذا البحث تم تقدير المركبات (SMX,TMP,CAF,HYO and PAR) باستخدام المشتقات الطيفية (الاولى , الثانية , الثالثة والرابعة). على شكل أمزجة ثنائية للأدوية بواسطة تطبيق التقاطع الصفري كما يلي:

1- مزيج السلفاميثا كسازول و التراي ميثوبريم باستخدام المشتقة الاولى و الرابعة في (288.0nm) و (257.8nm) ومدى للتراكيز الخطية (2-30 mg/L) و (2-25 mg/L) وكان منحنى المعايرة بمعامل ارتباط r لا يقل عن (0.9996) و (0.9992) وحد الكشف (0.750 mg/L و 0.360) للسلفاميثا كسازول على التوالي . اما التراي ميثوبريم فتم تعيينه باستخدام المشتقة الرابعة في (251.5nm) ومدى للتراكيز الخطية (2-30 mg/L) وكان منحنى المعايرة بمعامل ارتباط r لا يقل عن (0.9995) وحد الكشف (0.382 mg/L) وكان معامل الانحراف (1.136,0.280,0.255) على التوالي وتم تطبيقه على دواء (TRIMOL-400SMX, 80TMP mg) و (METHOPRIM-400SMX,80TMP mg).

2- مزيج الباراسيتامول مع الكافايين باستخدام المشتقة الثالثة في (275.8nm) ومدى للتراكيز الخطية (2-35 mg/L) وكان منحنى المعايرة بمعامل ارتباط r لا يقل عن (0.9987) وحد الكشف (0.445 mg/L) اما الكافايين فتم تعيينه باستخدام المشتقة الرابعة في (294.7nm) ومدى للتراكيز الخطية (2-35 mg/L) وكان منحنى المعايرة بمعامل ارتباط r لا يقل عن (0.9995) وحد الكشف (0.162 mg/L) وكان معامل الانحراف (0.130,0.222) على التوالي وتم تطبيقه على دواء (PANADOL EXTRA-500PAR, 65CAF mg).

3- مزيج الباراسيتامول و الهايوسين باستخدام المشتقة الاولى والثانية في (297.4nm) و (303.5nm) ومدى للتراكيز الخطية (2-30 mg/L) و (2-30 mg/L) وكان منحنى المعايرة بمعامل ارتباط r لا يقل عن (0.9998) و (0.9987) وحد الكشف (0.250 و 0.081 mg/L) للباراسيتامول على التوالي . اما الهايوسين فتم تعيينه باستخدام المشتقة الاولى في (215.9nm) ومدى للتراكيز الخطية (2-25mg/L) وكان منحنى المعايرة بمعامل ارتباط r لا يقل عن (0.9997) وحد الكشف (0.091 mg/L) وكان معامل الانحراف (0.342,0.400,0.107) على التوالي وتم تطبيقه على دواء (SPAZMOTEK PLUS-500PAR,10HYO mg).

تتضمن هذة الاطروحة ثلاثة فصول وكل فصل يحتوي على المعلومات التالية:

الفصل الاول: يشمل نبذة مختصرة عن خواص UV-visible وكذلك تطبيقات UV وDS في المستحضرات الصيدلانية وايضاً يتضمن تحليلات السلفاميثا كسازول , التراي ميثوبريم , الكافايين و الهايوسين و الباراسيتامول
الفصل الثاني: يشمل الجزء العملي وايضا يوضح المواد الكيميائية المستخدمة والاجهزة وطريقة تحضير المحاليل القياسية ونماذج الادوية المستعملة في البحث.
الفصل الثالث يشمل النتائج العملية ومناقشتها التي تسفر عن امكانية التطبيقات الناجحة التي استخدمت المشتقات الطيفية لتعيين تركيز كل مادة في الدواء.



جمهورية العراق
وزارة التعليم العالي والبحث العلمي
جامعة النهرين/كلية العلوم
قسم الكيمياء

التقديرات الطيفية للمركبات الاحادية والمتعددة للادوية

رسالة
مقدمة إلى كلية العلوم/ جامعة النهرين
كجزء من متطلبات نيل درجة الماجستير في علوم الكيمياء

من قبل
مروه صباح يونس
بكالوريوس 2010

إشراف
الاستاذ المساعد الدكتورة
خالدة حميد محمد السعيد

تشرين الأول
م 2014

ذو الحجة
هـ 1435